Identification And Characterization Of Mediators Of Toxicity Of A Oligomers By Genome Wide Screening In *Caenorhabditis Elegans*

Thesis

MATTEO STRAVALACI

Personal Identifier C4167464

Identification and Characterization of Mediators of Toxicity of Aβ Oligomers by Genome Wide Screening in *Caenorhabditis elegans*

Registered degree:

Doctor of Philosophy at The Open University

Life and Biomolecular Sciences

Affiliated Research Centre:

Mario Negri Institute for Pharmacological Research

September 2016

Abstract

Soluble oligomers of the amyloid-β (Aβ) protein play a key role in the pathogenesis of Alzheimer's disease (AD), although the underlying molecular mechanisms are poorly understood. In order to search for proteins involved in the formation and/or toxicity of Aβ oligomers, a transgenic *C. elegans* model of AD was used in which inducible expression of Aβ oligomers results in a complete paralysis; in these worms a genetic screen following chemical mutagenesis was applied to discover the genes involved in the Aβ-dependent paralysis (forward genetics). This analysis allowed identification of a mutated clone showing a complete lack of paralysis, despite this it not bear mutations in the Aβ coding region, and accumulates Aβ transcript and protein levels comparable to that of the non-mutated strain. This is the first *in vivo* model in which the expression of Aβ oligomers do not result in any toxic effect. The genome of the mutated worm was then sequenced and compared with that of the control strain to search for altered genes. Two genes, with no known function, were found to bear a stop codon mutation, likely resulting in the translation of an inactive protein. The rest of the mutations were missense mutations. Among them, point mutations were observed in some genes previously correlated with nematode lifespan and ageing. In *C. elegans* these biological processes are coordinated by the insulin/IGF-1-like signalling (IIS) pathway, which also regulates the response of the organism to toxic aggregated proteins. Thus, the activation of the IIS pathway was investigated in control and mutated worms. As expected, Aβ expression induced the up-regulation of two genes coding for small heat shock proteins (a class of chaperons known to be involved in AD) in the

control strain, whereas these genes were actually down-regulated in the mutated strain. Since heat shock proteins are known to bind Aβ oligomers, these chaperons could directly mediate the formation of toxic amyloid species. Moreover, the results of the whole genome sequencing indicate that several proteins could act as potential novel mediators of Aβ toxicity and could open up new insights for research on age-related, neurodegenerative diseases.

Acknowledgments

First of all, I wish to express my gratitude to Dr. Marco Gobbi for the great scientific and human support given to me in all these years spent in his laboratory. His high experience dramatically contributed to the development of my scientific career.

Also, I want to thank my supervisor Prof. Alun Williams for his guidance and his advices during my PhD studies.

I want to thank Dr. Luisa Diomede and all the members of her laboratory for their advices and suggestions with *C. elegans* studies.

Special thanks go to all the former and current members of PD/PK laboratory, and all the Department of Molecular Biochemistry and Pharmacology for making me grow professionally.

I would like to thank all the collaborators and colleagues of the Mario Negri Institute and I thank the director Prof. Silvio Garattini for giving me the chance to undertake my PhD.

The most important and sincere thanks go to Euge, my family and to my friends for their never ending care and encouragement.

Summary

Abstract **1**

Acknowledgments **3**

Summary **4**

List of Figures **7**

List of Tables **9**

INTRODUCTION **10**

1. Neurodegenerative diseases and protein misfolding **11**

1.1 Protein aggregation and amyloid formation 19

1.2 Mechanisms of neuronal death in neurodegenerative diseases 23

2. Alzheimer's disease **26**

2.1 The amyloid cascade hypothesis 28

2.2 APP processing and generation of Aβ 31

2.3 The role of Aβ oligomers in Alzheimer's disease 35

3. Transgenic *C. elegans* as a model in Alzheimer research **39**

3.1 Biology of *C. elegans* 40

3.2 Life Cycle 41

3.3 *C. elegans* as a genetic model organism 43

3.4 The IIS pathway in *C. elegans* links ageing to toxic protein aggregation 45

3.5 C. elegans models for Alzheimer's disease 49

4. Genetic screens in transgenic *C. elegans* models of protein misfolding diseases **53**

4.1 EMS mutagenesis 54

4.2 RNA interference 57

4.3 Genetic screens in *C. elegans* models for polyglutamine diseases 60

4.4 Genetic screens in *C. elegans* models for Parkinson's disease 63

4.5 Genetic screens in *C. elegans* models for Alzheimer's disease 65

AIMS 66

MATERIALS AND METHODS 68

5.1 *C. elegans* studies 69

5.2 Chemical mutagenesis of CL4176 worms and F2 screen 70

5.3 Analysis of Aβ DNA in transgenic worms 71

5.4 Total RNA extraction 72

5.5 Analysis of gene expression in transgenic worms by qRT-PCR 73

5.6 Total soluble Protein Extraction 74

5.7 Immunodot-blot analysis 75

5.8 Western blot analysis 76

5.9 Surface Plasmon Resonance studies 77

5.10 Whole genome sequencing of CL4176 and EMS-treated worms 78

RESULTS 80

6. Chemical mutagenesis of transgenic *C.elegans* AD model (CL4176 strain) 81

6.1 Time course of paralysis in new CL4176 worms 87

7. Analysis of Aβ expression in EMS-treated worms 89

7.1 Analysis of Aβ DNA in CL4176 and MN4176 worms 89

7.2 Analysis of genetic expression of Aβ in CL4176 and MN4176 worms 92

7.3 Analysis of Aβ oligomers in CL4176 and MN4176 worms 95

8. Genome wide sequencing of CL4176 and MN4176 worms 99

8.1 Results from the first whole genome sequencing. 99

8.2 Results from the second whole genome sequencing. 104

9. Analysis of IIS pathway activation in CL4176 and MN4176 worms 111

DISCUSSION 114

BIBLIOGRAPHY 122

List of Figures

Figure 1.1 A schematic energy landscape for protein folding 13

Figure 1.2 Regulation of protein folding in the Endoplasmic Reticulum (ER) 15

Figure 1.3 The proteostasis network 16

Figure 1.4 Extracellular and intracellular aggregates found in neurodegenerative diseases 20

Figure 1.5 Mechanism of amyloid formation 22

Figure 2.1 Cross sections of the brain show atrophy, or shrinking, of brain tissue caused by Alzheimer's disease.....27

Figure 2.2 The amyloid cascade hypothesis 30

Figure 2.3 APP structure and metabolism 33

Figure 2.4 APP mutations 34

Figure 2.5 Possible mechanisms of action of Aβ oligomers leading to neuronal death according to the amyloid hypothesis.....37

Figure 3.1 Anatomy of an adult hermaphrodite 40

Figure 3.2 Life cycle of *C. elegans* at 22°C 42

Figure 3.3 Light microscopy images showing male and hermaphrodite anatomy 43

Figure 3.4 The IIS pathway in *C. elegans* 46

Figure 3.5 Link between aging and protein aggregation in *C. elegans* 48

Figure 4.1 EMS mutagenesis scheme and F2 screen in *C. elegans* 55

Figure 4.2 RNA interference (RNAi) screening in *C. elegans* 58

Figure 6.1 Time course of paralysis in wild-type CL4176 worms 81

Figure 6.2 Representative picture outlining a typical F2 screen after EMS mutagenesis for the selection of mutated worms.....83

Figure 6.3 Paralysis kinetics of CL4176 and mutated worms selected after EMS mutagenesis 84

Figure 6.4 Time course of paralysis in the worms selected after the second mutagenesis experiment with EMS 85

Figure 6.5 Time course of paralysis of new CL4176 and MN4176 worms 87

Figure 7.1 Analysis of Aβ DNA by agarose gel electrophoresis 90

Figure 7.2 Basic local Alignment Tool (BLAST) analysis 91

Figure 7.3 Relative increase of Aβ mRNA levels in CL4176 and MN4176 worms 93

Figure 7.4 Fold change levels of Aβ mRNA in CL4176 and MN4176 worms 93

Figure 7.5 Temporal transcript accumulation of Aβ in CL4176 and MN4176 woms 94

Figure 7.6 Aβ protein expression in CL4176 and MN4176 worms 95

Figure 7.7 Detection of Aβ oligomers in CL4176 and MN4176 worms by Western blot analysis ...96

Figure 7.8 Studies with native Aβ oligomers extracted from CL4176 and MN4176 worms 98

Figure 8.1 Circle chart representing bacteria species found in CL4176 and MN4176 DNA 100

Figure 8.2 Detection of bacterial DNA in CL4176, CL802 and MN4176 worms by PCR 101

Figure 8.3 Detection of bacterial DNA in CL4176 and MN4176 worms after egg purification by PCR 103

Figure 8.4 Analysis of DNA sequence of C18E3.5 gene in CL4176 and MN4176 worms. 107

Figure 8.5 Analysis of DNA sequence of C17E4.10 gene in CL4176 and MN4176 worms 108

Figure 9.1 Induction of *daf-18* gene expression in CL4176 and MN4176 worms 109

Figure 9.2 Induction of *hsp* genes in CL4176 and MN4176 worms 110

List of Tables

Table 1.1 List of the main human neurodegenerative diseases and their pathological and biochemical features 18

Table 1.2 Human diseases associated with formation of extracellular amyloid deposits or intracellular inclusions with amyloid-like characteristics 19

Table 2.1 List of mutations causing early onset familial Alzheimer's disease 29

Table 4.1 Features of EMS mutagenesis versus RNA interference 53

Table 5.1 Sequences of primers used in qRT-PCR studies 73

Table 8.1 Oligonucleotidic primers used for detection of *S.maltophilia* and *B.thurigiensis* DNA in *C.elegans* 101

Table 8.2 Total number of mutations found in CL4176 and MN4176 DNA after whole genome sequencing 104

Table 8.3 Number and percentages of mutations found in MN4176 worms found identical in CL4176 worms 105

Table 8.4 Stop codon mutations found in MN4176 worms.....107

Table 8.5 Oligonucleotidic primers for stop codon mutations.....107

Table 8.6 Missense mutations found in MN4176 worms.....110

INTRODUCTION

1. Neurodegenerative diseases and protein misfolding

Proteins, which are synthetized by the genetic information encoded in the DNA, are involved in every biological process. The folding of proteins in complex and various three-dimensional structures has enabled living systems to develop tremendous diversity and selectivity in their chemical processes that lead to biological activity. Moreover, the precise folding of proteins is important for several biological processes, including molecular trafficking or cell growth and differentiation[1]. In addition, only functional proteins are stable in a crowded environment like that of a cell and are able to interact selectively with their targets. As a consequence, proteins which do not fold properly can give origin to severe pathological conditions, such as sickle cell anemia[2]. In this disease, a single point mutation in the β-globulin chain of haemoglobin (glutamic acid to valin) changes the protein conformation, exposing hydrophobic patches that lead to protein polymerization in individuals homozygous for the mutation[3,4]. This reduces the elasticity of red blood cells, causing extreme pain, extensive tissue destruction and anemia[5].

Under physiological conditions, proteins fold in structures that are the most thermodynamically stable[6]. However, the number of possible conformations of any polypeptide chain can adopt is so large[7] ($> 10^{30}$ for a protein 100 amino acids long), so that the folding process is inherently error-prone. This process mainly relies on the contact between residues that can be very distant in the amino acid

sequence[8]. Native-like interactions are generally more stable and persistent that non-native-ones, thus the polypeptide chain can adopt the lowest-energy structure by a process of trial and error. In this contest, hydrophobic interactions are particularly important in driving non polar amino acids into the core of the folding structure of soluble proteins, limiting the conformational space that must be searched during folding[9]. However, the free-energy surface (also called "landscape") toward the most thermodynamically stable structure is not plain, which means that the polypeptide chains need to cross several kinetic energy barriers and occupy various folding intermediates to reach the native conformation (Fig. 1.1).

Misfolded or incompletely folded proteins generally expose to the solvent hydrophobic structures that are buried in the native state, increasing the possibility to aggregate or inappropriately interact with other molecules[10]. Although most aggregates are amorphous, some proteins aggregate to form so-called amyloid fibrils (Fig. 1.1). Fibril formation is often preceded by the accumulation of oligomeric aggregates, which are thought to play a key role in several diseases.

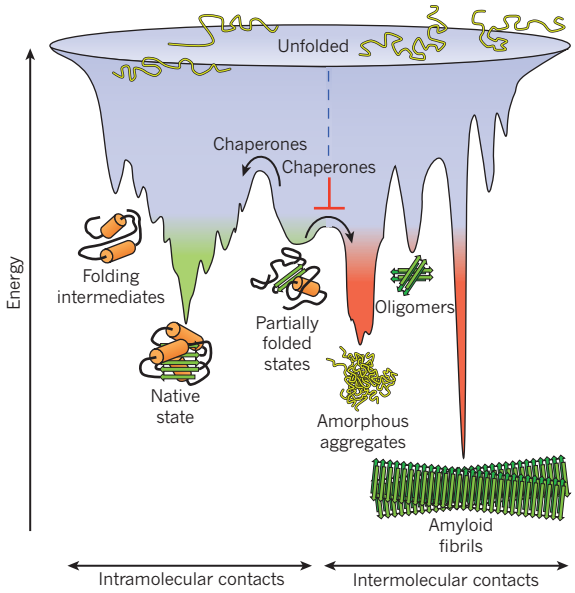

Figure 1.1 A schematic energy landscape for protein folding. During folding, proteins adopt various conformations in search of the most thermodynamically stable structure. Folding intermediates and partially folded states occupy low energy wells and are prone to aggregate in different forms (amorphous, oligomeric and fibrillar). Molecular chaperones can prevent these aberrant molecular assemblies by providing folding assistance (*taken from ref. 16*)

To prevent aberrant molecular interactions, living systems have evolved different strategies[11,12]. One of them involves the role of molecular chaperones that are present in all cell types and compartments. A molecular chaperone is a protein that interacts with, stabilizes, or helps another protein to acquire its functionally active conformation, without being present in its final structure[13-16]. Some chaperones interact with nascent polypeptide chains as they emerge from the ribosome (co-translational folding)[17], while others are involved in the assistance of later stages of protein folding[11,12]. Some classes of chaperons accelerate slow

steps in the folding process, e.g. peptidylprolyl isomerase increases the rate of cis-trans isomerization of peptide bonds involving proline residues, while disulphide isomerase increases the rate of formation of disulphide bonds[18]. However, in general, molecular chaperones act in protein folding by increasing the efficiency of the overall process and by reducing the probability of competing mechanisms, for example aggregation (Fig. 1.1).

Several lines of evidence suggest that molecular chaperones play an important role in preventing misfolding. It is also known that some molecular chaperones not only are able to protect proteins during their folding, but also to rescue misfolded and aggregated proteins (Fig. 1.1). These protective mechanisms in the folding process require energy, and ATP is mandatory for most of the known molecular chaperones to function properly.

Different stress factors, including high temperatures or oxidizing agents, induce the expression of various molecular chaperones by inducing specific transcriptional programs, which cooperate with protein synthesis and degradation to maintain proteome integrity. This complex machinery is generally called the proteostasis network (PN), and comprises about 1400 components in mammalian cells[19-21]. The main components of the PN are the cytosolic stress response[22], and the unfolded protein response (UPR) pathways of the endoplasmic reticulum (ER)[23]. ER is the destination of many newly synthetized proteins that have to be secreted from the cell. The ER contains a wide variety of molecular chaperones, and in addition, the proteins must satisfy a “quality-control” check, before their secretion through the Golgi apparatus[24] (Fig. 1.2). This control-quality system is

characterized by a series of glycosylation and deglycosylation reactions that allow correctly folded proteins to be distinguished from misfolded ones[24].

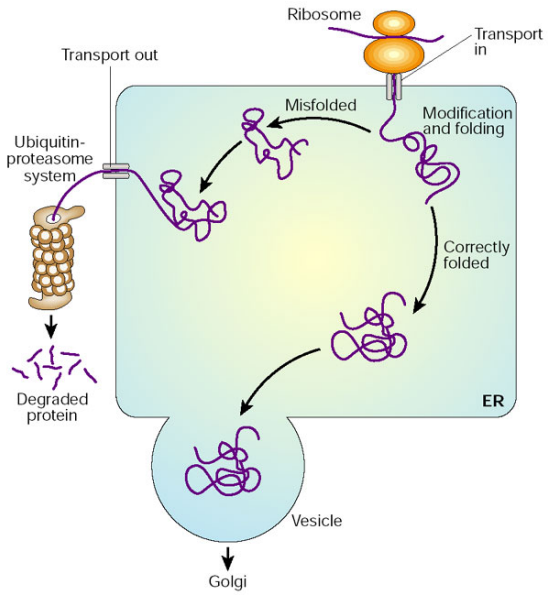

Figure 1.2 Regulation of protein folding in the Endoplasmic Reticulum (ER) (*taken from ref. 2*)

Misfolded proteins are targeted to degradation, which is performed mainly by the ubiquitin-proteasome system (UPS, Fig. 1.2)[25,26]. Clearance of aggregated proteins by the UPS system requires disaggregation prior to degradation, which is operated by the Hsp70 system (Fig. 1.3). Protein aggregates that resist degradation may be cleared by selective autophagy and lysosomal degradation[26].

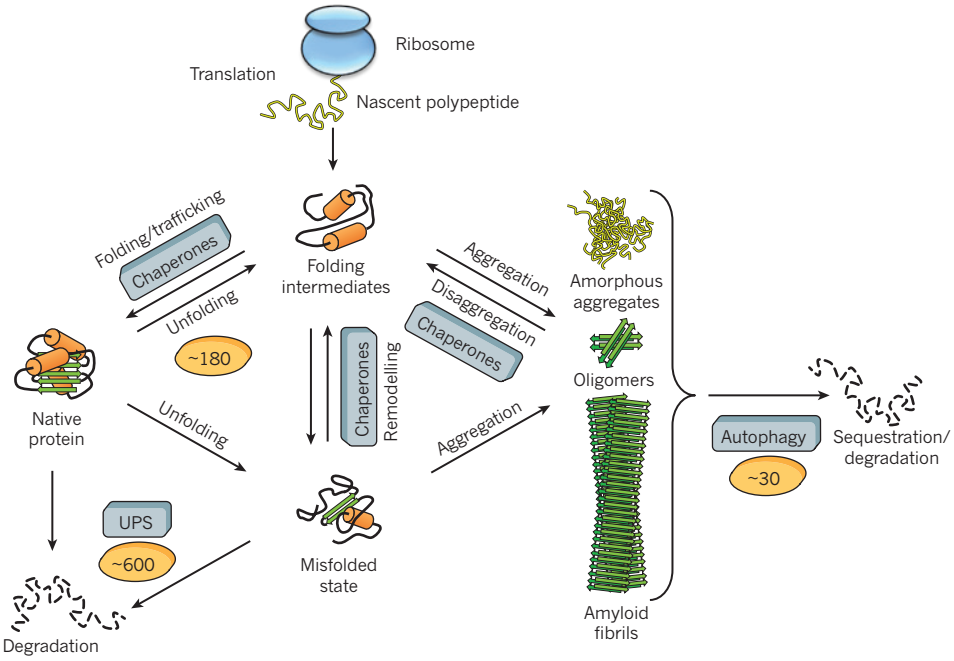

Figure 1.3 The proteostasis network *(taken from ref. 16)*.

As outlined above, all biological processes, including protein turnover, trafficking and cellular localization require a correct protein folding. Improper degradation of misfolded proteins can thus contribute to the development of more severe diseases. The most known example is provided by the disease cystic fibrosis, which is caused by mutations in cystic fibrosis transmembrane conductance regulator (CFTR), a plasma membrane chloride channel. The most common causative mutation in cystic fibrosis is deletion of a phenylalanine residue at position 508 (ΔF508) in CFTR. This mutation causes the protein to be misfolded and targeted for degradation[27].

Because many proteins that localize to specific organelles must fold correctly in order to be trafficked properly, mutations that destabilize the correct fold can lead to wrong subcellular localization. This can result in dysfunction via both loss of

function of the protein at its appropriate location as well as gain-of-function toxicity if it accumulates in an incorrect location. One example of this dual toxicity is provided by α1-antitrypsin, a secreted protease inhibitor that, when mutated, leads to emphysema in a recessive loss-of-function manner and liver damage in a dominant gain-of-function manner[28]. Mutant forms of this protein fail to complete proper folding and are retained in the ER. The misfolded protein is not degraded, unlike other misfolded proteins, so it accumulates in the ER of hepatocytes – the site of synthesis – resulting in liver damage[29,30]. Furthermore, because the mutated α1-antitrypsin is not secreted, it is unable to perform its normal cellular function, which is to inhibit the action of proteases, including neutrophil elastase, in the lung. This, in turn, causes extensive damage to the lung's connective tissue.

In other pathologies, however, proteins with a high propensity to misfold escape all the protective mechanisms cited above and may form either intracellular or extracellular aggregates termed amyloids.

Many neurodegenerative disorders can be classified as "protein misfolding" diseases. This heterogeneous group of diseases includes Alzheimer's disease (AD), Parkinson's disease (PD), Huntington's disease (HD), transmissible spongiform encephalopathies (TSEs; also known as 'prion diseases') and amyotrophic lateral sclerosis (ALS) (Table 1.1). Despite the differences in clinical symptoms and disease progression, all these disorders are characterized by the accumulation of amyloid aggregates in the brains of affected patients[31].

Pathology	Mode of Transmission	Clinical features	Affected regions of the brain	Protein involved	Cellular localization of aggregates
Alzheimer's	Sporadic (95%) or inherited (5%)	Progressive dementia	Hippocampus, cerebral cortex	Amyloid-β and tau protein	Extracellular, cytoplasmic
Parkinson's	Mostly sporadic	Movement disorder	Substantia nigra, hypothalamus	α-Synuclein	Cytoplasmic
Huntington's	Inherited	Dementia, motor and psychiatric problems	Striatum, cerebral cortex	Huntingtin	Nuclear
Amyotrophic lateral sclerosis	Sporadic (90%)or inherited(10%)	Movement disorder	Motor cortex, brainstem	Superoxide dismutase	Cytoplasmic
Transmissible spongiphorm encephalopathies	Sporadic (90%) Inherited (8%) or infectious (2%)	Dementia, ataxia, psychiatric problems and insomnia	Various regions., depending on disease	Prion protein	Extracellular

Table 1.1 List of the main human neurodegenerative diseases and their pathological and biochemical features (*adapted from ref. 31*).

1.1 Protein aggregation and amyloid formation

Amyloid diseases are characterized by the aggregation of a specific protein. Although the features of the soluble forms of the proteins associated to these diseases are very different (Table 1.2) – they can range from globular proteins to unstructured peptides – their aggregated forms show common characteristics[32] (Fig. 1.4). This suggests that the main interactions within the fibril are made through the common protein backbone and not by the individual amino acid side chain residues[33].

Disease	Aggregating protein or peptide
Neurodegenerative diseases	
Alzheimer's disease (AD)	Amyloid β peptide
Prion diseases (TSEs)	Prion protein
Parkinson's disease (PD)	α-Synuclein
Dementia with Lewy bodies	α-Synuclein
Frontotemporal dementia	Tau
Amyotrophic lateral sclerosis (ALS)	Superoxide dismutase 1
Huntington's disease (HD)	Huntingtin with polyQ expansion
Spinocerebellar ataxias	Ataxins with polyQ expansion
Spinal and bulbar muscular atrophy	Androgen receptor with polyQ expansion
Nonneuropathic systemic amyloidoses	
AL amyloidosis	Immunoglobulin light chains
AA amyloidosis	Fragments of serum amyloid A protein
Senile systemic amyloidosis	Wild-type transthyretin
Familial amyloidotic polyneuropathy	Mutants of transthyretin
Hemodialysis-related amyloidosis	β2-microglobulin
ApoAI amyloidosis	N-terminal fragments of apolipoprotein AI

Table 1.2 Human diseases associated with formation of extracellular amyloid deposits or intracellular inclusions with amyloid-like characteristics (*adapted from ref. 39*).

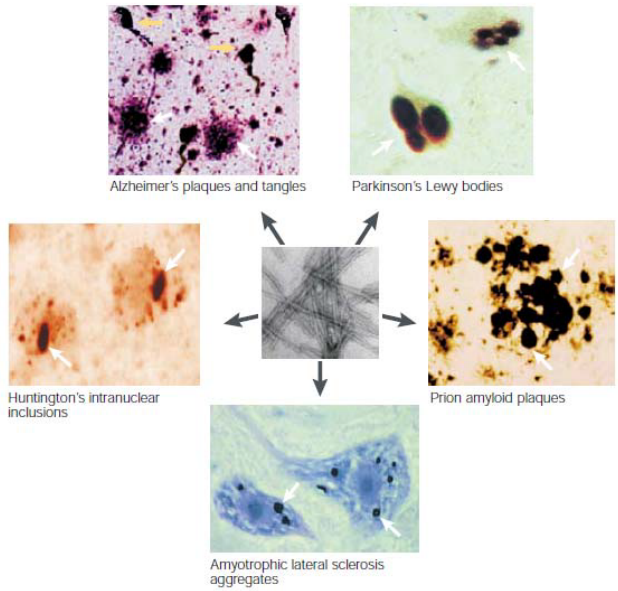

Figure 1.4 Extracellular and intracellular aggregates found in neurodegenerative diseases (*adapted from ref. 31*).

Additional evidence for the intrinsic nature of amyloid formation came from the observation that polythreonine and polylysine sequences could form amyloid fibrils *in vitro*[33]. Electron microscopy analysis showed that amyloid fibrils are long, unbranched and often twisted structures with a diameter of 7-13 nanometers. X-ray diffraction patterns of fibrils display a characteristic "cross-β" configuration, indicating that the core structure is composed of β-strands oriented perpendicular to the fibril axis[32]. This specific structural organization is recognized by the dyes Congo Red and thioflavin T. When bound to fibrils, these compounds display green birefringence and enhanced fluorescence, respectively[34]. Apart from these common features, heterogeneity in fibril structures also occurs. Variation can exist at the level of amino acid side-chains as in the loops connecting intramolecular β-sheets. This variation can also be observed between fibrils of the same protein

that, under given conditions, adopt a different internal organization due to thermodynamic or kinetic determinants[35]. Several genetic and environmental factors have been associated with protein misfolding and aggregation. The mechanism by which mutations lead to conformational change and disease is probably destabilization of the normal proteinconformation, promoting misfolding and subsequent aggregation. Environmental factors that might favour this process include change in metal ions, pathological chaperone proteins, pH or oxidative stress, macromolecular crowding and increases in the concentration of unfolded and partially folded proteins[36,37]. Many of these alterations have been associated with aging, consistent with the late onset of neurodegenerative diseases[38].

The unfolded and partially folded states initially form disordered aggregates that can further assemble to form amyloid fibrils[39]. *In vitro* experiments indicate that their formation is generally characterized by a lag phase, followed by a period of rapid growth[40,41]. The critical event is the formation of protein oligomers that acts as a nucleus to direct further growth of aggregates. The lag phase can be suppressed by the addition of preformed aggregates to fresh solution, a process called seeding[42,43]. An alternative model of aggregation is the “template-assistance model”[44-46]. In this model, the native soluble form of a protein interacts with the misfolded form. As a consequence of this interaction, the native form alters its conformation; this new homodimer may then dissociate allowing the interaction of each misfolded polypeptides with other native proteins, thus propagating the misfolding reaction.

There are striking similarities in the aggregation process of different peptides and proteins (Fig. 1.5)[40,41]. At least two intermediates have been identified in the pathway from the native monomeric protein to the fibrillar structure. The first are

soluble, low-molecular weight oligomers, and their structural and biochemical characterization has been so far challenging because they are transient and very unstable molecular assemblies. The second intermediates are short, flexible, rod-like structures defined as protofibrils[47,48]. Protofibrils are unbranched polymers that are 3-6 nanometer in diameter and up to 100 nanometers long. *In vitro*, they are found in equilibrium with oligomers and are the direct precursor of amyloid fibrils[48]. The evidence suggests that these intermediates, along with the monomeric protein and the fibrils, are present simultaneously and in a dynamic equilibrium[37].

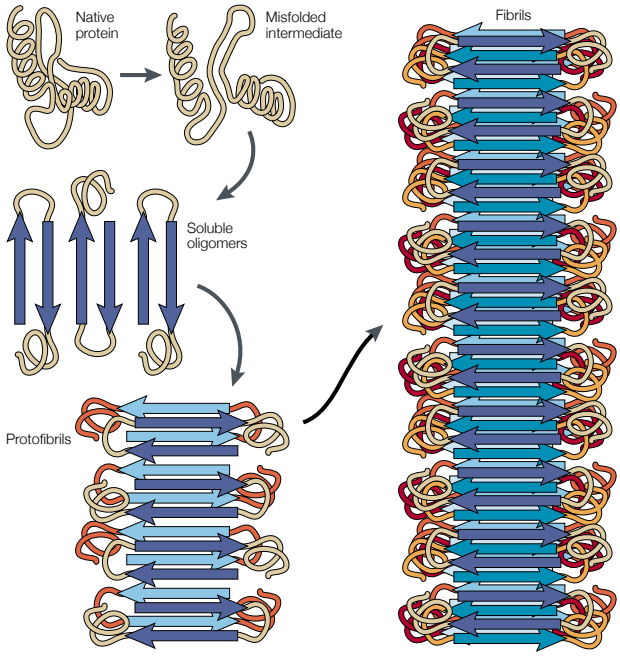

Figure 1.5 Mechanism of amyloid formation. A protein loses its monomeric native state by conversion into an oligomer which can grow further into amyloidogenic fibrils and ultimately into insoluble amyloid aggregates (*taken from ref. 31*)

1.2 Mechanisms of neuronal death in neurodegenerative diseases

Many neurodegenerative diseases share typical toxic biological features, such as synaptic alterations, inflammation mediated by activated microglia and selective neuronal loss, and, ultimately, neuronal death and neurodegeneration[49]. What differs, among diseases, is the most affected region of the brain and the localization of the aggregates (extracellular vs intracellular), which determine the clinical symptoms of each. For instance, neuronal death in AD occurs mainly in regions of the brain that are implicated in memory and abstract thinking, such as the hippocampus, amygdala, and association areas of the neocortex. PD is characterized by neuronal loss in the substantia nigra and depletion of dopaminergic neurons in the striatum. In HD, there is severe neuronal loss initially in the neostriatum and later in the cerebral cortex. The cell death process in ALS is relatively selective for lower motor neurons in the spinal cord and brainstem, and for upper motor neurons in the motor cortex. One striking feature of genetic prion diseases is their phenotype heterogeneity[50,51]. *PRNP* mutations are associated with different clinical and neuropathological phenotypes: Creutzfeld-Jakob disease (CJD), fatal familial insomnia (FFI), Gerstmann-Straüssler-Scheinker (GSS) syndrome and PrP cerebral amyloid angiopathy (PrP-CAA). CJD is a subacute spongiform encephalopathy, mostly involving the cerebral cortex, striatum and cerebellum, and recognized clinically by dementia and motor abnormalities[52]. FFI is characterized clinically by sleep alterations and autonomic dysfunctions, and neuropathologically by severe degeneration of the anterior ventral and mediodorsal nuclei of the thalamus[53,54]. GSS is a slowly progressive ataxia with

prion amyloidosis mainly in the cerebellum and basal ganglia[55]. PrP-CAA is a slowly progressive dementia with PrP amyloid deposits in blood vessels of the central nervous system.

Neuronal loss in neurodegenerative diseases can occur by programmed cell death or apoptosis[56]. Several hypotheses have been proposed to explain how protein misfolding and aggregation might be associated with neuronal apoptosis.

One of the most widely accepted theories of brain degeneration in neurodegenerative diseases proposes that misfolding and aggregation result in the gain of a neurotoxic function by the misfolded protein. This assumption is based on the direct induction of neuronal apoptosis by aggregates of several misfolded proteins *in vitro*[57]*.* Further support to this theory derives from experiments with transgenic animals in which the incorporation of the mutated gene that codes for the misfolded protein can trigger the neurodegeneration[58-62].

A crucial biological process involved in neurodegenerative diseases is autophagy, an intracellular degradation pathway that is responsible for the digestion and recycling of nutrients via autophagosomes[63]. These intracellular double-membrane structures engulf cytoplasmic proteins and organelles and deliver them to the lysosome for degradation, maintaining homeostasis within the cell[64]. Autophagy plays a key regulatory role of the levels of intracytoplasmic, aggregate-prone proteins that cause neurodegenerative diseases, including polyglutamine-expanded huntingtin (HD)[65], mutant α-synuclein (PD)[66], mutant TDP-43 (ALS)[67], and wild-type and mutant tau[68,69]. The clearance of such substrates is retarded when autophagy is compromised, and clearance is induced when autophagy is stimulated. In Alzheimer's disease, altered autophagy lead to lysosome

dysfunction and accumulation of autophagic vescicles in affected neurons[70,71].

Several mechanisms have been proposed for the neurotoxic activity of the aggregates derived by protein misfolding, and it's likely that different pathways act on the basis that aggregates accumulate inside or outside the cell. The extracellular aggregates could activate specific signal transduction pathways that lead to synaptic damage and, ultimately, to apoptosis, by interacting with specific cellular receptors[72]. For example, RAGE (receptor for advanced glycation end products), a multi-ligand immunoglobulin superfamily cell-surface molecule, binds amyloid-like fibrils comprising amyloid-β peptide (Aβ), PrP, amylin and amyloid-A, thereby inducing cellular stress and activation of NF-κB[73-76]. It has also been demonstrated that both toxic PrP aggregates and Aβ oligomers localize at lipid rafts, which are cell membrane domains enriched in cholesterol and sphingolipids[77-79]. This, in turn, triggers synapse damage by altering cell membranes, increasing cholesterol and activating cytoplasmic phospholipase A2[80,81], a key event in many neurodegenerative diseases[82,83].

Intracellular deposits could damage the cells by sequestering in the fibrillar aggregates essential factors for the cell life[84]. Components of the proteasome, chaperone proteins, cytoskeletal proteins and transcription factors have been found in huntingtin and α-synuclein aggregates[85,86].

Another proposed mechanism for Aβ neurotoxicity and prion protein is the disruption of the plasma membrane and its depolarization mediated by the formation of ionic channels, resulting in an alteration of ion homeostasis,

eventually leading to death cell[87]. Finally, protein aggregates could induce oxidative stress by producing free radical species, leading to protein and lipid oxidation, intracellular calcium increase and mitochondrial dysfunction[88,89].

2. Alzheimer's disease

Dementia syndrome is linked to a large number of underlying brain pathologies, including Alzheimer's disease (AD), which is the most common. About 50-75% of patients with dementia suffer from Alzheimer's disease and the number of patients could be tripled by 2050[90]. Currently, the total cost related to the medical and social care are rated to exceed globally 600 billion US dollars[91]. The increasing number of patients will challenge society on social, medical and economical levels. Presently, there is no cure or treatment to halt or reverse disease progress.

AD is a progressive neurodegenerative disease characterized by pathological neuronal cell death and corresponding loss of neuronal function and synaptic connections. Neuronal loss occurs gradually throughout different brain regions and eventually leads to severe shrinkage of the brain (Fig. 2.1). The first brain region affected is the hippocampus, important for the formation of new memory processes and recalling recent memories. Neurodegeneration then spreads to the cerebral cortex responsible for thought, attention, language and reasoning. In the last stages of the disease neurodegeneration extends to all the brain[92].

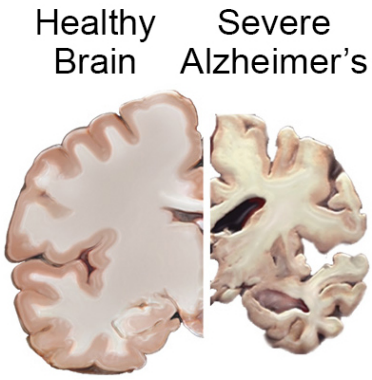

Figure 2.1 Cross sections of the brain show atrophy, or shrinking, of brain tissue caused by Alzheimer's disease (Image taken from www.nia.nih.gov/alzheimers).

The first definition of AD came in 1906, when a German physician, Dr Alois Alzheimer, first described an agglomeration of pathologic abnormalities in the autopsied brain of a woman who had been affected by memory problems, confusion and language dysfunction for some years. He reported the accumulation of extracellular deposits (amyloid plaques) and neurofibrillary tangles within the brain cells[93].

2.1 The amyloid cascade hypothesis

At the molecular level, the amyloid plaques in AD were found to be composed of extracellular fibrils of the amyloid β-proteins (Aβ) [94,95].

The purification and partial sequencing of the Aβ protein from meningovascular amyloid deposits in AD and Down's syndrome[96], a genetic disorder caused by the presence of a third chromosome 21, enabled the subsequent cloning of the gene encoding the β-amyloid precursor protein (APP), a large type 1-transmembrane glycoprotein located on the chromosome 21, consistent with the observation that middle aged patients affected by Down's syndrome developed amyloid plaques and neurofibrillar tangles typical of AD[97]. Neurofibrillary tangles (NFTs) are the second major hallmark of Alzheimer's disease in the brain. NFTs are intracellular aggregates, primarily composed of paired helical filaments (PHF)[98]. The major component of the NFTs is the protein tau, a microtubule associated protein (MAP)[99], which binds to microtubulin to provide structural stability to cells. Under pathological conditions, dissociation of the tau protein from microtubulin leads to tau hyperphosphorylation and aggregation into PHF[100,101].

Early-onset familial AD (EOFAD), which typically develops before the age of 65 years and accounts only for a small portion (<1%) of AD cases, is primarily caused by overproduction of Aβ owing to mutations in either the *APP* gene or genes encoding presenelin 1 (*PSEN1*) or presenilin 2 (*PSEN2)*[102-106], essential components of the γ-secretase complexes responsible for cleavage and release of Aβ (see below) (Table 2.1).

The majority of AD cases are sporadic and occur late in life (>65 years). Commonly are referred to as late-onset AD (LOAD). Although multiple genetic and environmental risk factors are involved in LOAD pathogenesis, overall impairment in Aβ clearance is probably a major contributor to disease development[107]. Genetically, the ε4 allele of the apolipoprotein E (*APOE*) is the strongest risk factor for LOAD[108-110]. In AD patients, the frequency of the ε4 allele is increased to ~40%[111].

Locus Name	Proportion of EOFAD	Gene Symbol	Chromosomal locus	Protein name
AD 3	20-70%	*PSEN1*	14q24.3	Presenilin 1
AD1	10-15%	*APP*	21q21	Amyloid ß
AD4	Rare	*PSEN2*	1q31-q42	Presenilin 2

Table 2.1 List of mutations causing early onset familial Alzheimer's disease (EOFAD)

Based on these findings Hardy and Selkoe proposed the "amyloid cascade hypothesis" suggesting that the processing of APP to generate Aβ is the key event in developing AD[112]. The subsequent aggregation of Aβ and the formation of senile plaques then triggers a cascade of events such as the formation of neurofibrillary tangles leading to neuronal death and dementia. In its current form, the hypothesis emphasizes the importance of soluble toxic oligomers: in particular, these species can start a slow but fatal cascade that can leads to synaptic alterations, astrocytic and microglial activation and tau aggregation, and progressive neuronal loss associated to neurotransmitter deficiencies[113] (Fig. 2.2).

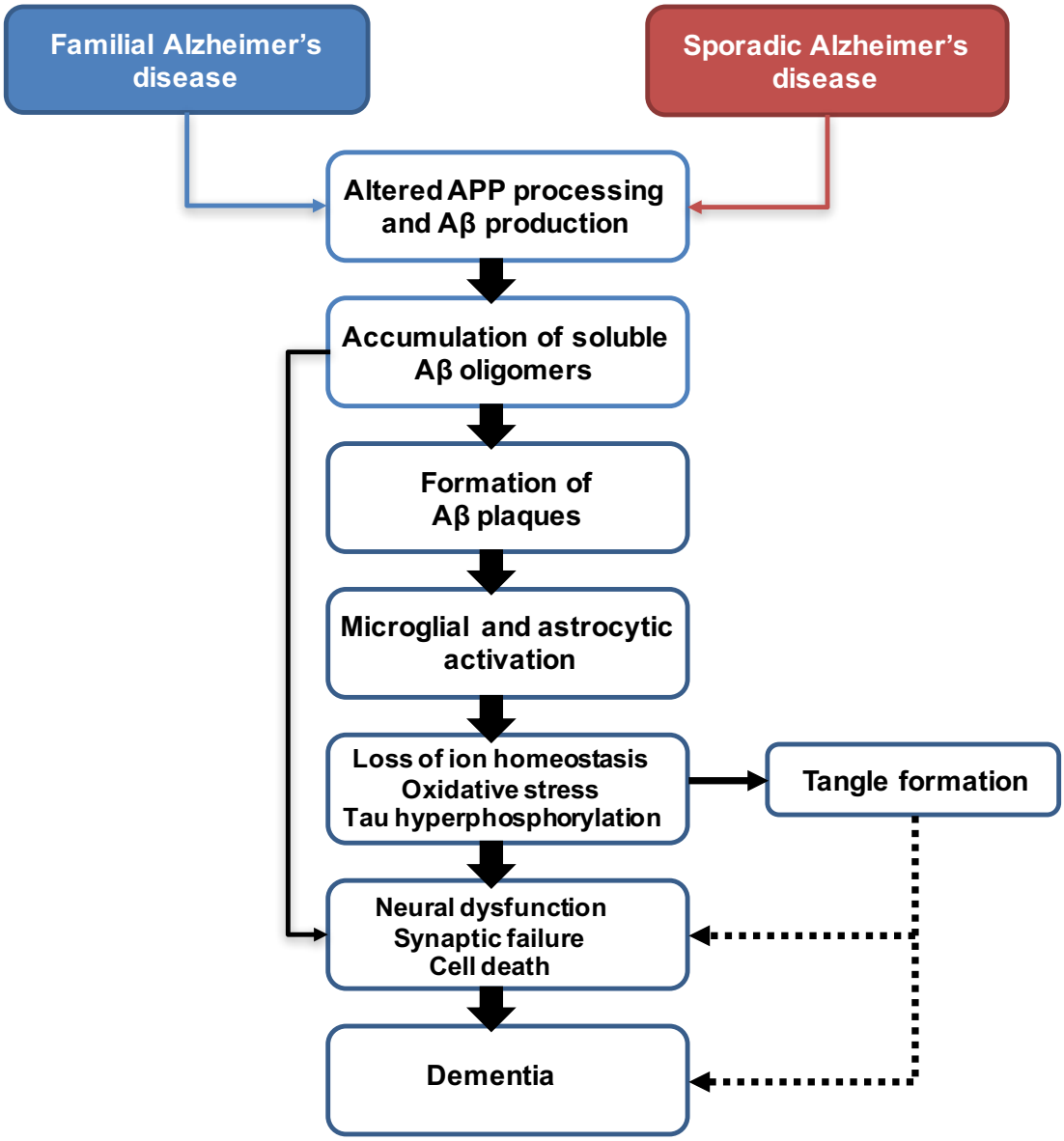

Figure 2.2 The sequence of major pathogenic events leading to AD proposed by the amyloid cascade hypothesis.

2.2 APP processing and generation of Aβ

The Aβ peptide is generated from APP by a finely regulated proteolytic cleavage. The proteolysis of APP can occur through two pathways[114] (Fig 2.3). Both pathways release an extracellular soluble fragment (APPs) and a second membrane-spanning C-terminal fragment (CTF)[115]. The non-amyloidogenic pathway is selected when APP is first cleaved by α-secretase, a member of the ADAM family of membrane-anchored metalloproteases, which generates a soluble ectodomain region (APPsα) and CTF83. This cleavage precludes the generation of Aβ as the α-secretase cleavage site is located within the Aβ sequence.

The amyloidogenic pathway is entered when APP is first cleaved by β-secretase instead of α-secretase. The β-secretase, also known as BACE (β-site APP cleaving enzyme), is a transmembrane aspartic protease[116] and it cleaves at the N-terminus of the Aβ sequence, releasing APPsβ and CTF99. The CTF83 and CTF99 fragments are subsequently cleaved by γ-secretase and generate the p3 and Aβ peptides, respectively, as well as an APP intracellular domain (AICD). The soluble secreted APPsβ is reported to have a neuroprotective function and it is important for neurogenesis[117]. In contrast, AICD impairs generation of new neurons[118], has a signalling function and is a transcription regulator[119]. The p3 peptide is generally accepted as non-amyloidogenic although it has been reported as highly hydrophobic, aggregating and has been found in amyloid plaques[120].

γ-secretase is a large proteolytic complex in which the catalytic core is composed by five essential subunits: presenelin-1 and -2 (PS-1 and PS-2), nicastrin, APH-1 and PEN-2[121]. The γ-secretase complex cleaves different sites inside the APP

transmembrane domain, generating various Aβ peptides of 38-43 amino acids[122]. Almost 90% of secreted Aβ is represented by Aβ1-40, while Aβ1-42 represents less than 10% of the total. It was shown that Aβ1-40 is the major component of cerebral vascular amyloid deposits, while Aβ1-42 is the main component of neuritic plaques[123,124]. In addition to these two predominant isoforms, several other C-terminal truncated Aβ isoforms have been discovered, including Aβ1-15/16 and Aβ1-37/38/39[125,126]. *In vitro* studies have identified a number of longer Aβ variants like Aβ1-43 and Aβ1-48 in cell lines. Longer Aβ isoforms have also been identified in transgenic mice models of AD[127-129].

Further heterogeneity of Aβ can be obtained at the N-terminus during proteolytic release. Instead of aspartate that is normally found in the first position of the peptide, these Aβ variants possess different N-termini[95,130-132]. *In vitro* experiments have showed that shortening of N-terminus enhances Aβ aggregation[133]. Finally, various post-translational modifications of Aβ have been described[134], such as pyroglutamylation[135,136], oxidation[134,137,138], isomerization[134,139]or racemization[140-142]. All these modifications have been found in AD patients, and could play a role in the progression of the disease[143].

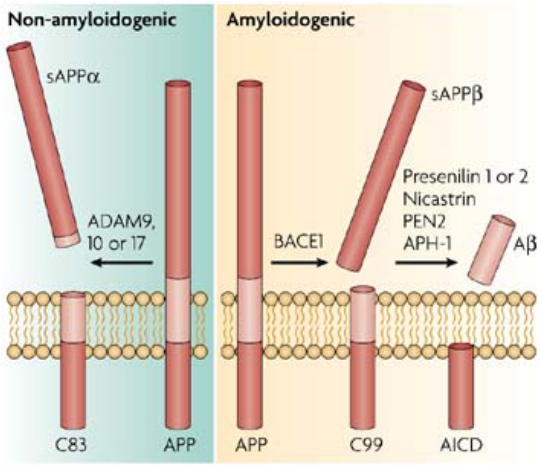

Figure 2.3 APP structure and metabolism. APP processing by secretase is divided into the non-amyloidogenic pathway (left) and the amyloidogenic pathway (right) (*taken from ref. 114*).

Almost all APP mutations causative of familial AD (FAD) are clustered at the β-secretase and γ-secretase, releasing the Aβ peptides into the luminal/extracellular compartments[144] (Fig. 2.4). The KM670/671NL Swedish APP mutation increases total Aβ production, as observed in Swedish APP transfected cells and skin fibroblasts from carriers of the mutation[145-148]. Other FAD mutations occur after the γ-secretase cleavage site and most of them enhance the production of the longer and more aggregating Aβ1-42 peptide[149-151]. This strongly supported a causative role of the longer Aβ1-42 peptide, which in animal models is essential for senile plaque formation[152]. Finally, mutations within Aβ increase the aggregation properties of Aβ peptides[153], and most of them are causative of cerebral amyloid angiopathy (CAA)[144]. At the molecular level, these mutations change the charge distribution and thereby likely affect the peptide structure, ultimately promoting fibril formation[154,155]. *In vitro* studies with the E22Q (E693Q) Dutch peptide showed

that it is more prone to oligomerize[156,157] and is more neurotoxic[158,159] than the wt peptide. Transgenic animal models expressing Dutch APP recapitulate the human pathology, with the amyloid deposition mainly located within the vasculature[160].

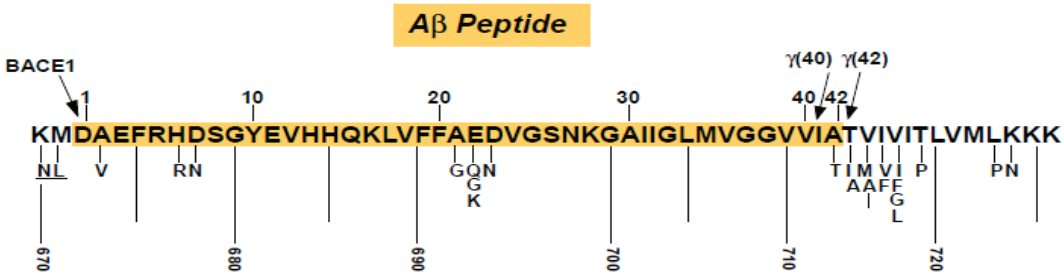

Figure 2.4 APP mutations. The APP transmembrane domain extends from the glycine-700 to the lysine-723. The Aβ42 peptide is highlighted in yellow. Depicted by arrows are the β-secretase (BACE1) cleavage site, the γ-secretase cleavage sites generating Aβ40 and Aβ42. Amino acid exchanges causative of either familial Alzheimer's disease (FAD) or cerebral amyloid angiopathy (CAA) are shown below the peptide sequence (*adapted from ref. 144*).

2.3 The role of Aβ oligomers in Alzheimer's disease

The central feature of the first version of the "amyloid cascade hypothesis" was that neuronal death was caused by the deposition of fibrillar Aβ into plaques.

However, the number and the density at different anatomical locations of Aβ plaques in the brains of the patients affected by AD does not correlate with the cognitive deficits observed[161,162]. Further indicating a disconnection between plaque pathology and memory impairment, several groups reported that cognitive deficits in transgenic mouse models of AD appeared before Aβ plaque deposition or detection of insoluble amyloid aggregates in their brains[163-165].

The apparent controversy on how Aβ toxicity correlated with cognitive decline and memory impairment in AD began to be resolved when it was demonstrated that Aβ spontaneously forms small, soluble oligomeric assemblies with neurotoxic properties, which were termed Aβ-derived diffusible ligands (ADDLs)[166]. In agreement with these findings, other studies confirmed that Aβ oligomers can alter various mechanisms associated with brain synaptic transmission, such as dendrite spine morphology and long term potentiation, which is believed to be essential for neuronal plasticity and learning phenomena[167,168]. It was also shown that the levels of several presynaptic proteins were reduced in the brains of AD patients and after treatment with Aβ oligomers[169,170].

Further studies have demonstrated that soluble Aβ oligomeric species can be extracted with saline buffers from the brain tissue of patients with AD and that their

presence correlated better with disease symptoms than the presence of amyloid plaques[171,172]. Aβ oligomers are increased in AD brains[173-180] and can be detected using oligomer-sensitive antibodies[175,181-183], but are not detected by conventional histopathological techniques, such as staining with thioflavin S or Congo Red. Different type of brain-derived toxic Aβ oligomers have been described in the literature, including dimers and trimers[178,184-187], or larger assemblies such as Aβ tetramers and dodecamers[188,189]. Overall, available studies generally support the existence of a mixture of soluble Aβ assemblies that induce synaptic failure, but it remained to be clarified whether this toxicity can be specifically associated with dimers, timers or larger species[190].

Experiments with synthetic Aβ peptides have demonstrated that Aβ oligomers may be metastable intermediates on the pathway to insoluble fibrils, but some types of oligomers could be “off-pathway” species that have different secondary structures and do not further aggregate to amyloid fibrils. Therefore, different *in vitro*-generated oligomers may have different toxicities[191-193]. However, it is not yet clear if these synthetic Aβ oligomers occur *in vivo* or which species are more relevant for the pathogenesis of AD.

Many experiments investigating the mechanisms of Aβ oligomers toxicity have been based on the assumption that oligomers are stable structures that interact specifically with neuron receptors. For example, several studies have described the interaction of Aβ oligomers with postsynaptic NMDA and AMPA receptors[194], with the nicotinic acetylcholine receptor[195], or with the insulin receptors[196]. Recently, the cellular prion protein was found to be a specific receptor for Aβ

oligomers[197], although the putative biological effects of this interaction have been questioned[198-204] (Fig. 2.5).

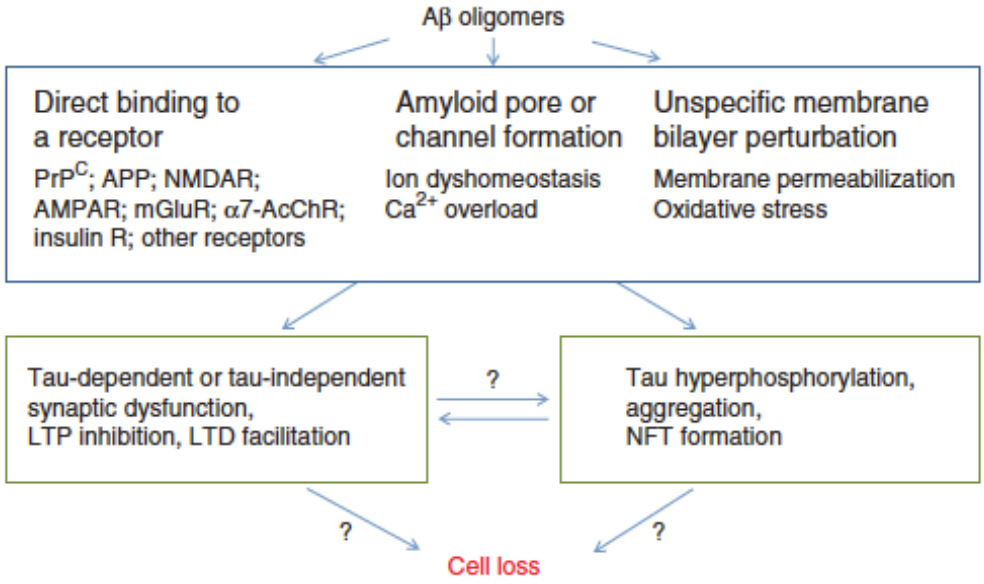

Figure 2.5 Possible mechanisms of action of Aβ oligomers leading to neuronal death according to the amyloid hypothesis (*adapted from ref. 190*).

These data clearly suggest that a unique mechanism cannot explain all the features of Aβ oligomer toxicity. Amphiphilicity, aggregation state, covalent modifications and the organization of hydrophobic residues within an oligomeric assembly can influence the toxic effects of such soluble aggregates. Recently, it has been suggested that the toxicity of oligomers is not due to their morphology or size, rather could be due to their specific conformation[205,206]. This conformation could lead to the exposure to the solvent of "toxic surfaces", e.g. hydrophobic stretches that are very prone to interact with different classes of molecules[206,207].

Accordingly, it has been suggested that Aβ oligomers might exert their toxic effects by binding to different membrane proteins, targeting membrane lipids, changing membrane dielectric properties and ion permeability[208,209] (Fig. 2.5).

3. Transgenic *C. elegans* as a model in Alzheimer research

The nematode C. *elegans* provides an excellent *in vivo* system to evaluate the molecular mechanisms involved in neurobiology and in particular in neurodegenerative disorders. The mechanisms underlying different processes like, for example, neuronal generation, synapse formation, neuronal degeneration or cell death have been well studied and characterized[210,211]. The distinct tissue and the cell types have been extensively characterized and behavioural assays that monitor their functionality are well described[212,213]. The transparency of these nematodes allows the generation of transgenic lines expressing fluorescently tagged aggregation-prone proteins that can be visualized in any tissue during development and throughout adulthood. With a relatively short lifespan of 2-3 weeks, it is feasible to perform experiments to assess the roles of chaperones and cytoprotective pathways on longevity.

The use of *C. elegans* also allowed research to discover new techniques, which were subsequently adapted and applied to other biological systems. For example, the whole genome of *C. elegans*, which contains 19000 genes, was the first to be completely sequenced and published in 1998[214]. At least 38% of the *C. elegans* protein-coding genes have predicted orthologs in the human genome[215], 60-80% of human genes have an ortholog in the *C. elegans* genome[216], and 40% of genes known to be associated with human diseases have clear orthologs in the *C. elegans* genome[217]. Another discovery that led to a novel technique with broad biological impact was gene silencing by RNA interference (RNAi)[218], which allows researchers to silence gene expression of any gene.

3.1 Biology of *C. elegans*

C. elegans is a small, free-living nematode of about 1,5 mm in length that can be found in soil environments feeding on different bacteria, including *Escherichia coli*. Adults are hermaphrodites composed of only 959 somatic cells, and the complete cell lineage, which is invariant between animals, has been established[219,220]. For example, the nervous system of the adult hermaphrodite is composed of 302 neurons[221]; the majority of them are localized in ganglia in the head, in the ventral cord and in the tail.

Worms are enclosed by a cuticle which is a tough but flexible exoskeleton-like structure to which the muscles are attached. Food is taken in through the mouth, compacted and pumped into the intestine by the pharynx. The intestinal lumen of the nematode runs through the entire length of the body from the pharynx to the anus[222,223] (Fig. 3.1).

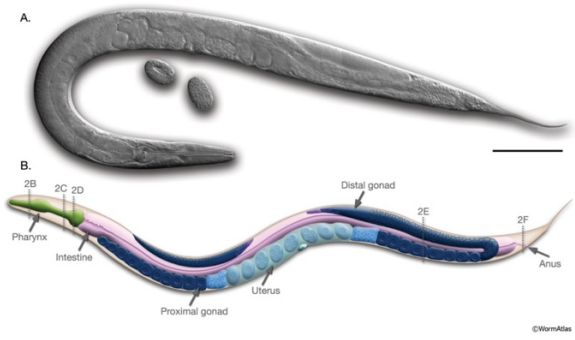

Figure 3.1 Anatomy of an adult hermaphrodite (Image taken from Worm Atlas, www.wormatlas.org). A. DIC (differential interference contrast) image of an adult hermaphrodite, Scale bar 0.1 mm. B. Schematic drawing of anatomical structures, left lateral side.

3.2 Life Cycle

The lifecycle of *C. elegans* starts with an embryonic stage, followed by four larval stages (named L1-4) and then adulthood[224]. This lifecycle is observed in favourable conditions, where food is not limited and the population is not at such a high density that overcrowding occurs. If conditions are not favourable, for example when bacteria (food source) are depleted and the animals are crowded, then the worm activate an alternative life cycle and enter into a new larval stage called dauer[225]. Worms can remain in the dauer state for up to 4 months, as they have high fat stores, and are highly resistant to stress. When conditions become favourable, dauers are able to re-enter the lifecycle at L4 stage (Fig. 3.2) and progress through adulthood as normal[224]. The developmental time from egg to adult takes about 2-3 days at 25°C. The lifespan of an adult worm is approximately 12-14 days at 25°C[226].

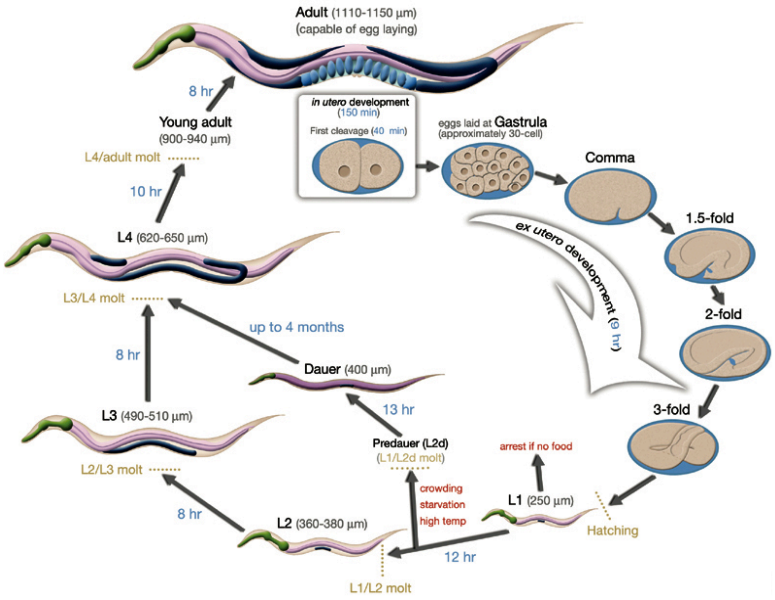

Figure 3.2 Life cycle of *C. elegans* at 22°C (Image taken from Worm Atlas, www.wormatlas.org). Life cycle from egg through four larval stages (L1-L4) to adulthood.

3.3 *C. elegans* as a genetic model organism

C. elegans have two sexes determined by the presence or absence of a second X chromosome. Males have only one copy of the X chromosome (XO), whereas hermaphrodites possess two copies (XX)[227]. Hermaphrodites can either self-fertilize or mate with males, but cannot mate with other hermaphrodites. The frequency of males in a colony is usually very low, approximately 0.1-0.2% of the progeny. However, if hermaphrodites mate with males, then progeny will be 50:50 male: hermaphrodite, as half of the progeny will not receive a copy of the X chromosome from sperm. Male animals are generally smaller than hermaphrodites, but they can be readily be distinguished by sensory rays on their tail[227] (Fig. 3.3).

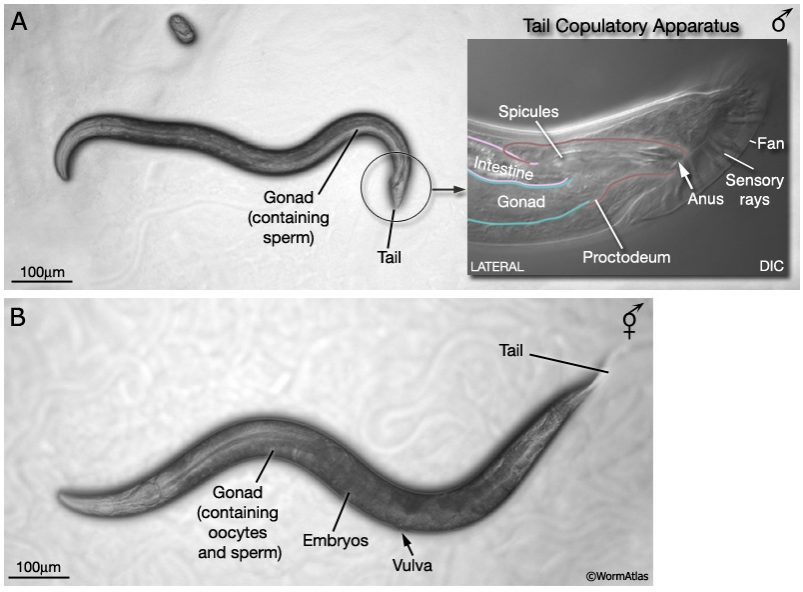

Figure 3.3 Light microscopy images showing male and hermaphrodite anatomy. A) male. Inset shows a magnified view of the tail. B) hermaphrodite (Image taken from Worm Atlas)

Self-fertilizing hermaphrodites provide several advantages for genetic analysis. First, self- fertilization simplifies maintaining stocks because a single animal can give rise to an entire population. Second, strains that are mutagenized are essentially isogenic because populations of hermaphrodites tend to lose heterozygosity. Third, self-fertilization follows the standard Mendelian rules of segregation, so a parent that is heterozygous for a recessive trait will produce the standard 1:2:1 pattern of segregation, such that 25% of the progeny will be homozygous for the mutant allele and display the autosomal recessive trait.

The traditional use of genetics in *C. elegans* (often referred to as “forward genetics”) begins with a screen or selection to find mutants with a particular phenotype followed by inference of the wild-type role of the gene from the nature of the mutant phenotype[228]. A variety of mutagens have been used[229], including ethyl methylsulfonate (EMS), an alkylating reagent that causes principally GC-to-AT transition mutations and small deletions[227].

Once mutant strains have been obtained and give mutant individuals in the next generation, they can be mapped using classical genetic tools[227]. Originally, mapping involved linkage crosses to identify the chromosome containing the mutation followed by multiple three-factor crosses to refine its map position.

Today, however, this process is much more rapid due to advances in whole-genome sequencing[230-232]. Finally, recent advances in efficient genome-editing methods (TALEN and CRISPR/Cas9) in *C. elegans* now allow investigators to create targeted mutations in nearly any location in the genome in any genetic background[233,234].

3.4 The IIS pathway in *C. elegans* links ageing to toxic protein aggregation

A hallmark of many neurodegenerative diseases is the age-associated onset of phenotypes due to (amyloidogenic) protein aggregation and toxicity. These characteristics can be investigated in *C. elegans* models of protein misfolding; further, it has been demonstrated that genes that regulate longevity suppress misfolding, in part by enhancing chaperone levels[235,236]. *C. elegans* has been an invaluable model organism for the discovery of pathways that modulate lifespan, including the insulin/insulin-like growth factor-1 signalling (IIS) pathways[226,237,238].

Under normal conditions, the nematode IIS cascade (Fig. 3.4), that is nearly identical to that in humans[239], is initiated when an as-yet-undefined ligand binds to DAF-2, the worm insulin/IGF receptor[226,237]. Following such binding, DAF-2 can recruit IST-1 and AGE-1, a phosphatidylinositol 3-kinase that mediates the production of phosphatidylinositol-3,4,5-triphosphate. In turn, this activates members of the AKT family.

The IIS pathway has an internal negative regulator: the phosphatase DAF-18 (a PTEN orthologue), which act in opposition to AGE-1, reducing its activity[240].

Activated AKT phosphorylates the downstream protein DAF-16, which is the exclusive *C. elegans* FOXO forkhead transcription factor. Phosphorylated DAF-16 is prevented from entering the nucleus and thus cannot regulate the expression of its target genes, such as the small heat-shock protein (small HSPs) chaperones. Therefore, the IIS pathway negatively regulates the activity of DAF-16 by modifying its intracellular localization. Another key transcription factor that is

required for the worm lifespan extension that is facilitated by reduced IIS is heat-shock factor 1 (HSF-1), a highly conserved leucine-zipper-containing transcription factors that, once activated, enters the nucleus and regulates the expression of its target genes[241].

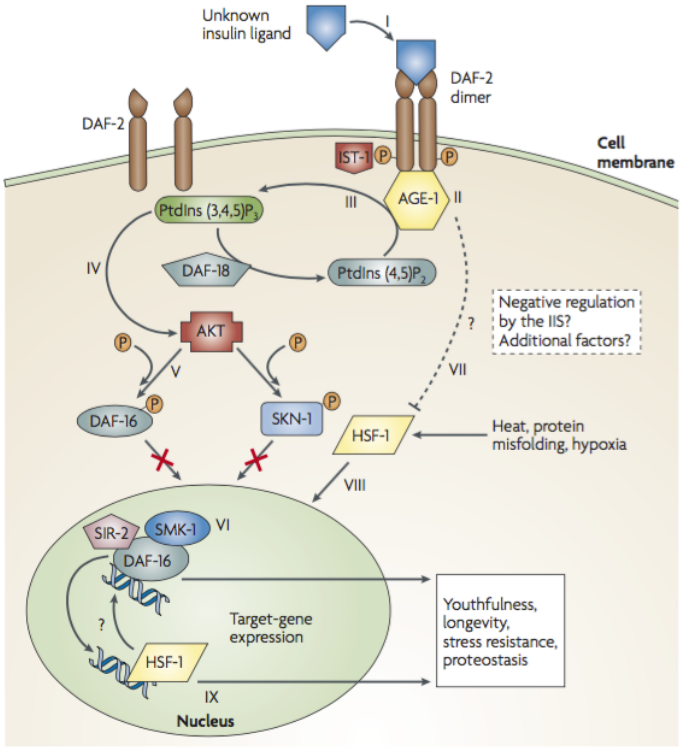

Figure 3.4 The IIS pathway in *C. elegans* (*taken from ref. 238*)

Several studies performed in *C. elegans* proteotoxicity models indicate that the IIS pathway directly links aging to the onset of toxic protein aggregation. Examples of these studies come from the use of transgenic nematodes expressing fluorescently tagged PolyQ repeat in body-wall muscle cells[236]. In young worms, at least 40 glutamine repeats were necessary for aggregation. However, the threshold number of repeats needed for aggregation decreased as the worms

aged. Moreover, a decrease in the expression of AGE-1 protected worm embryos from polyQ82 aggregates and these protective effects were dependent on DAF-16. Thus, these studies indicate that a decrease in the activity of the IIS pathway can reduce the toxicity associated with aggregated proteins, although the mechanisms of this protection are still obscure. Even in worms models of AD, that expresses human Aβ1-42 in the body-wall, it has been demonstrated that a reduction of the IIS pathways is protective[235]. Using different techniques, it has been also reported that the amount of Aβ aggregates with high molecular mass does not correlate with toxicity. In fact, a reduction of IIS resulted in reduced toxicity but caused an increase in the levels of high-molecular-mass Aβ aggregates. Conversely, inhibition of DAF-16 reduced the amount of high-molecular-mass Aβ aggregates but increased the toxicity[235]. Furthermore, RNAi versus *hsf-1* mRNA drastically elevated both toxicity and the amounts of high-molecular-mass of Aβ assemblies[235]. These findings suggest that the IIS cascade controls at least two anti-proteotoxic activities: disaggregation mediated by HSF-1 and protective aggregation that is regulated by DAF-16 (Fig. 3.5).

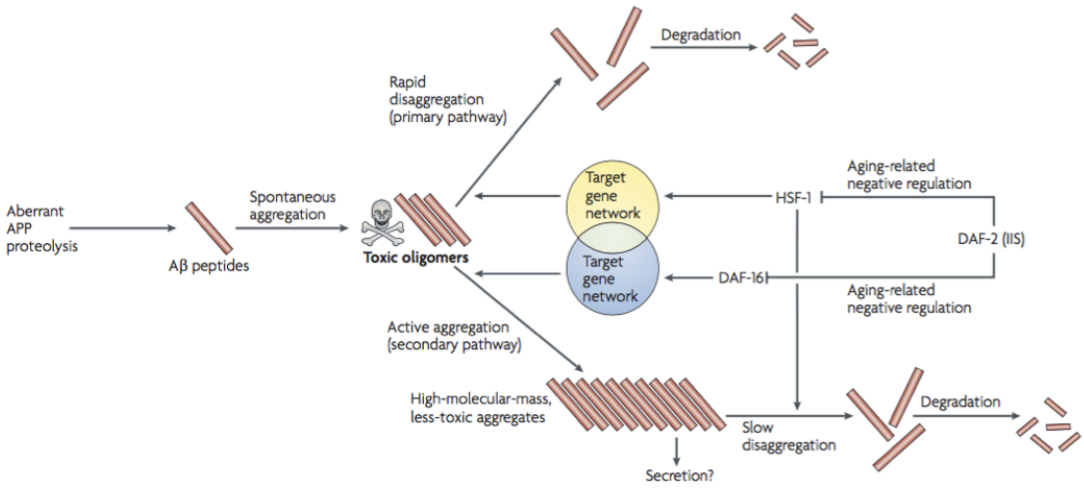

Figure 3.5. Link between aging and protein aggregation in *C. elegans* (*adapted from ref. 238*).

Different studies have been successively done to identify DAF-16- and HSF-1-regulated genes. Several classes of genes were identified, however the most consistently discovered subset was the Heat Shock Protein (HSP) family, in particular the small HSPs, such as the HSP-16 family[242,243]. The role of HSPs in assisting correct protein folding and in mediating the clearance of misfolded and aggregated proteins[244] supports that defects in protein homeostasis are key players in the ageing process.

3.5 *C. elegans* models for Alzheimer's disease

In the first attempts to develop a mutant strain by targeting endogenous APP gene, it was found that the *C. elegans* genome includes genes that encode proteins related to human APP (*apl-1*). Analogously to human APP, the invertebrate APP-family members are composed of single-pass transmembrane proteins with a large extracellular domain and a short intracellular domain, which can be cleaved to release intracellular and extracellular proteolytic fragments. However, APP-like genes in *C. elegans* do not possess the region encoding the neurotoxic Aβ. A transgenic *C. elegans* model was therefore developed which that can express human Aβ peptide intracellularly in the body wall muscle with a transgene-induced paralysis phenotype[245]. Although the *C. elegans* model obviously lacks the neuronal cognitive complexity of mammals, it turns out to be a valid model to replicate cellular processes that may underlie AD.

The first transgenic *C. elegans* model of AD (named CL2006), constitutively expressed Aβ1-42. These transgenic animals showed a progressive, irreversible paralysis[245]. Staining these transgenic worms with a human Aβ specific antibody revealed an accumulation of Aβ deposits, which reacted with Congo Red, thioflavin S and X-34, all markers of of Aβ deposits[246,247]. Ultrastructural examination of the Aβ deposits, however, showed that the aggregates were located in the cytoplasm of the muscle cells[248] rather than as extracellular deposits or plaques as seen in AD brains[249]. This intracellular localization was not expected given that the human Aβ1-42 construct was made with an artificial signal

sequence that should have led to the extracellular release of Aβ1-42. The artificial signal sequence is functional, although cleavage occurs after the signal sequence so that the Aβ sequence corresponds to amino acids 3-42 rather than 1-42[250]. Collectively, these results demonstrated that after production, Aβ is targeted either by the endoplasmic reticulum (ER) quality control system and retrotranslocated for degradation[245] and/or sequestered into intracellular inclusions by autophagic vescicles[251].

In the CL2006 strain Aβ aggregates co-immunoprecipitated with some chaperone proteins[252]. From early studies it was shown that increased expression of HSP-70 class and αB-crystallin related proteins might have effects on the formation of plaques in AD brain. In the *C. elegans* model, one of these chaperone proteins is HSP-16, which was closely colocalized with intracellular Aβ. HSP-16 was found to colocalize with anti-Aβ antibody 4G8 immunoreactive deposits, but not with the Aβ aggregates stained by the amyloid-specific dye X-34. These findings may suggest a possible interaction between HSP-16 and prefibrillar Aβ oligomers. Intracellular Aβ seems play a crucial role in AD pathogenesis[253] and some Aβ transgenic mouse models that display AD behavioural phenotypes also show intracellular Aβ accumulation rather than extracellular plaque formation[167,254]. In another transgenic *C. elegans* model of AD, CL4176, the toxic phenotype was suggested to be induced by the specific production of Aβ oligomers, as detected by immunogold staining with A11 antibody and by western blot analysis[255,256]. Although Aβ expression is limited to the muscle cells, this specific strain allows the researchers to establish a relationship between Aβ oligomers expression and their toxicity.

To investigate possible mechanisms of Aβ oligomer toxicity in transgenic *C. elegans*, Link et al. employed DNA microarray technique to reveal global gene expression changes in the CL4176 strain[257]. Among the top induced genes, they found that the *hsp-16* gene was up-regulated, corresponding with their prior observation that a GFP reporter transgene derived by the *hsp-16-2* promoter could be induced by constitutive Aβ expression. To verify the experimental results, quantitative RT-PCR experiments were performed to measure the expression of αB-crystallin (CRYAB), which is homologous to the HSP-16 gene, in post mortem AD brain. RNA of this gene increased considerably in parts of the superior frontal gyrus and the cerebellum of AD patients compared with the controls[257].

In a more recent set of experiments, alterations in gene expression induced by human Aβ peptide in *C. elegans* CL4176 strain were compared to those caused by a non-disease associated, aggregation-prone protein (GFP:degron) to identify Aβ-specific effects[258]. Among identified genes, many were involved in aging, proteasome and mitochondrial function.

Recently, new transgenic *C. elegans* models of AD have been developed, which express either Aβ1-40 or Aβ1-42 at the neuronal level[259,260]. In these models the intraneuronal expression of Aβ lead to postsynaptic deficits involving alterations of acetylcholine receptors, as indicated by the resistance of the worms to paralysis induced by aldicarb or levamisole, which are cholinergic agonists[259]. Notably, the expression of Aβ1-40 carrying the mutation A2V, which causes early-onset dementia in humans in the homozygous state[261], resulted in the formation of

oligomers. Nematodes expressing the mutant peptide had a shorter lifespan than WT, and a worse impairment of locomotor activity and pharyngeal pumping[259].

4. Genetic screens in transgenic *C. elegans* models of protein misfolding diseases

Sydney Brenner first introduced the nematode *C. elegans* as a genetic model organism in 1974 and since then this model has been widely used in different research fields, from developmental biology to aging and neuroscience[227]. Genetic screens are extensively used in *C. elegans* to discover gene function. Such screens can be easily applied to discover which gene mutations are responsible for a specific phenotype of interest (forward genetics) or, the gene function can be altered to assess what is the consequence in terms of development, behaviour or alterations in specific biological processes (reverse genetics). The two most employed genetic screens are ethyl methane sulfate (EMS) screens[262] and (genome-wide) RNAi screens[263]. The characteristics of both type of screens are summarized in Table 4.1

EMS mutagenesis	RNA interference
Inactivation or alteration of gene function	Reduction or depletion of gene function
Requires identification of gene mutation	Candidate gene is known
Permanent mutation	Possible to select developmental stage for depletion. No effects on embryos in the first generation
Can select for non-essential genes	Can identify roles of essential genes in a post-developmental process Limited penetrance to neurons Limited efficiency if the protein that is encoded by the targeted gene is very stable

Table 4.1 Features of EMS mutagenesis versus RNA interference (*adapted from ref. 263*).

4.1 EMS mutagenesis

The most common method to mutate the genome of *C. elegans* is the treatment with EMS, which induces mutations in the sperm and oocytes of hermaphrodites. EMS has relatively low toxicity and it has a good efficiency[264]. The fact that *C. elegans* mainly exist as hermaphrodite allows easy maintenance of a mutation as a homozygous worm will pass to all the progeny through self-fertilization.

Mutations can be identified using a simple F2 screen first described by Brenner in 1974[227]. Thousands of copies of any particular gene can be analyzed in a typical EMS screen. The frequency of a null mutation at any particular locus of the genome is one for every 2000 copies by using standard concentrations (50 mM) of the mutagen[262]. This means that one can expect to identify approximately 6 mutations per particular gene in a typical experiment of 12000 genomes. The mutagenized worms are placed on Petri dishes and grown for two generations to produce homozygous mutants (Fig. 4.1). Worms from the F2 generation showing a specific phenotype of interest are further singled to new plates to determine whether the phenotype is transmitted to the next generation.

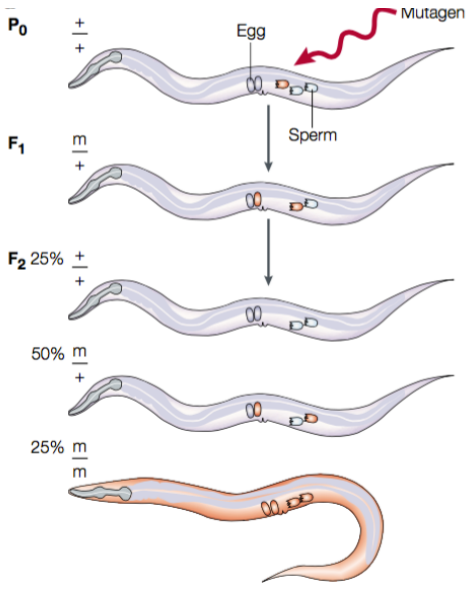

Figure 4.1 EMS mutagenesis scheme and F2 screen in *C. elegans* (*adapted from ref. 228*).

Once a worm with a specific phenotype is isolated, the responsible mutation has to be identified. By using single nucleotide polymorphisms (SNPs) of the Hawaiian wild type strain in comparison of the Bristol strain (natural variation wild type) it is possible to map a mutation first to a certain chromosome[265] and then to a specific region on that chromosome. When a mutation is mapped to a gene region, sequencing or the specific knockdown of every single gene in that area by RNAi can be used to identify the mutated gene. The development of new sequencing methods like deep sequencing or next generation sequencing facilitates the identification of mutations and can save laborious fine mapping[230-232].

In the first EMS screen ever performed, 619 mutants were identified with visible phenotype especially from the uncoordinated class[227]. This group of genes impair wild type movements when mutated. Many of these mutants have revealed

important information about molecules and mechanisms involved in human disease[266,267].

In addition to mutations in the uncoordinated class, Brenner also identified mutants with aberrant appearance like animals with small bodies, blistered cuticles, rolling locomotion, long bodies or bent heads[227].

EMS screens are often used to identify different mutations with the same phenotype to further investigate if those genes function in the same process. Using this approach, Sulston and Horvitz searched for mutants that presented defects in the differentiation of a vulva from epidermal cells[268]. Molecular analysis revealed that animals that lack a vulva had mutations in two signalling pathways: the epidermal growth factor (EGF)/RAS pathway and the Notch signalling pathway[269,270]. These studies in *C. elegans* have increased the understanding of these molecular pathways involved in oncogenesis in humans.

4.2 RNA interference

RNA interference was first discovered and investigated in *C. elegans* and published in 1998[218]. The discovery of dsRNA-mediated gene silencing has revolutionized genetic studies in *C. elegans*, as well as in other model organisms. Similar to EMS screens, RNAi screens can be used to identify genes that, when depleted, result in a certain phenotype or enhance or suppress a mutant phenotype.

RNAi in *C. elegans* is systemic, which, to date, is not the case for any other animal models. Therefore, it is sufficient to introduce dsRNA into one specific tissue to get RNA silencing also in distant cells because of an amplification process called transitive RNAi[271]. This systemic effect is advantageous for large-scale-genome-wide RNAi screens in *C. elegans*. Different methods have been developed to silence gene expression in *C. elegans*. The dsRNA can be delivered into the worm by i) injection into any region[218], ii) feeding with dsRNA-producing bacteria[272], iii) soaking in dsRNA[273] or iv) *in vivo* production of dsRNA from transgenes under the control of specific promotors[274].

The possibility to feed nematodes with dsRNA-producing bacteria enables to perform high-throughput RNAi screens in *C. elegans*[275] (Fig. 4.2). For efficient induction of RNA interference, the choice of the dsRNA-coding region is essential. In *C. elegans*, long dsRNA fragments (more than 100 bp) trigger gene silencing via RNAi. For most genes, dsRNA is about 200-1000 nucleotides or even longer and covers exon-regions of the targeted gene. The fragment should only target one gene. Once the coding region is chosen it can be cloned into a specific vector

encoding the production of the specific dsRNA. The L4440 vector contains two bacteriophage T7 RNA polymerase promotors flanking the multiple cloning site in which the cDNA of a specific gene has been inserted. The construct can be transformed into *E. coli* strain HT115. This strain is deficient for the bacterial RNA polymerase III and its production of bacteriophage T7 polymerase from the construct can be induced by the addition of isopropyl β-D-1-thiogalactopyranoside (IPTG). The bacteria are then synthesizing two complementary RNA strands that form a duplex RNA which mediates RNAi[218].

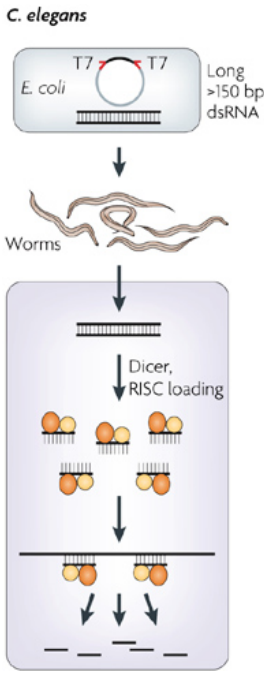

Figure 4.2 RNA interference (RNAi) screening in *C. elegans*. Age-synchronized animals are transferred to microtiter plates containing different clones of HT115 E. coli bacteria. Every clone produces a specific dsRNA which is taken up by the nematodes and induces a knockdown of the corresponding gene (*adapted from ref. 263*).

RNAi libraries are commercially available which includes one library of bacteria clones containing cDNAs of 17,575 genes which represents about 87% of the *C. elegans* genome[276]. Positive scored clones subsequently can be sequenced to confirm that they target the predicted gene. The target of RNAi is known. This is the major difference to EMS mutagenesis that cannot be directed to specific genes. However, RNAi can silence only gene activity and that is not a full knockout of the gene. It is estimated that about 10-30% of candidates are scored as false negatives as the RNAi is not efficient enough to result in an obvious phenotype. Moreover, RNA interference acts at the mRNA level, only influencing the expression of a protein. That means that already generated, stable-proteins and their activities, are not affected by RNAi.

One advantage of *C. elegans* is that it is amenable to generate “humanized” models of human neurodegenerative diseases. Neuropathological hallmarks found in the human brain can be successfully recapitulated in the nematode, such as protein aggregation[277]. Several nematode models have been generated to recapitulate molecular aspects of diseases, including Huntington’s disease, Parkinson’s disease, or Alzheimer’s disease. Although they do not exhibit the clinical aspects of the neurological disease, they provide the means to understand the molecular mechanisms in these pathologies. Genetic screens performed in some of these models represent quick, unbiased methods that have enabled insights into the underlying mechanisms of neurodegeneration[278] (see below). Indeed, many of the disease modifiers discovered so far in *C. elegans* were found to be reproducible in human-cell based models and other animal models such as

mice, confirming the validity of using nematodes to study complex human diseases.

4.3 Genetic screens in *C. elegans* models for polyglutamine diseases

Polyglutamine diseases comprise a subset of neurodegenerative disorders that include Huntington's disease, spinocerebellar ataxias, Machado-Joseph disease and spinobulbar muscular atrophy[279]. The common characteristic of polyglutamine diseases is an abnormal expansion of CAG triplets (which encode glutamine) in the coding region of the disease-related gene. Although the length of the CAG repeat may vary from individual to individual, the threshold to develop disease is around 40 CAG repeats, which cause a polyglutamine expansion in the protein, increasing the propension to aggregate. The larger the CAG repeat the earlier onset will occur and the more severe the disease phenotype will be[280].

Similarly to what occurs in humans, the length of the CAG repeats also determines the aggregation phenotype in *C. elegans*. At least three models have been generated to induce polyglutamine-associated toxicity in neurons by expressing expanded polyglutamine stretches in sensory neurons, touch receptors neurons or the entire nervous system of *C. elegans*[281-283]. Polyglutamine aggregation has been modelled also in the body-wall muscle cells of *C. elegans*[236]. In this model, expanded polyglutamine stretches are fused to a yellow fluorescent protein (YFP) under the *unc-54* promotor, which is specific to the body-wall muscle. The aggregation and toxicity phenotype is dependent of the length of polyglutamine. As the animal ages, the accumulation of protein aggregates increases, which is

associated with toxicity[236]. This model has been widely used to perform genetic screens to discover enhancers or suppressors of polyglutamine-induced proteotoxicity. Two genome-wide RNAi screens revealed modifiers genes and classified them according to their biological function[284,285]. In the first screen, Q35 nematodes were fed with dsRNA-producing bacteria and scored for genes whose downregulation accelerated polyglutamine aggregation[284]. The major functional classes for these protective genes included RNA synthesis and processing, protein synthesis, folding, transport and degradation and component of the proteasome. In the second screen, the authors selected genes whose downregulation suppresses polyglutamine-induced aggregation[285]. In this study a new subset of aggregation-promoting genes was described including other biological functions, for example cell cycle, cell structure, energy and metabolism.

Forward genetics has also been employed to identify modifiers of proteotoxicity. This screen consisted in treating Q40-expressing worms with EMS. The screen revealed MOAG-4 (modifier of aggregation) as a general aggregation-promoting factor in polyglutamine, Parkinson's and Alzheimer's disease models[277]. Inactivating MOAG-4 rescued worms from the aggregation and toxicity induced by polyglutamine; moreover, this effect was functionally conserved in the human orthologs SERF1A and SERF2. New evidence has shown that SERF1A is a specific aggregation promoting factor, since it was able to interact with different amyloidogenic proteins, including alpha-synuclein, prion protein, amyloid-β and huntingtin, but not to non-amyloidogenic proteins[286].

Genetic screens have also been used to find regulators of proteotoxicity in the *C. elegans* neurons. An RNAi screen performed in a *C. elegans* model expressing 128 polyQ stretches in the touch receptor neurons resulted in 662 genes that

either enhanced or suppressed neuron degeneration, as measured by loss of touch response[287]. Comparison of these disease-modifier genes to gene expression data in two mouse models of HD showed that there was an overlap of 49 genes that were dysregulated in the striatum of either models, emphasizing the power of using *C. elegans* to find novel regulators of proteotoxicity relevant in human diseases[287].

4.4 Genetic screens in *C. elegans* models for Parkinson's disease

Parkinson's disease (PD) is the second most common neurodegenerative (after AD) that affects 1% of the population over the age of 50. Clinically, it is characterized by resting tremors, rigidity, bradykinesia and postural instability[288,289]. Pathologically, the disease is characterised by the accumulation of aggregates of alpha-synuclein in susceptible neurons in the form of Lewy Bodies[290].

Alpha-synuclein is a small (140 amino acids) soluble, monomeric protein that is predominantly expressed in the brain and is enriched in presynaptic terminals[291]. Although the precise function of this protein remains unclear, it is thought to be involved in the regulation of dopamine neurotransmission, vesicular trafficking and modulation of synaptic function and plasticity[292,293]. Three different mutations in the alpha-synuclein gene have been associated with an autosomal-dominant PD. Genetic screens performed with this model have discovered an important relationship between alpha-synuclein and vesicle transport. The *C. elegans* model of PD expresses the human alpha-synuclein fused to YFP in the body-wall muscle[294].

A genome-wide RNAi screen with this model showed 80 protective genes that, when downregulated, caused premature alpha-synuclein inclusion formation[294]. Further studies have discovered *tdo-2*, a gene involved in tryptophan degradation, as a general regulator of protein homeostasis during aging[295]. Moreover, 49 of the original 80 modifier genes had human homologs, which were enriched for genes related to vesicular trafficking functions.

A subset of candidate genes found in the initial screen was then further analyzed in another *C. elegans* model, expressing alpha-synuclein in the dopaminergic neurons. This study revealed five candidate genes that were able to protect form alpha-synuclein-induced dopaminergic neurodegeneration. Again, the most representative class of genes described was associated with vesicular trafficking. Also, a serine/threonine kinase involved in axonal elongation, UNC-51, was found to be homologous to the previously associated risk factor ULK-2, as revealed by a genome-wide association study (GWAS) performed in PD patients[296].

Genome-wide RNAi screens in a *C. elegans* model expressing pan-neuronal alpha-synuclein revealed two genes, *apa-2* and *aps-2*, that, when downregulated, increase alpha-synuclein toxicity[297]. These two genes encode for subunits of the AP-2 adaptor complex, which mediates the internalization of cargo into the cell from the extracellular pace via clathrin-mediated endocytosis[298].

4.5 Genetic screens in *C. elegans* models for Alzheimer's disease

To date, genetic screens in *C. elegans* models for AD have been scarce and, at the start of this thesis, there had been no genetic screen performed in any of the models expressing amyloid-β. There is only one report on genome-wide RNAi done in a tau-expressing model[299]. In that model, 60 modifier genes were discovered to belong to several functional classes including kinases, chaperons, proteases and phosphatases. Of these, 38 had homologs in humans, and, more importantly, 6 had already been associated with disease either in humans or other animal models. One of these modifiers was the nicotinic acetylcholine receptor, alpha-7 (nAchR), a ligand-gated ion channel expressed in the human brain and known to contribute to tau phosphorylation[300].

Overall, genome wide screening in *C. elegans* models of neurodegenerative diseases have revealed that a complex network of processes is involved in maintaining protein homeostasis. These modifiers include proteins with a confirmed role in modifying the toxicity of aggregation-prone proteins in human cell models, including chaperons, and proteins involved in proteasomal degradation and autophagy.

Recent studies, however, have demonstrated that other functionally distinct proteins may have a role in the toxicity mediated by protein misfolding and aggregation, even if they act independently of the well-known molecular pathways related to protein homeostasis mechanisms.

These findings suggest that other proteins, not yet identified, can be important in toxicity mechanisms mediated by misfolded proteins and may represent new pharmacological targets.

AIMS

This project aimed to take advantage of *C. elegans* to identify genes involved in the toxicity of Aβ oligomers, by performing a genome wide screening in a transgenic *C. elegans* model of AD. So far, no genome wide screening have been employed in transgenic *C. elegans* expressing toxic Aβ oligomers. However, a systematic search for mediators of Aβ oligomers toxicity, including proteins involved in their formation and those involved in their direct, down-hill, toxic effects on cells, could help elucidate the mechanisms of action of these transient species, in order to develop new and effective therapeutic strategies.

For these studies, we have employed the CL4176 *C. elegans* strain, engineered to express human Aβ peptide in muscle cells upon induction (raise of temperature) [245,257]. These nematodes, when the temperature is raised, become rapidly paralyzed and it was shown that paralysis is strictly associated to the appearance of Aβ oligomers[255]. Thus, the CL4176 strain represents a very convenient tool where the formation and/or the action of Aβ oligomers can be detected by a clear read-out of toxicity.

This allowed us to perform genome wide screenings for genes which, upon mutation, suppress paralysis, therefore identifying the proteins involved in the toxic effects of Aβ oligomers, which could be either those involved in the formation of oligomers or those mediating oligomer toxicity.

MATERIALS AND METHODS

5.1 *C. elegans* studies

The transgenic CL4176 strain (*smg-1(cc546ts)*I; *dvIs27*[pAF29 (*myo-3*/Aβ1-42/letUTR) + pRF4 (*rol-6*(*su1006*)]) expressing human Aβ1-42 in the body-wall muscle[257] and the control CL802 strain (*smg-1(cc546ts)*I; *rol-6*(*su1006*)) were obtained from the Caenorhabditis Genetic Center (CGC, USA) and propagated on solid Nematode Growth Medium (NGM) seeded with OP50 *E. coli* (CGC, USA) for food[213]. Transgenic CL4176 worms contain the expression vector pPD118.60, which has the *myo-3* body-wall specific myosin promoter and an abnormally long 3'untranslated region, which makes the transgenes expression dependent on *smg-1* function (mRNA surveillance system). The *smg-1* in *C. elegans* becomes inactive at the non-permissive temperature of 24°C, which allows the translation of the stabilized transgenes mRNA for human Aβ1-42. Age-synchronized worms were obtained by transferring nematodes to fresh NGM plates to reach maturity at three days of age and lay eggs overnight. For the paralysis assay, synchronized eggs were obtained by bleach treatment and incubated in M9 buffer for 24 hours. Total viable L1 worms were measured by counting the number of worms in 10 uL of worm suspension. Then, 100 L1 worms were placed at 16°C on fresh NGM plates (35 x 10 mm culture plates,) seeded with OP50 *E. coli*. Aβ1-42 expression was induced by putting worms at 24°C, 24 hours after plating. Paralysis of the nematodes was evaluated after 24, 48 or 72 hours (where indicated), by scoring worms that did not move or only moved their head when gently touched with a platinum loop.

5.2 Chemical mutagenesis of CL4176 worms and F2 screen

Chemical mutagenesis of CL4176 worms was performed by treatment with ethyl methan sulfonate (EMS, Sigma-Aldrich, USA), using standard procedures[227,228]. Prior to mutagenesis, a parental population of CL4176 was synchronized and left grow at 16°C until the fourth larval state (L4). In this stage, the number of germ-line nuclei is near its maximum, thus increasing the efficiency of mutagenesis with EMS, and increasing the number of nematodes that can be mutagenized. Then, L4 nematodes were mutagenized with 50 mM EMS for 4h at 20°C. After that, mutagenized worms were plated to recover, and then, 10 L4 were transferred to a new plate (10 nematodes for 10 plates), and incubated at 16°C overnight, and allowed to lay F1 progeny.

The day after, the parental adults were removed and F1 left to grow until adulthood.

After one day of egg laying, the F1 progeny was removed from F2 eggs by a synchronization step with bleach. F2 progeny was left to grow until larval L2 stage, then transferred to 24°C for paralysis screening. Paralysis was scored after 48 hours from the increase of temperature (time at which nearly about 100% of the CL4176 nematodes are paralyzed. Nematodes resistant to paralysis were individually removed to a fresh NGM plates and inspected in the following generations to determine if the phenotype bred true.

5.3 Analysis of Aβ DNA in transgenic worms

Staged populations of CL4176, EMS-treated CL4176 and CL802 worms were washed twice with sterile water and harvested in M9 buffer (20 mM KH_2PO_4, 42 mM Na_2HPO_4, 86 mM NaCl, 1 mM $MgSO_4$). Genomic DNA (gDNA) was extracted using Promega Maxwell 16 DNA Purification Kit (Promega Corporation, USA). DNA concentration and purity was determined by a Nanodrop Spectrophotometer. Aβ coding sequence was amplified by standard Polymerase Chain Reaction (PCR) analysis using 2X Biomix (Bioline Reagents Ltd, UK) and the following oligonucleotide primers (kindly provided by Dr. Christopher Link): Forward primer: 5'- CTTTCTGGCACCAGCAGGTAC-3';Reverse primer: 5'- CTTGCAGACTTCTCGCTGCTAG-3'. PCR products were stained with Gel Red Nucleic Acid stain (VWR International s.r.l., Italy) and separated by electrophoresis on a 1,5% agarose gel. A 100 base pair (bp) DNA ladder (Promega Corporation, USA) was run in parallel as a size reference indicator. Aβ DNA was then purified from agarose gel using the Wizard SV Gel and PCR Clean-Up System kit (Promega Corporation, USA) and sequenced by an external company (Eurofin, Italy). The sequencing results were analyzed by the software Finch TV 1.4 (Geospiza Inc, Seattle, USA).

5.4 Total RNA extraction

Egg-synchronized CL4176 and EMS-treated CL4176 worms were placed for 24 hours at 16°C on fresh NGM plates seeded with OP50 *E. coli*. The temperature was then raised at 24°C. After 48 hours worms were washed in M9 buffer and pelleted by centrifugation. The nematodes were sucrose floated and washed with M9 buffer according to standard techniques. The pellets were resuspended in 10% (m/v) Homogenization Buffer (Promega Corporation USA), vortexed for 1 min, subjected to three freeze-thaw cycles and then stored at -80°C until extraction. After thawing, RNA was extracted according to manufacturer's instructions (Promega Corporation USA). The quality and concentration of extracted RNA was determined using a Nanodrop Spectrophotometer (A260:A280 and A260:A230 ratio).

5.5 Analysis of gene expression in transgenic worms by qRT-PCR

Single-stranded cDNA was prepared from the total RNA samples by reverse transcriptase reaction using random hexamer with the Applied Biosystem kit (Life Technologies, USA) Quantitative Real Time PCR was performed on the cDNAs using the SYBR green master mix (Life Technologies, USA) on an Applied Biosystem 7900HT instrument. Relative measure of target gene expression levels was determined by dividing expression values by the corresponding geometric means of three non-variable control genes (*rpb-12*, *rps-7*, *ama-1*)[257,258], and analyzed using the comparative $2^{-\Delta\Delta Ct}$ method[301]. Where indicated, fold change values were calculated using the following equation:

fold change = $2^{-\Delta Ct\ induced}$ / $2^{-\Delta Ct\ not\ induced}$

The oligonucleotide primers used in this thesis are listed in Table 5.1

Gene target	Forward Primer	Reverse Primer
Aβ transgene	CCGACATGACTCAGGATATGAAGT	CACCATGAGTCCAATGATTGCA
Y46H3A.D (*hsp-16.2*)	GGTGCAGTTGCTTCGAATCTT	TCTTCCTTGAACCGCTTCTTTC
Y46H3A.E (*hsp-16.41*)	AAACAAAATCGGAACATGGATACTT	TGGAGCCTCAATTTGGAGTTTTC
daf-18	AGCCCTGAAAACTCGAGAACA	GCTCGATTTGCACACGATGA
F23B2.13 (*rpb-12*)	CGCCGAAAATGAAATCAAAC	GGGCGTCGTACACCATCA
ZC434.2 (*rps-7*)	GGCAAGCTTTTGAAGTCCGA	GGAAAGCCTTGAGTTGTGGG
F36A4.7 (*ama-1*)	CCGCTGAAATCGATCAAGCA	TGACCAACTCCTGCAGCTTA

Table 5.1 Sequences of primers used in qRT-PCR studies. Oilgonucleotidic primers for Aβ, Y46H3A.D, Y46H3A.E and F23B2.13 were taken from ref. 257. Primers for *daf-18*, ZC434.2 and F36A4.7 were taken from ref. 258.

5.6 Total soluble Protein Extraction

Transgenic CL4176 and EMS-treated CL4176 worms, induced or not for 48 hours at 24°C, as described above, were collected with M9 buffer, centrifuged at 1100 ×*g* for 4 min and washed twice to eliminate bacteria. Pellets of worms were suspended in 5 volumes of lysis buffer (5.0 mM NaCl, 5.0 mM EDTA, 1.0 mM dithiothreitol and protease inhibitor mixture (Roche Diagnostic Gmbh, Germany) in 25 mM Tris/HCl buffer, pH 7.5). The suspension was homogenized with an Ultra-Turrax T10 roto-stator grinder rotating at 20000 rpm for three 30 sec bursts separated by 1 min rests on ice. The homogenate was centrifuged at 10,000 x *g* for 20 min at 4^{o}C. Total protein concentration of worm lysates was determined by Bradford Protein Assay (BIO-RAD, CA) and the supernatants were frozen at -20^{o}C until use.

5.7 Immunodot-blot analysis

For dot-blot analysis, equal amounts of protein (25 µg) were spotted onto nitrocellulose membranes (Millipore). The membranes were incubated with an anti-Aβ mouse monoclonal WO2 antibody (1:1000, Millipore). To minimize background staining due to non-specific membrane-binding of the antibody, the membranes were saturated for 1 h at room temperature by incubation with 10 mM Tris buffer S, pH 7.5 containing 150 mM NaCl 0.1% (v/v) Tween 20 (TBST), 5% (w/v) low-fat dry milk powder and 2% (w/v) bovine serum albumin. Peroxidase-conjugated anti-mouse IgG (1:20.000, Sigma) was used as secondary antibody. A 0.1% Ponceau Red solution (Sigma Aldrich) was used to stain the blotted membranes for total protein visualization. The mean volumes of dot-blot immunoreactive spots and of Ponceau-dyed spots were analyzed using Quantity One 1-D Analysis Software (Bio-Rad).

5.8 Western blot analysis

Aβ species in lysates from transgenic *C. elegans* strains were identified by immunoblotting using 15% Tris-glycine gel, and by Western blotting. After heating samples in sample buffer containing 5% β-mercaptoethanol (1:1 vol/vol, Bio-Rad), 50 µg of total protein lysates were loaded in each lane of the gel. The membranes were blocked with 10 mM Tris-HCl solution, pH 7.5, containing 150 mM NaCl and 0.1% (vol/vol) Tween 20, 5% (w/v) low-fat dry milk powder and 2% (w/v) bovine serum albumin. Membranes were then incubated overnight with 6E10 antibody (1:1000, Covance). Peroxidase-conjugated anti-mouse IgG (1:20.000, Sigma) was used as the secondary antibody.

5.9 Surface Plasmon Resonance studies

The Surface Plasmon Resonance (SPR) apparatus used for the present study (ProteOn XPR36 Protein Interaction Array System; Bio-Rad) has six parallel flow channels that can be used to uniformly immobilize strips of six ligands on the sensor surface. The fluidic system can automatically rotate 90° so that up to six different analytes can be injected, allowing simultaneous monitoring of up to 36 individual molecular interactions in a single run on a single chip. Anti Aβ 4G8 antibody (Covance) was immobilized in parallel flow channels of GLC sensor chips (Bio-Rad) using amine coupling chemistry, as previously described[207]. Briefly, after surface activation, 4G8 (30 µg/ml in 10 mM acetate buffer, pH 5.0) was injected for 5 min at a flow rate of 30 µl/min, and the remaining activated groups were blocked with ethanolamine, pH 8.0. The final immobilization levels were 5000 resonance units (1 RU = 1 pg of protein/mm^2). A “reference” surface was always prepared in parallel using the same immobilization procedure but without addition of the antibody.

After rotation of the microfluidic system, lysates from either CL4176 or EMS-treated CL4176 worms were injected over immobilized 4G8 for 3-5 minutes. Dissociation was followed for the next 11 minutes. The running buffer, also used to elute samples, was 10 mM phosphate buffer, pH 7.4, containing 150 mM NaCl and 0,005% Tween-20 (PBST). All the experiments were done at 25°C.

5.10 Whole genome sequencing of CL4176 and EMS-treated worms

Whole genome sequencing of CL4176 and EMS-treated worms was performed by Illumina Next Generation Sequencing (NGS) chemistry. The first step consisted of DNA library preparation, which is prepared by random DNA fragmentation, followed by ligation of specific 5' and 3' adapters. For library preparation, high quality and high molecular weight DNA was purified from staged populations of CL4176 and EMS-treated CL4176 worms, or from synchronized L1 worms obtained after worm eggs purification, using Promega Maxwell 16 DNA Purification Kit (Promega Corporation, USA), as described above. DNA concentration was measured using the Quant-iT PicoGreen dsDNA assay kit (Invitrogen), using manufacturer's instructions. After checking for integrity using 1% agarose gel, DNA samples (380 ng DNA in 100 µL water) were fragmented using the Bioruptor sonicator (power setting LOW, cycle 30 sec ON / 90 sec OFF, time 6 minutes) in carefully degassed water, at 4°C. Optimal fragmentation (550 base pairs fragments) was confirmed with the Agilent High Sensitivity DNA kit on the 2100 Bioanalyzer (Agilent). Then, DNA library preparation was performed using the TruSeq Nano DNA kit (Illumina), according to the manufacturer instructions. The library was loaded onto the Illumina flow cell and the fragments were hybridized to the flow cell surface. Each bound fragment was amplified allowing cluster generation.

Finally, paired end sequencing was performed on a NextSeq500 platform (Illumina) with NextSeq 500/550 High Output Kit (300 cycles). Paired end sequencing involves sequencing both ends of the DNA fragments in a sequencing library and aligning the forward and reverse reads as read pairs. In addition to

producing twice the number of reads for the same time and effort in library preparation, sequences aligned as read pairs enable more accurate read alignment and the ability to detect indels. During sequencing, fluorescently labeled nucleotides are added and the first base is incorporated. The flow cell is imaged and the emission from each cluster is recorded. The emission wavelength and intensity are used to identify the base. This cycle is repeated “n” times to create a read length of “n” bases.

Paired end (2x121 bp) reads were mapped to reference genome (ce10) by using bowtie2[302] aligner. Determination of the depth of coverage and and variant calling, including SNPs and insertions or deletions, was performed using the GATK pipeline through a multi-step procedure[303]. The GATK architecture is designed to divide complex computations in two separate modules; traversal modules, which divide and prepare the data, and walkers modules, which provide efficient analysis of the data obtained from next generation sequencing. We first determined mismatches between the individual *C. elegans* strains and the reference genome and then compared the two strains directly. Finally, DNA-mutations occurring in the mutant and not in the wild-type strain were characterized using the variant annotation tool provided by UCSC[304]. To limit the number of false-positives and potentially biologically meaningless results we discarded from the analysis both mismatches occurring in non-protein-coding portions of the genome and synonymous mutations. Thus, we restricted the analysis to mutations that resulted in insertion of stop codons, frame-shifts and non-synonymous translation.

RESULTS

6. Chemical mutagenesis of transgenic *C.elegans* AD model (CL4176 strain)

In transgenic *C. elegans* strain CL4176, the inducible expression of Aβ leads to a rapid Aβ oligomers-induced paralysis and death[255,257], that is complete after 48 hours from induction (Fig. 6.1).

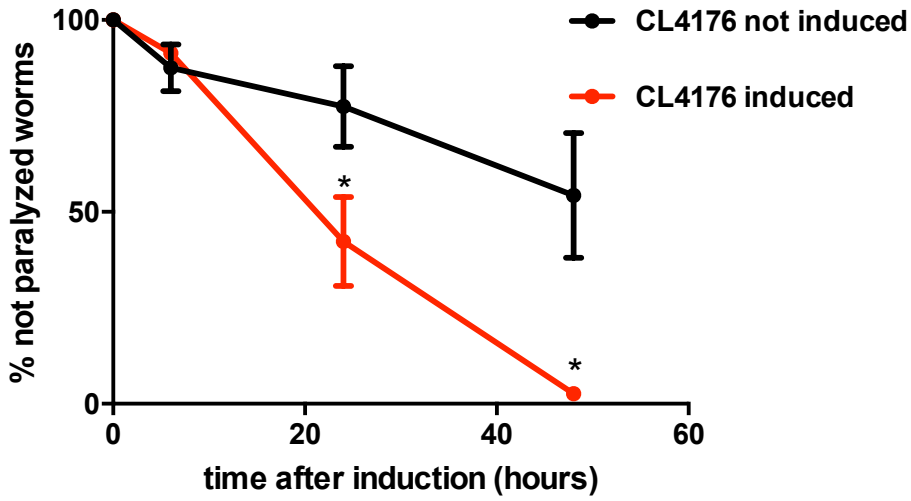

Figure 6.1 Time course of paralysis in wild-type CL4176 worms. Egg-synchronized worms were placed for 48 h at 16 °C, until they are in the larval stage L2, and the temperature was then raised to 24 °C, to induce Aβ expression (blue line) and paralysis was scored at different time points up to 48h. Control worms remained at 16°C (Aβ not induced, red line). *p<0,05 t-test induced vs not induced (mean ± SD, n=100, three independent assays).

To identify the genes involved in the production of this obvious phenotype, a genome wide screening was performed by chemical mutagenesis induced by EMS. For this, we followed the scheme depicted in Figure 6.2 with minor modifications (see Material and Methods for a detailed description of the experiment).

CL4176 worms were mutagenized and then screened for paralysis resistance. Analysis of 15000 mutagenized worms in the F2 progeny revealed 8 nematodes that did not paralyze after temperature upshift were selected. These were transferred to new plates and let to self-fertilize at permissive temperature. Only three clones were able to grow in the F3 progeny, possibly because random mutagenesis by EMS could cause sterility or death in some mutated worms (Fig. 2). The surviving clones (named MN4176, MN4176-2, and MN4176-3, respectively) were expanded for two generations and screened again in the paralysis assay. Briefly, the different clones were left to grow at permissive temperature until larval stage L2, and then they were transferred to 24°C. Paralysis was scored just before the temperature upshift, after 24 hours and after 48 hours (Fig. 6.3).

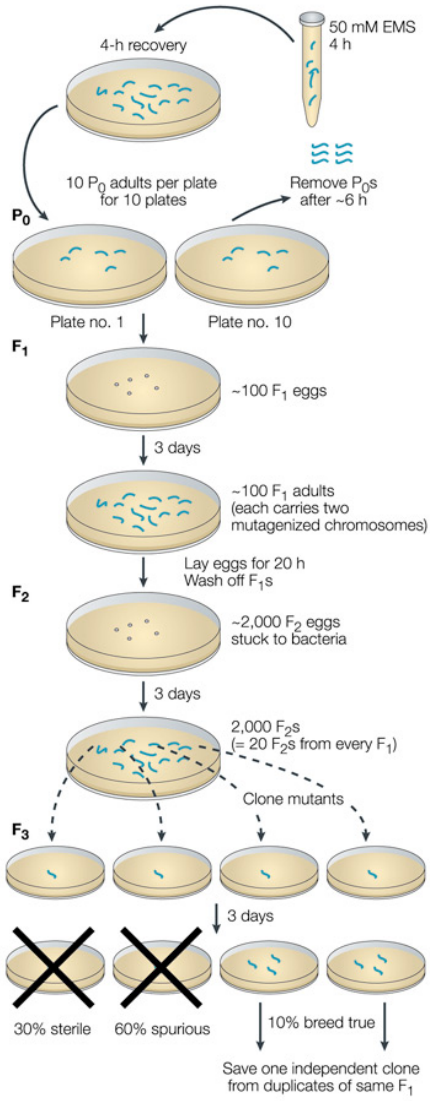

Figure 6.2 Representative picture outlining a typical F2 screen after EMS mutagenesis for the selection of mutated worms (*adapted from ref. 228*).

Data shown in Figure 6.3 show that only the MN4176 mutant strain confirmed the lack of paralysis after 48 hours at 24°C, whereas the other clones became progressively paralyzed after 48 hours of temperature upshift, although with different paralysis kinetics. These clones, false positive at the first screening, could be the result of somatic mutations that arose after EMS treatment that cannot be transmitted to the following progeny. Another reason could be that the mutations

generated by EMS did not result in a complete penetrance of the phenotype, as suggested by the different kinetics of paralysis of the mutated clones, compared to that of the control CL4176 strain.

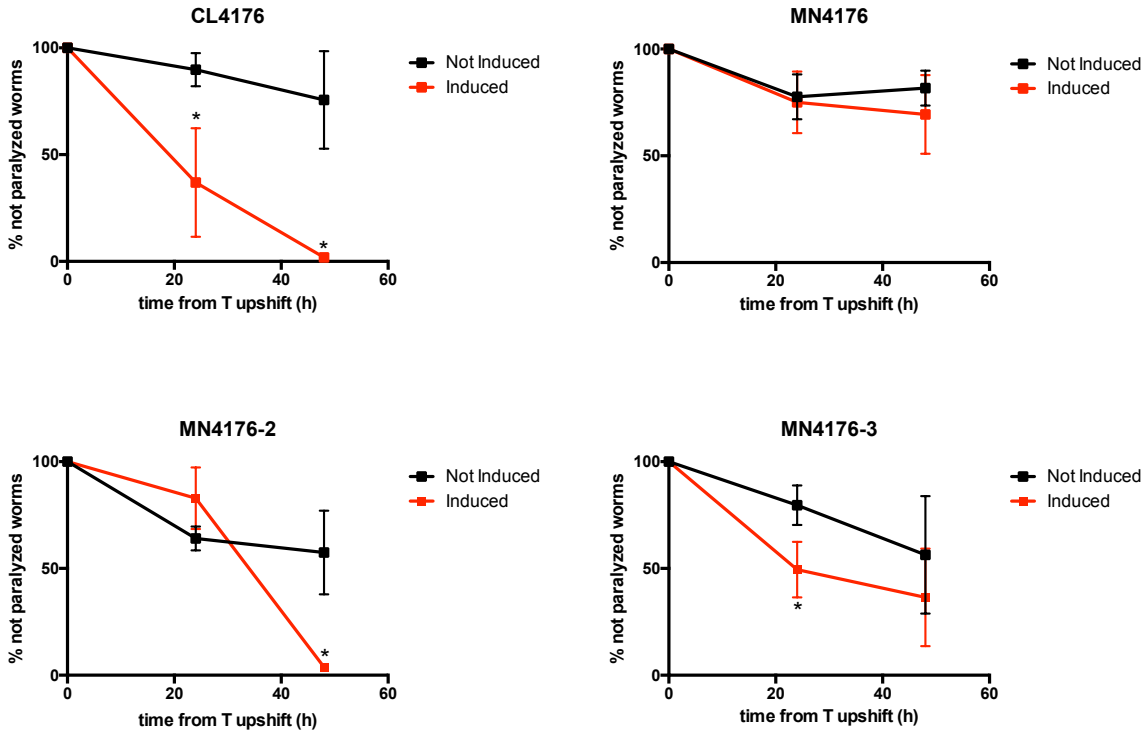

Figure 6.3 Paralysis kinetics of CL4176 and mutated worms selected after EMS mutagenesis. Egg-synchronized worms were placed for 48 h at 16 °C, until they are in the larval stage L2, and the temperature was then raised to 24 °C, to induce Aβ expression (red line) and paralysis was scored after 24 and 48h. Control worms remained at 16°C (Aβ not induced, black line). *p<0,05 t-test induced vs not induced (mean ± SD, n=100, three independent assays).

To possibly increase the number of mutated clones resistant to Aβ-induced paralysis, another EMS mutagenesis session in CL4176 worms was performed. After the F2 screen, two clones (MN4176-4 and MN4176-5) were selected, which did not paralyze after 48 hours of temperature increase to 24°C. However, these

observations were not confirmed when the paralysis assay was replicated in the following generations of the mutated nematodes (Fig. 6.4).

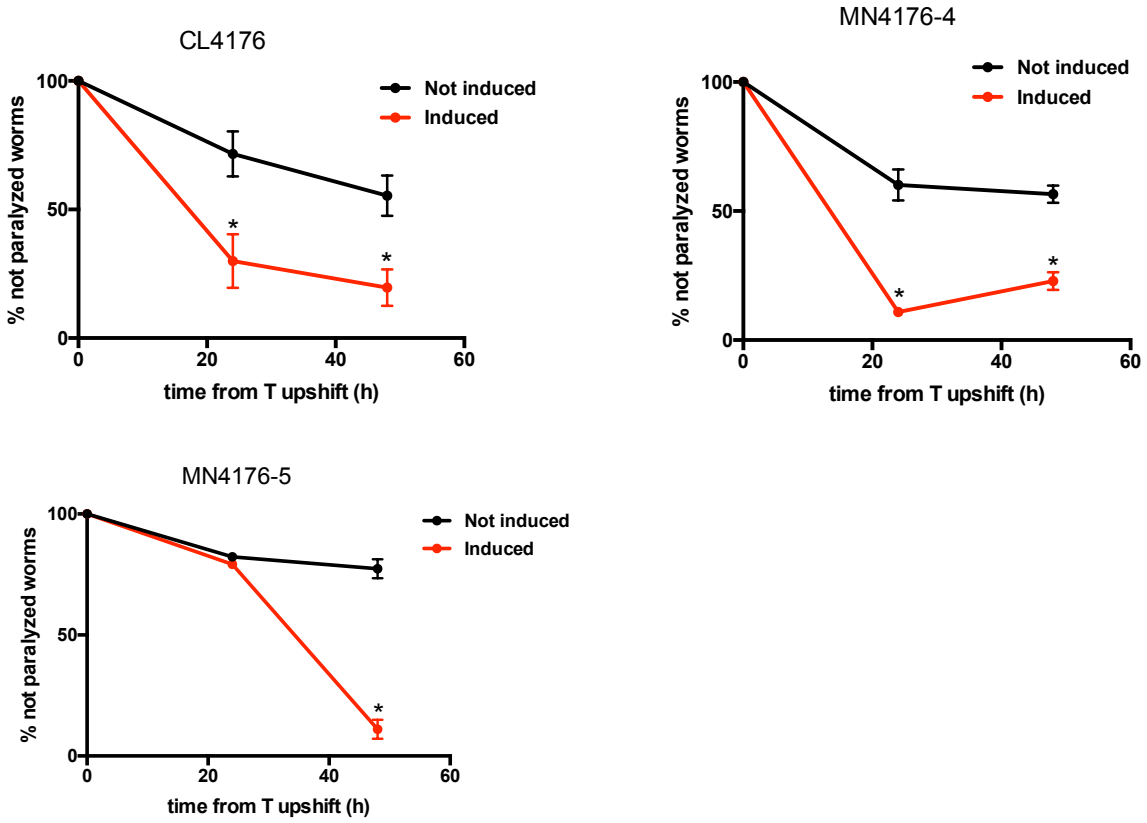

Figure 6.4 Time course of paralysis in the worms selected after the second mutagenesis experiment with EMS. Egg-synchronized MN4176-4 and MN4176-5 worms were placed for 48 h at 16 °C, until they are in the larval stage L2, and the temperature was then raised to 24 °C, to induce Aβ expression (red line) and paralysis was scored after 24 and 48h. Control worms remained at 16°C (Aβ not induced, black line). *p<0,05 t-test induced vs not induced (mean ± SD, n=100, three independent assays).

In conclusion, EMS-mediated chemical mutagenesis resulted in the generation of different mutated worms with different paralysis kinetics, compared to the control strain. The majority of clones obtained after mutagenesis showed a delayed paralysis, after the increase of temperature. However, we obtained only one clone (MN4176) which was almost completely resistant to paralysis induced by the increase of temperature, and this clone was chosen for further characterization.

6.1 Time course of paralysis in new CL4176 worms

During the course of the project it was observed that the presence of the Aβ minigene in CL4176 wild type worms appeared to be deleterious (even under non-induced conditions), and presumed spontaneous deletions in these transgenes were observed multiple times (e.g., loss of the *rol-6* marker). A possible explanation of this effect is that the deletions occur when large worm populations are maintained by "chunking", presumably due to constant low-level selection against the transgene.

Thus, another copy of this strain was obtained from the CGC. The new strain showed a slower time course of paralysis, reaching complete paralysis after 72 hours from the temperature upshift (Fig. 6.5). We found however, that MN4176 worms did not paralyze even after 72 hours from temperature increase, indicating that mutagenesis did not delay the onset of paralysis (Fig. 6.5).

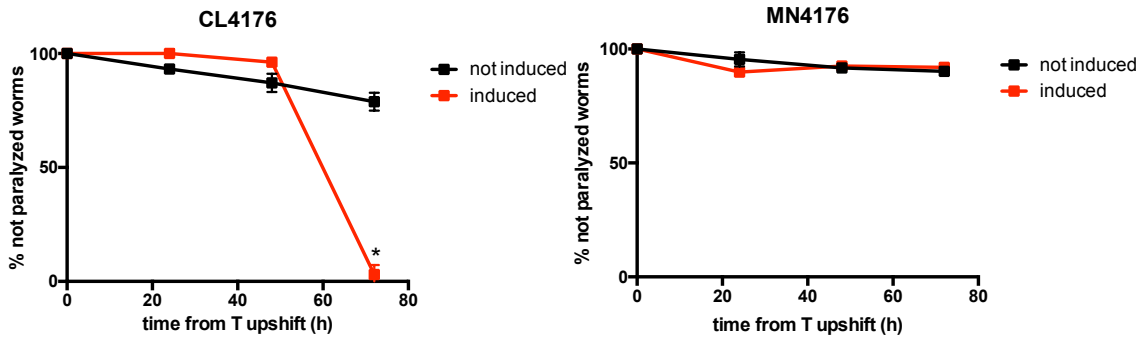

Figure 6.5. Time course of paralysis of new CL4176 and MN4176 worms. Egg-synchronized CL4176 and MN4176 worms were placed for at 16 °C on fresh NMG plates seeded with OP50 *E. coli*. After 48 h the temperature was raised from 16 to 24 °C (red lines) and paralysis was scored at 24, 48 and 72 hours from the temperature upshift. Data are shown as percentages ± SD of worms not paralyzed. *p<0,05 t-test induced vs not induced (mean ± SD, n=100, three independent assays).

The variability observed in the paralysis kinetics among various CL4176 strains could be due to different causes, whose determination fell outside of the scope of this project. However, these discrepancies had already been reported in literature. In fact, some reports indicate a complete paralysis of induced CL4176 worms after 48 hours[255], whereas others research groups have showed faster kinetics of paralysis, reaching 100% of paralyzed CL4176 after 24 hours from the temperature upshift[258].

7. Analysis of Aβ expression in EMS-treated worms

7.1 Analysis of Aβ DNA in CL4176 and MN4176 worms

Once obtained a mutated clone resistant to paralysis induced by temperature upshift (MN4176), possible alterations in the expression of Aβ were evaluated. First, the DNA sequence coding for human Aβ1-42 in CL4176 and in MN4176 worms was analyzed. The majority of mutations inside the Aβ sequence are known to increase the oligomerization properties, and thus the toxicity, of the peptide[144]. Recently, however, the mutation A2T has been shown to be protective[305], and *in vitro* experiments showed that this mutation delays the aggregation properties of Aβ peptide[306]. Moreover, nonsense mutations could arise after EMS treatment, resulting in the generation of inactive truncated peptides. To verify these possibilities, genomic DNA (gDNA) was extracted from staged populations of control and mutated CL4176 strains using standard procedures. The DNA yield was determined by measuring its concentration by absorbance at 260 nm. The ratio of the readings at 260 nm and 280 nm (A260/A280) provided an estimate of the purity of DNA with respect to contaminants that absorb UV, such as proteins. Good ratio values, ranging from 1.8 to 2.0, were obtained for each DNA extraction (data not shown).

After DNA extraction, the Aβ1-42 gene was amplified by polymerase chain reaction (PCR) analysis. The forward primer used for this analysis targets the 3' end of the signal peptide, whereas the reverse primer targets DNA sequences in

the 3'UTR resulting in a PCR product of about 240 base pairs (bp). After the amplification, DNA bands were visualized by agarose gel electrophoresis (Fig. 7.1)

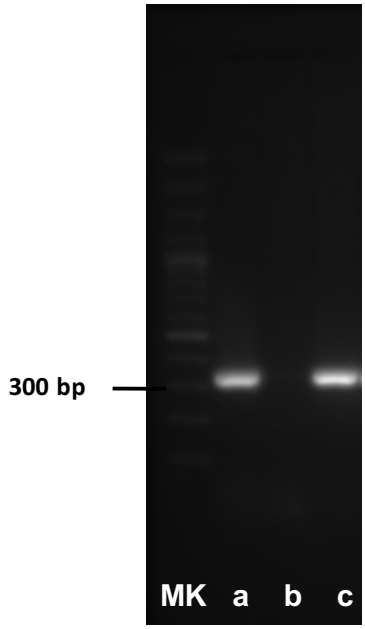

Figure 7.1 Analysis of Aβ DNA by agarose gel electrophoresis. gDNA was extracted and Aβ sequence was amplified by PCR with the primers listed in Material and Methods. Then, PCR products were stained and run on a 1,5% agarose gel. Bands were visualized by UV luminescence. *MK*: DNA molecular ladder; *lane a*: band amplified from DNA of CL4176 worms; *lane b*: band amplified from DNA of CL802 worms; *lane c*: band amplified from DNA of MN4176 worms.

Figure 7.1 shows the results of the PCR reaction. In parallel to the DNA of MN4176 (lane c), DNA was also extracted from CL4176 worms (lane a, positive control), and from CL802 worms (lane b). CL802 is a transgenic strain which carry the same plasmid of CL4176 worms, but without the Aβ1-42 minigene, thus representing the negative control[255]. A single DNA band was observed in

CL4176 and MN4176 worms, with a molecular size of approximately 300 base pairs. As expected, no amplified products in the DNA of CL802 worms were observed, because of the lack of the Aβ1-42 gene in that strain. To investigate the presence of possible mutations in the Aβ DNA sequence in EMS-treated worms, the DNA bands of CL4176 and MN4176 strains were purified and sequenced.

Analysis of the DNA sequences obtained from both strains showed a 100% identity with the human DNA sequence coding for Aβ inside the APP gene (Fig. 7.2).

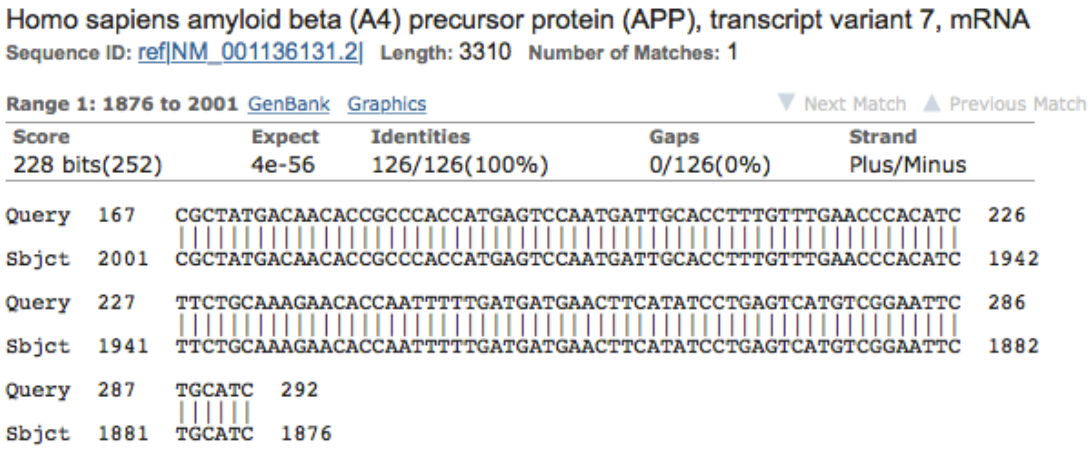

Figure 7.2 Basic Local Alignment Sequence Tool (BLAST) analysis (via NCBI) of MN4176 DNA amplified with primers specific for Aβ1-42. The analysis resulted in 100% identity with the 126 bp sequence present in the human APP gene, coding for Aβ1-42.

Taken together, these data suggest that the lack of paralysis observed in MN4176 worms after temperature upshift is not due to any mutation in the DNA sequence of the Aβ transgene.

7.2 Analysis of genetic expression of Aβ in CL4176 and MN4176 worms

Once it was demonstrated that there was an absence of any mutation in the DNA of Aβ coding sequence in MN4176 worms, their Aβ expression was next investigated, by measuring the levels of Aβ mRNA induced by temperature upshift. Transgenic CL4176 and MN4176 worms were propagated at 16°C until they reached the larval stage L2, and then they were shifted to the non-permissive temperature of 24°C for 48 hours. Control not induced populations were maintained at 16°C until they reached the same developmental stage (L4). At this time point, worms were collected and the relative levels of Aβ mRNA levels were measured by quantitative real-time PCR (qRT-PCR).

Results are shown in Figure 7.3. Either CL4176 and MN4176 worms showed a significant increase in their levels of Aβ mRNA when shifted to 24°C for 48 hours, compared to the control, not induced, worms. Differences in the relative levels of Aβ mRNA between the two strains, with higher values for the wild type strain. It is worth noting that the *smg-1ts*-dependent silencing of transgenic CL4176 worms is often leaky, allowing for low levels of Aβ expression at permissive temperatures. This effect could vary between the two strains, also taking in consideration that the CL4176 strain used for this analysis was not the same from which the mutated clone was originated.

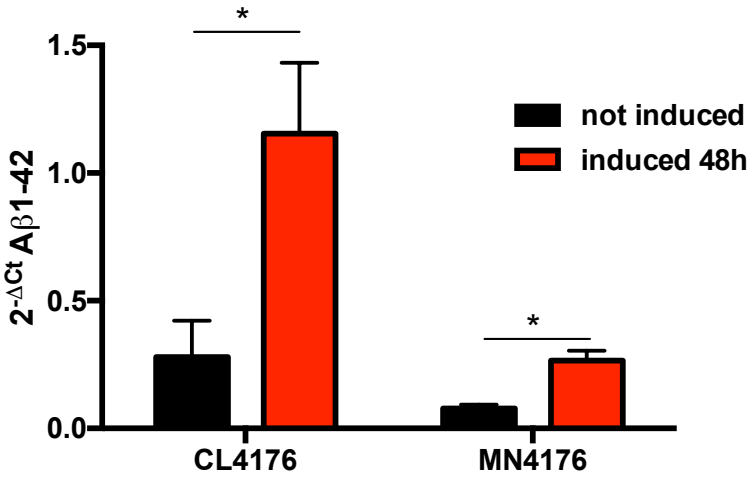

Figure 7.3 Relative increase of Aβ mRNA levels in CL4176 and MN4176 worms resulting from 48 hours upshift of the worms from 16°C to 24°C, determined by qRT-PCR. *p<0,05 t-test induced vs not induced (mean ± SD, n=6).

To better compare the increase of Aβ mRNA of the two strains, the fold change levels of Aβ mRNA expression were calculated (Fig. 7.4). Although relative Aβ mRNA levels were different between the two strains, fold change values appeared to be very similar.

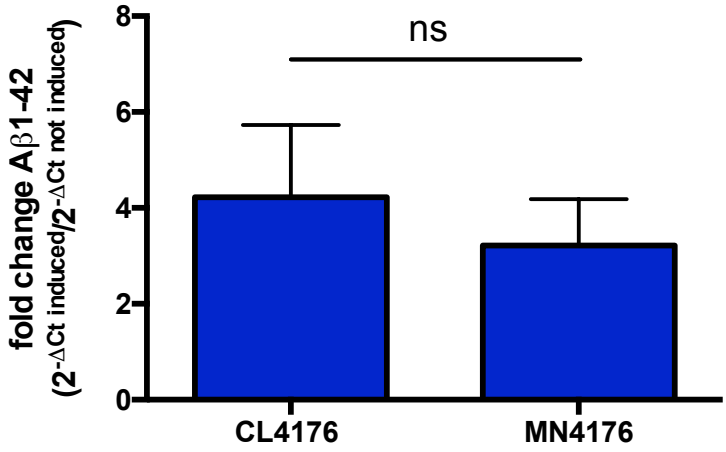

Figure 7.4 Relative increase of Aβ mRNA levels in CL4176 and MN4176 worms resulting from 48 hours upshift of the worms from 16°C to 24°C, determined by qRT-PCR. (mean ± SD, n=6). ns=not significant, p>0,05 t-test MN4176 vs CL4176

Finally, the kinetics of induction of Aβ mRNA in CL4176 and MN4176 worms were compared. Nematodes were propagated at 16°C until they reached the larval stage L2, and then they were shifted to 24°C. After 24, 48 or 60 hours, worms were harvested and relative Aβ mRNA levels were measured (Fig. 7.5).

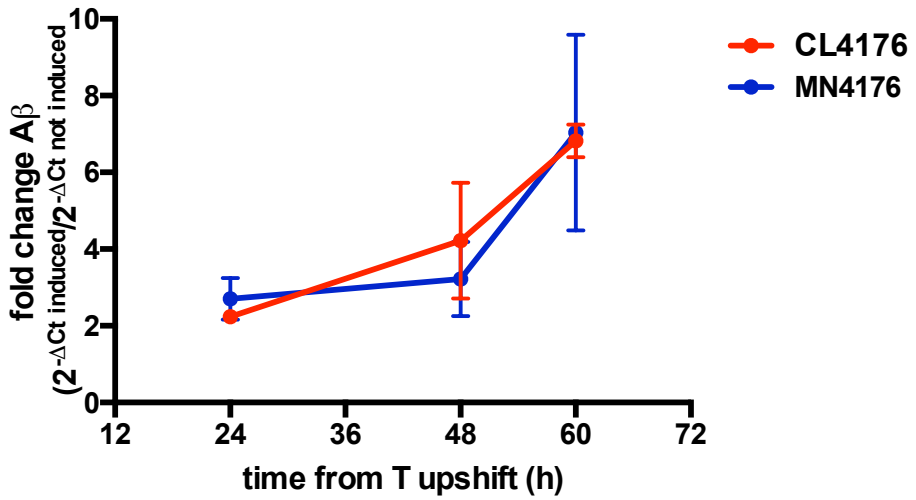

Figure 7.5. Temporal transcript accumulation of Aβ in CL4176 and MN4176 worms. (mean ± SD, n=3-4 for each time point taken in consideration)

Data in Figure 7.5 show that the increase of temperature resulted in a time-dependent induction of Aβ mRNA, with expression kinetics almost overlapping between CL4176 and MN4176 strains.

7.3 Analysis of Aβ oligomers in CL4176 and MN4176 worms

It was then investigated if the induction of Aβ mRNA levels in MN4176 worms was followed by Aβ protein expression. Figure 7.6 shows that Aβ levels were comparable in wild type and mutated worms, as assayed by immuno-dotblot analysis.

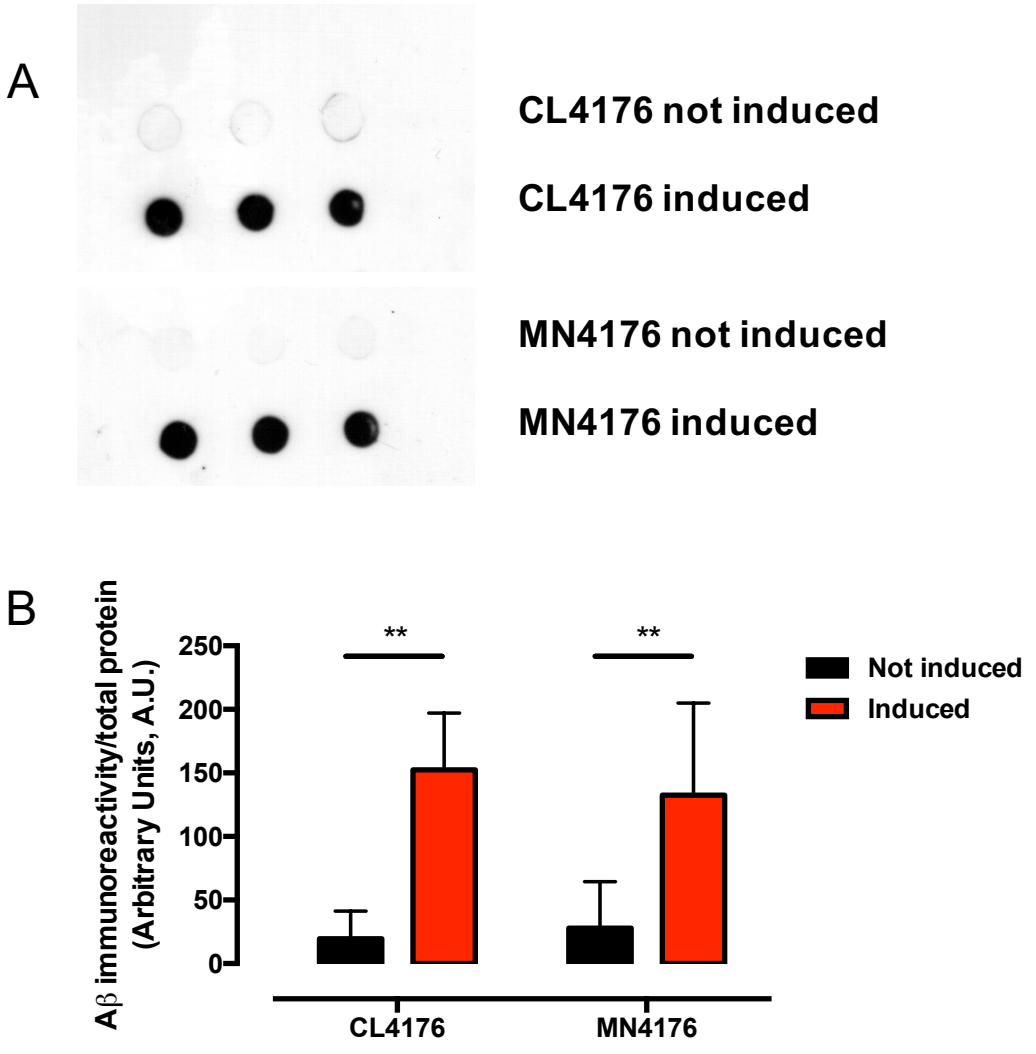

Figure 7.6 Aβ protein expression in CL4176 and MN4176 worms, 48 h after temperature upshifting. A) Representative immunodot-bot in which equal amounts of protein worm lysates (25 μg) were spotted in triplicate. Total proteins on the blotted membranes were stained using 0.1% Ponceau

Red solution and were used to normalize the immuno-specific signal for protein loading. B) Densitometric analysis of total Aβ immunoreactivity, expressed as the mean ± SD of three experiments. ***p*<0,05 t-test analysis of induced vs not induced.

The presence of Aβ oligomers in induced MN4176 worms was then evaluated, in comparison with the control strain. Western blot analysis revealed the presence of a specific Aβ-immunoreactive band running between 27 and 34 KDa (Fig. 7.7), suggesting the formation of Aβ aggregates.

Despite previous reports indicated the co-existence of Aβ monomers with oligomeric species[255,256], low molecular weight Aβ species were not detected, both in CL4176 and MN4176 worms. A possible explanation of this observation could be that at longer induction times, the progressive aggregation of Aβ, eventually leading to worm paralysis, shifted the monomers-oligomers equilibrium versus the aggregated species.

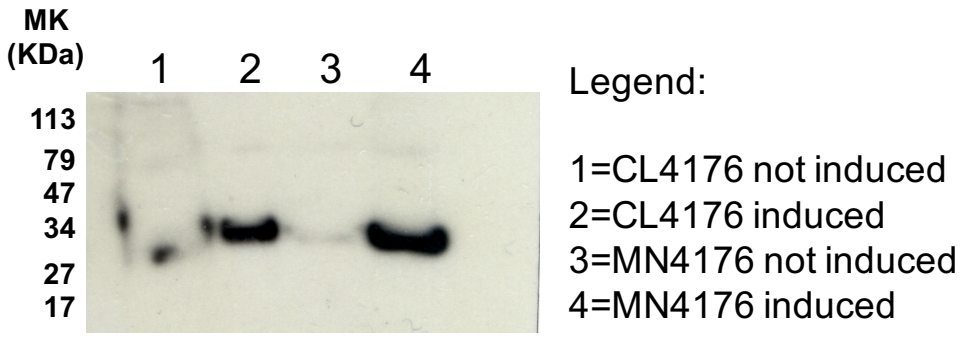

Figure 7.7 Detection of Aβ oligomers in CL4176 and MN4176 worms by Western blot analysis. Equal amounts of each protein worm lysate (50 μg) was run on a 12% SDS-PAGE and transferred to a PVDF membrane. After blocking, membrane was immunoblotted with anti Aβ antibody (6E10). This experiment was replicated twice with similar results.

Finally, the presence of Aβ oligomers in MN4176 worms was investigated by using a novel immunoassay based on Surface plasmon resonance (SPR)[207]. SPR is a powerful technique used to study macromolecular interactions in real time without any molecule labelling. In a SPR experiment, one of the two interacting partner is immobilized on a sensor chip surface, and the other molecule is flowed over the immobilized one. Binding is measured in real time as a change of mass at the surface, and association and dissociation kinetics can be estimated, as well as its affinity.

By using immobilized anti Aβ 4G8 antibody as a detecting agent, it was found that the SPR-based immunoassay was able to specifically detect Aβ oligomers which are transiently formed during the incubation of synthetic Aβ peptide, discriminating them from monomers and higher order aggregates[207]. This assay also allowed the detection of Aβ oligomers in lysates from transgenic CL4176 worms[207].

Thus, lysates from CL4176 and MN4176 worms upshifted to 24°C for 48 hours were flowed over immobilized 4G8 in the SPR assay. Lysates from noninduced worms of both strains were used as control (Fig. 7.8). Although the injection of lysates obtained from noninduced MN4176 worms resulted in a binding signal higher than the signal observed injecting lysates from noninduced CL4176, the binding levels of the lysates prepared from induced CL4176 and MN4176 worms to immobilized 4G8 were comparable. These results indicated a specific binding signal due to the presence of Aβ oligomers in induced MN4176 worms.

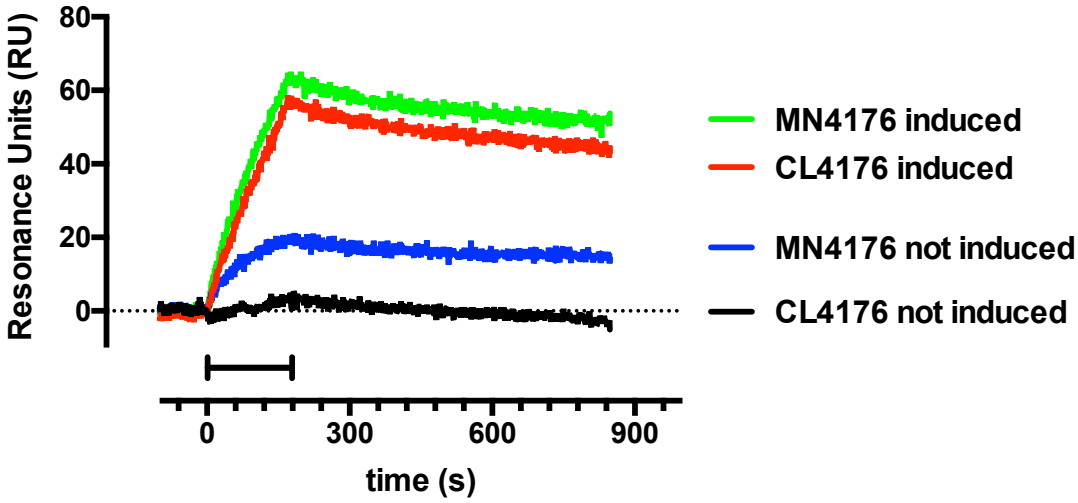

Figure 7.8 SPR studies with native Aβ oligomers extracted from CL4176 and MN4176 worms. Lysates obtained from CL4176 and MN4176 strains 48 hours after the temperature rise were injected for three minutes (bar) onto immobilized 4G8. Dissociation was followed for the following 11 min. Lysates from not induced CL4176 and MN4176 nematodes were injected in parallel as control. The shape of the curves, in particular the slow dissociation rate, suggested that the binding was due to oligomeric species[207]. This experiment was replicated twice, with similar results.

Notably, these data also indicate that the lack of paralysis observed in induced MN4176 worms is not due to differences in the production of Aβ (oligomers), in comparison with CL4176 worms, and suggests that the mutation(s) affects downstream mechanisms activated by Aβ oligomers.

8. Genome wide sequencing of CL4176 and MN4176 worms

8.1 Results from the first whole genome sequencing.

Total Genomic DNA (gDNA) from CL4176 and MN4176 worms was sequenced and compared at first with the reference genome of founder Bristol N2 worms. Unexpectedly, 80-90% of sequenced DNA, both from wild type and EMS-treated worms, did not align with the reference genome. A BLAST analysis was carried out to identify the source of the non-matching DNA, indicating that the exogenous DNA belonged to several bacteria. A more detailed analysis revealed that the bacterial DNA mostly was ascribable to that of *Stenotrophomonas maltophilia*, in particular the strains K279a and R551-3. Another relevant source of bacterial DNA came from *Bacillus thuringiensis* and from different strains of *Pseudomonas* (Fig. 8.1)

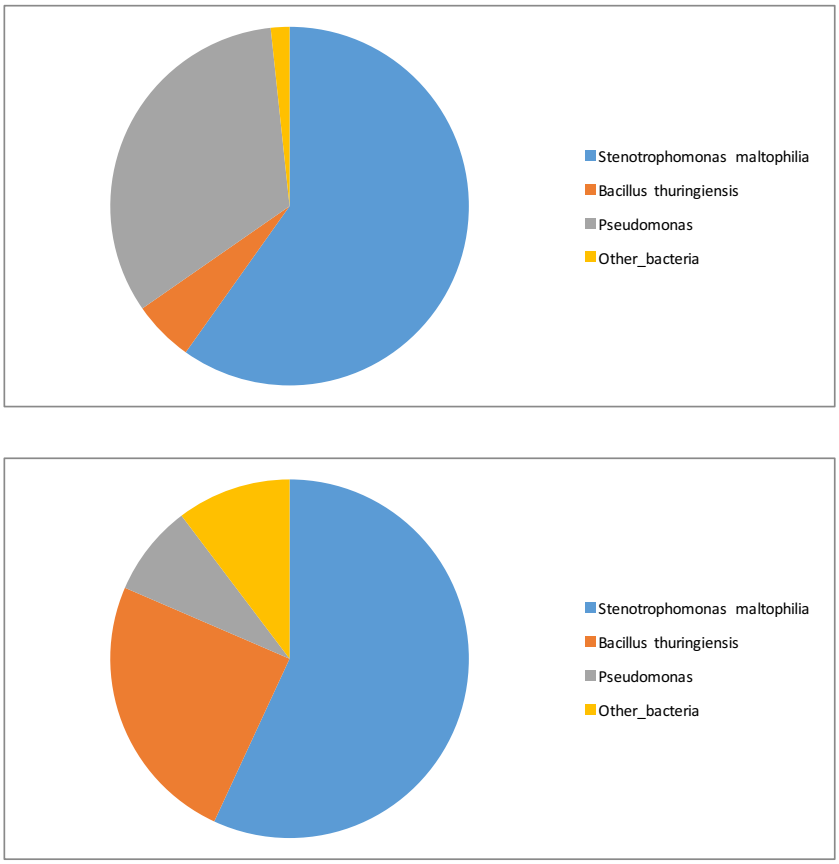

Figure 8.1. Circle charts representing the proportions of the various bacterial DNA found in CL4176 wild type worms (top panel) and MN4176 worms (bottom panel).

To verify the bacterial contamination in the DNA of worms, PCR analysis with oligonucleotidic primers designed to specifically distinguish two strains of *Stenotrophomonas maltophilia* and a set of primers to recognize *Bacillus thuringiensis* was performed (Table 8.1).

Primers	Sequence
S Malt Seq1_Forward	TCGTGAAGGCCGTTATTCGG
S Malt Seq1_Reverse	TGACGATCGAGTTCCTGGTG
S Malt Seq2_Forward	GCTGGTCGATCCTTACGGTG
S Malt Seq2_Reverse	ATCAGCGCCATGGTCTCTTC
B.Thur_Forward	TGTAGTCTGAGCGAAGCAAGA
B.Thur_Reverse	GACTGCATTTCAGCATCCGT

Table 8.1 Oligonuecleotidic primer specific for *S. maltophilia* (S. malt Seq-1 and S. malt Seq-1) and for *B. thuringiensis* (B. thur).

For each worm strain two DNA samples obtained from independent experiments, and DNA from CL802 worms were included in the analysis. PCR products were separated on a 1.5% agarose gel and specific bands were visualized by staining with a DNA binding dye. Results of the PCR analysis are shown in Figure 8.2.

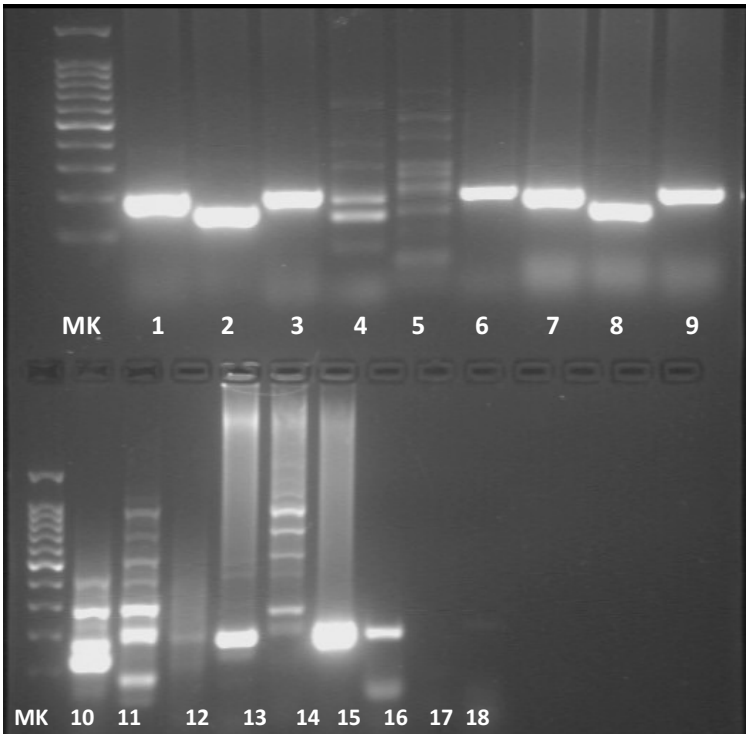

Samples

MK) Molecular Marker
1) CL4176 DNA-S.malt Seq-1
2) CL4176 DNA-S.malt Seq-2
3) CL4176 DNA-B.thur
4) MN4176 DNA-S.malt Seq-1
5) MN4176 DNA-S.malt Seq-2
6) MN4176 DNA-B.thur
7) CL802 DNA-S.malt Seq-1
8) CL802 DNA-S.malt Seq-1
9) CL802 DNA-B.thur
10) CL4176 DNA 2-S.malt Seq-1
11) CL4176 DNA 2-S.malt Seq-2
12) CL4176 DNA 2-B.thur
13) MN4176 DNA 2-S.malt Seq-1
14) MN4176 DNA 2-S.malt Seq-2
15) MN4176 DNA 2-B.thur
16) Blank-S.malt Seq-1
17) Blank-S.malt Seq-2
18) Blank-B.thur

Figure 8.2. Detection of DNA from bacteria in CL4176, MN4176 and CL802 by PCR analysis. genomic DNA was extracted from CL4176, MN4176 and CL802 worms and probed with primers for *S.maltophilia* (S.malt Seq-1 and -2, Table 8.1) and *B.thuringiensis* (B.thur, Table 8.1). Blank reactions were prepared with PCR mixture without any DNA.

A large bacterial contamination in the DNA of all nematode strains analyzed was found. This contamination extended not only to transgenic worms, but also to N2 wild type worms maintained in our laboratories and to other nematodes strains not related to this project (data not shown).

Stenotrophomonas maltophilia is a Gram-negative bacterium acting as opportunistic pathogen in immunocompromised individuals. Although some reports described that *S. maltophilia* strains can infect *C. elegans*, their pathogenicity has been debated. As previously reported[307], we hypothesized that *S. maltophilia* K279a and R551-3 were avirulent, since transgenic *C. elegans* strains maintained under normal conditions did not exhibit a reduction in survival.

Bacillus thuringiensis is a Gram-positive soil bacterium which is known to produce toxins which are pathogenic for *C. elegans*[308,309]. As for *S. maltophilia*, infection of *B. thuringiensis* did not appear to have pathogenic activity on our *C. elegans* strains.

To overcome the bacteria contamination and to obtain *C. elegans* DNA samples suitable for whole genome sequencing, we purified eggs from a population of nematodes. Briefly, a population of gravid CL4176 wild type and mutated worms underwent a strong bleach treatment, which resulted in the complete elimination of bacteria and worms, leaving intact the eggs, due to their resistant shell. Following this treatment, isolated eggs were recovered and incubated 24 hour in solution, to obtain viable worms in the larval stage 1 (L1). Total DNA from L1 worms was extracted and PCR analysis was performed to verify the presence of any bacterial contamination (Fig. 8.3).

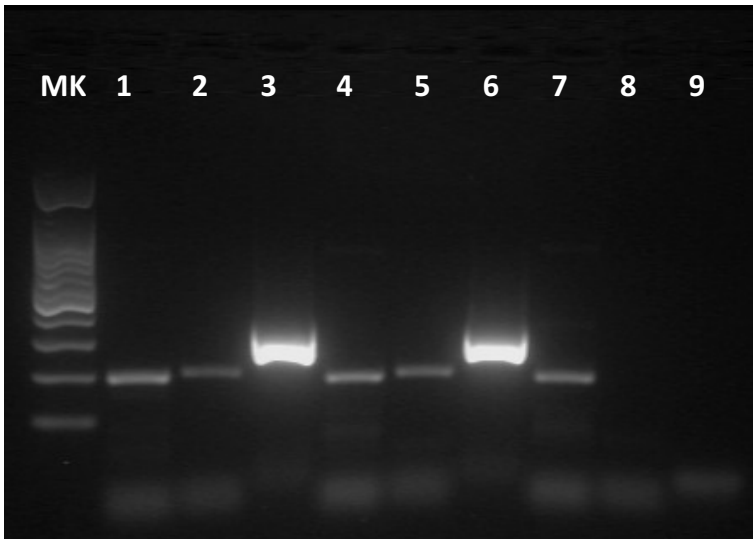

Samples:

MK: DNA ladder
1) CL4176 L1 DNA-S.malt Seq-1
2) CL4176 L1 DNA-B.thur
3) CL4176 L1 DNA phsp16
4) MN4176 L1 DNA-S.malt Seq-1
5) MN4176 L1 DNA-B.thur
6) MN4176 L1 DNA phsp16
7) Blank-S.malt Seq-1
8) Blank-B.thur
9) Blank-B.thur

Figure 8.3. Detection of DNA of *S. maltophilia* and *B. thurigiensis* in CL4176 and MN4176 L1 worms by PCR analysis after egg purification. 100 ng of genomic DNA were amplified with primer specific for *S.maltophilia* (S.malt Seq-1, Table 8.1), *B.thurigiensis* (B.thur, Table 8.1) or the *C.elegans* promoter of *hsp-16* (phsp16, Forward: TCTGAGCCCGCTTTCCTTAT; Reverse: AGAACATTCGAGCTGCTTGT).

Data shown in Figure 8.3 clearly demonstrated a very low amplification of the DNA of bacterial origin in both *C. elegans* strains, in comparison with the amplification of the DNA sequence of the promoter of the *C. elegans* gene *hsp-16* (lane 3 and 6, Fig. 8.3), here used as positive control.

8.2 Results from the second whole genome sequencing.

Having demonstrated the complete absence of any bacterial contamination in *C. elegans*, a second whole genome sequencing of wild type and EMS-treated CL4176 DNA was performed. After alignment with DNA of the N2 founder worms, bioinformatics algorithms were used to call newly acquired base substitution, or small insertion or deletions, listed in Table 8.2.

For both strains, a huge amount of mutations in their DNA was discovered, compared to the deposited reference genome of N2 worms (Table 8.2).

type of mutations	CL4176		MN4176	
	n°	%	n°	%
downstream gene variant	7199	**32,445466**	6892	**32,1380275**
frameshift variant	111	**0,50027042**	101	**0,47097225**
intron variant	5566	**25,0856319**	5182	**24,1641408**
missense mutations	771	**3,47485127**	811	**3,78176731**
non coding transcript exon variant	95	**0,42815937**	102	**0,47563535**
splice region variant	117	**0,52731206**	96	**0,4476568**
stop gained	12	**0,05408329**	22	**0,10258802**
stop lost	1	**0,00450694**	1	**0,00466309**
synonymous variant	938	**4,22751037**	996	**4,64443926**
upstream gene variant	7378	**33,2522084**	7242	**33,7701096**

Table 8.2 Total number of mutations found in CL4176 and MN4176 worms after whole genome sequencing.

Similar numbers of mutations were found between the two *C. elegans* strains, suggesting that most of these mutations were not due to treatment with EMS, because they were also present, in similar percentages, in control CL4176 (Table 8.2). These variant could be originated by the irradiation of CL4176 worms with γ-rays, a procedure used to integrate the plasmid DNA carrying the Aβ minigene in the chromosomal DNA[257]. Indeed, as shown in Table 8.3, a large proportion of mutations in the DNA of MN4176 worms (ranging from 40 to more than 60%) was found identical in the DNA of CL4176 worms. The majority of the mutations fell, for both worm strains, in non coding regions of DNA (downstream gene variant and upstream gene variant) or inside intronic regions.

type of mutations	n°	**%**
downstream gene variant	4531	**65,75**
frameshift variant	60	**60,39**
intron variant	3334	**64,35**
missense mutations	466	**57,58**
non coding transcript exon variant	66	**65,68**
splice region variant	50	**53,12**
stop gained	9	**40,9**
stop lost	1	**100**
synonymous variant	532	**53,41**
upstream gene variant	4412	**60,92**

Table 8.3 Number and percentages of mutations found in MN4176 worms found identical in CL4176 worms, afterwhole genome sequencing.

Mutations that likely altered gene functions, including for example frameshift variants, missense mutations and stop gained mutations, represented less than 5% of the total amount of mutations found in worms. Finally, less than 20% of the total mutations were found to be unique for each worm strain analyzed.

To gain insight of a specific effect of EMS in mutagenized worms, we focussed on our attention on mutations that likely affected protein functions. In addition, only mutations with an allelic frequency of 1, (i.e. mutations found in homozygous state), were considered. In this way, only mutations that effectively could be generated by treatment with EMS were selected. These mutations, once transmitted to the following generations in homozygous state, possibly generated the phenotype of interest.

Notably, in CL4176 wild type worm no mutations in the homozygous state affecting protein function were found. On the contrary, in EMS-treated worms several specific mutations leading to putative loss of protein function were identified. Most of the mutations generated by EMS treatment in MN4176 worms were G to A or C to T transitions, as previously reported in literature[227].

The identified mutations were:

1) Point mutations that led to premature stop codons, which resulted in a truncated and likely inactive protein (Table 8.4). The genes found were C18E3.5, which is predicted to code a protein involved in egg laying and C17E4.10. However, no data about its function is available.

Gene	Consequence	Amino acid change	Codon change	Process
C18E3.5	stop_gained	W/*	tGg/tAg	Ovipostion
C17E4.10	stop_gained	W/*	tgG/tgA	Protein binding

Table 8.4. Stop codon mutations in MN4176 worms. Annotations were from Wormbase

To confirm that the stop codon mutations were not due to any sequencing errors, a set of oligonucleotidic primers was designed in order to amplify regions of DNA sequence of C18E3.5 and C17E4.10 containing the mutations (Table 8.5).

Sequence Name	Sequence
C18E3.5stop_forward	GTTTTGGACGCGGAATTAAA
C18E3.5stop_reverse	CATTTGAGGACCTCGACGAT
C17E4.10stop_forward	CCTCGATTCTCCATCCAAAG
C17E4.10stop_reverse	TGTATTTGGAGCATCTGACTGAG

Table 8.5. Oligonucleotidic primers for stop codon mutations.

Then, genomic DNA from CL4176 and MN4176 was extracted and amplified by PCR with the primers listed in Table 8.5. PCR products were separated on agarose gel, then DNA was purified and sequenced by Sanger analysis.

As shown in Figure 8.4 and Figure 8.5, the expected single point substitution G to A was found in C18E3.5 and C17E4.10 genes of MN4176 worms, confirming the results of the whole genome sequencing. Moreover, the presence of a single peak, corresponding to a single base in that specific position, indicated the homozygosity of the stop codon mutation for both the interested genes, as predicted by whole genome sequencing analysis.

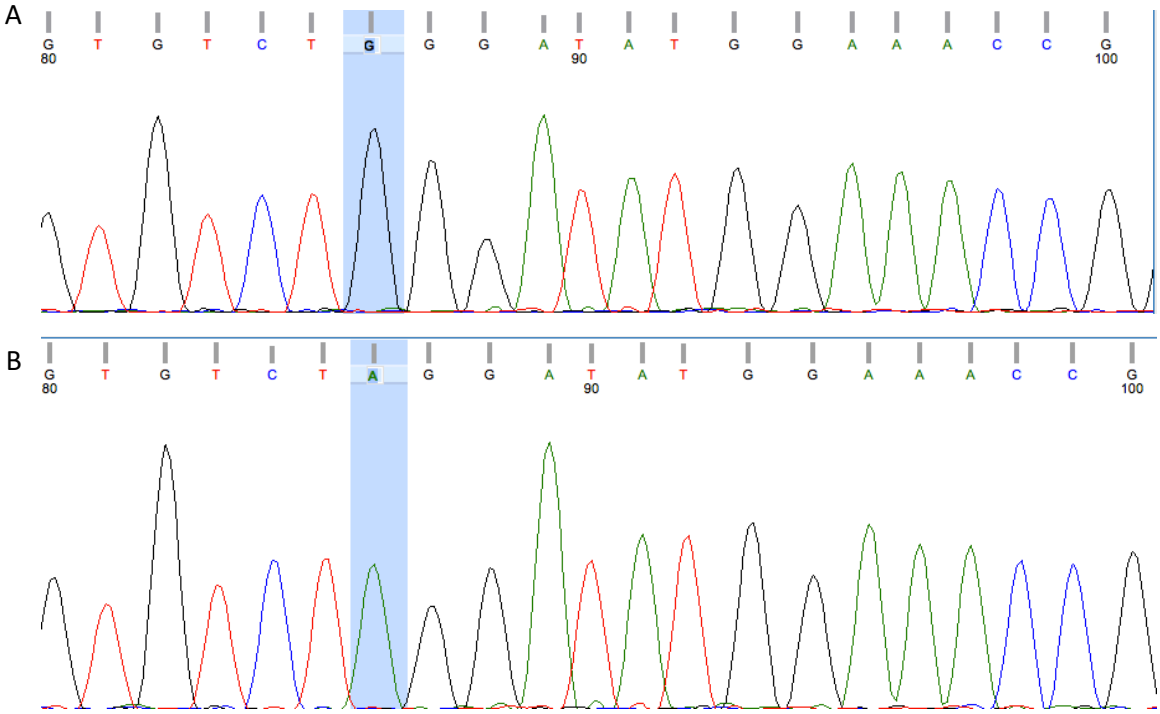

Figure 8.4. Analysis of DNA sequence of C18E3.5 gene in A) CL4176 and B) MN4176 worms. DNA sequences were obtained by PCR using oligonucleotidic primers listed in Table 8.4. The site of mutation is highlighted in blue.

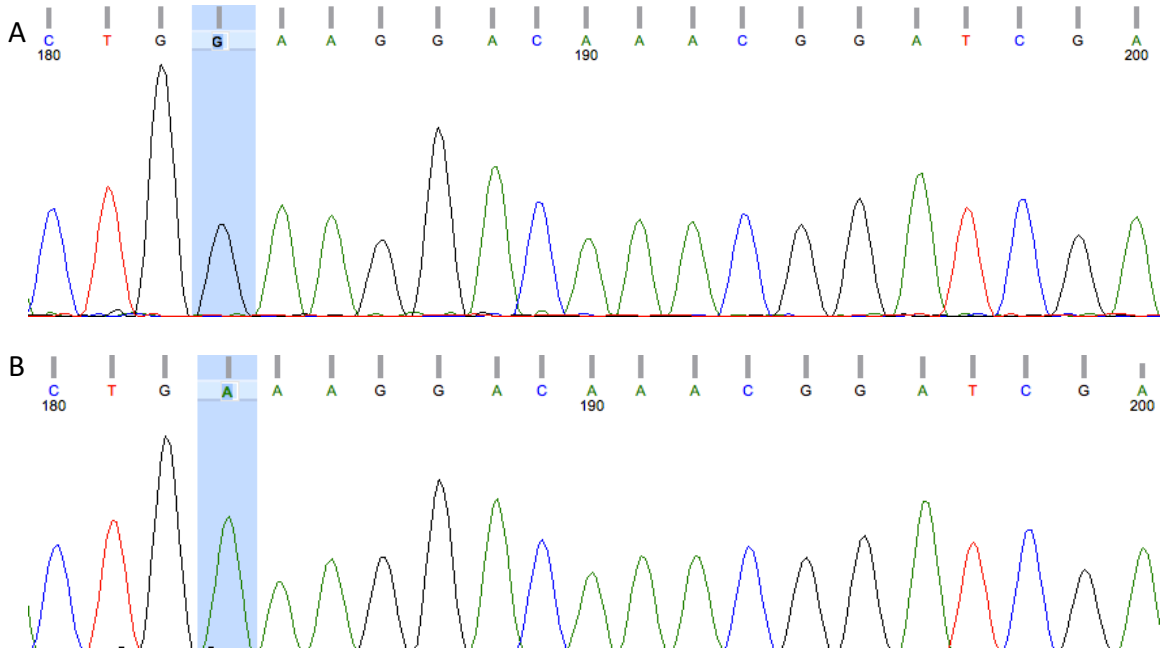

Figure 8.5. Analysis of DNA sequence of C17E4.10 gene in A) CL4176 and B) MN4176 worms. DNA sequences were obtained by PCR using oligonucleotidic primers listed in Table 8.4. The site of mutation is highlighted in blue.

2) point mutations that led to missense substitutions, which resulted in the change of a single amino acid (Table 8.6). 19 genes with missense mutations were found in MN4176 worms, encoding for proteins involved in different biological processes, such as reproduction, protein transport and lipid storage and metabolism. Most importantly, several genes found in this category were previously described to regulate worm longevity. For example, three genes (B0205.10, Y47H9C.9 and Y39F10C.1) were correlated with the determination of lifespan in *C. elegans*. While RNAi-mediated deletion of B0205.10 and Y47H9C.9 shortened lifespan[310,311], inactivation of Y39F10C.1 increases longevity[312].

Gene	Consequence	Amino acid change	Codon change	Process
F53G12.9	missense_variant	R/Q	cGa/cAa	Unknown
mbtr-1	missense_variant	R/C	Cgt/Tgt	Regultion of transcription
Y51F10.3	missense_variant	V/I	Gtt/Att	Unknown
lpd-3	missense_variant	P/L	cCg/cTg	Lipid storage
ZK973.1	missense_variant	D/N	Gac/Aac	Nucleic acid metabolism
ubr-4	missense_variant	S/T	Tcg/Acg	stability of MEC-2 complex
pnk-1	missense_variant	V/M	Gtg/Atg	Lipid storage
F26B1.5	missense_variant	R/K	aGa/aAa	Protein dephosphorylaton
hpo-11	missense_variant	S/L	tCa/tTa	Lipid storage
fcp-1	missense_variant	A/V	gCt/gTt	Embryo development
sec-8	missense_variant	G/R	Gga/Aga	Protein transport
B0205.10	missense_variant	I/F	Att/Ttt	Adult lifespan
Y47H9C.9	missense_variant	F/L	ttC/ttA	Adult lifespan
F41D3.9	missense_variant	A/T	Gca/Aca	Unknown
clec-13	missense_variant	A/T	Gcc/Acc	Innate immunity
clec-15	missense_variant	A/T	Gcc/Acc	Innate immunity
acox-1	missense_variant	G/E	gGa/gAa	Lipid metabolism
ZK1225.1	missense_variant	D/N	Gat/Aat	Unknown
Y39F10C.1	missense_variant	P/S	Cca/Tca	Adult lifespan

Table 8.6 Missense mutations found in MN4176 worms. Annotations were from Wormbase

Overall, the second genome wide screening identified several genes with single point mutations that could have an impact on protein function. However, many of these genes have not yet fully characterized, thus it's difficult to predict a possible interaction with Aβ oligomers or with pathways that mediate their toxicity.

9. Analysis of IIS pathway activation in CL4176 and MN4176 worms

In *C. elegans*, the Insulin/Insulin-like growth factor signalling (IIS) cascade regulates worm longevity, under DAF-16 mediated-expression of different genes[313]. It has been previously shown that the expression of Aβ oligomers in transgenic CL4176 worms leads to the induction of specific genes involved in stress-mediated response, including those related to the IIS pathway[257,258].

The *C. elegans* IIS cascade is nearly identical in mammals, and several studies performed in *C. elegans* models of proteotoxicity indicate that this pathway links aging with the onset of protein aggregation and neurodegeneration[235,251].

It was investigated if, even in EMS-treated CL4176 worms, the expression of Aβ oligomers resulted in the induction of *daf-18,* the sole regulator of the IIS cascade. To do so, qRT-PCR analysis was performed in CL4176 and MN4176 worms induced for 48 hours.

After 48 hours of temperature rise, MN4176 worms increased the expression of *daf-18* mRNA, with levels comparable to that of induced CL4176 worms (Fig. 9.1).

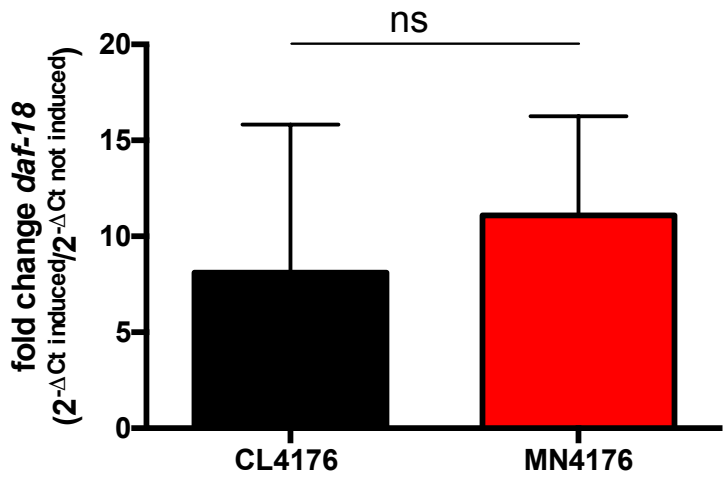

Figure 9.1 Induction of *daf-18* gene expression in CL4176 and MN4176 worms. Data are expressed as fold change (mean ± SD, n=4) ns = not significant, *p*>0,05 t-test analysis of MN4176 vs CL4176.

Then, the expression of the target genes of DAF-16 was analyzed, in particular the heat small proteins (HSP) chaperons family, including *hsp-16.2* and *hsp-16.41.* The upregulation of these genes due to the expression of toxic Aβ oligomers had also been previously demonstrated[257,258].

Figure 9.2 shows the results of RT-QPCR assay for the gene expression of *hsp-16.2* and *hsp-16.41* in CL4176 and in MN4176 worms.

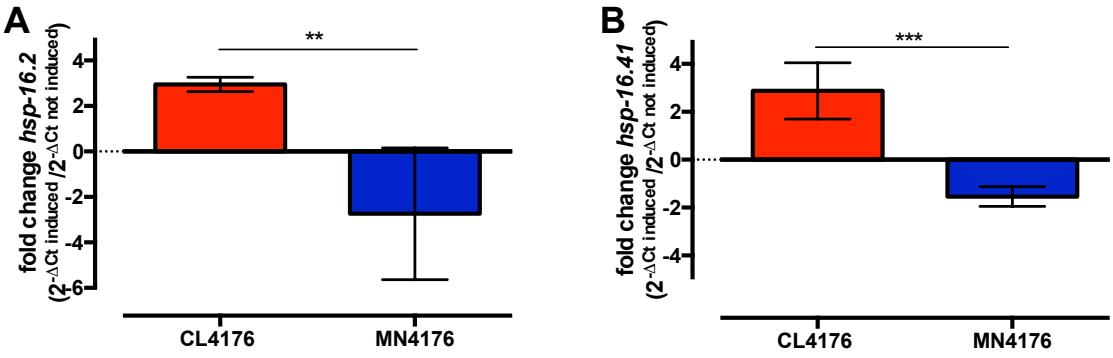

Figure 9.2 Induction of *hsp* genes in CL4176 and MN4176 worms. A) relative *hsp-16.2* mRNA and B) relative *hsp-16.41* mRNA levels. **, *** $p<0,05$ t-test analysis of MN4176 vs CL4176.

In CL4176 worms it was observed, as expected, that the raising of temperature enhanced the transcription of *hsp-16.2* and *hsp-16.41* (Fig. 9.2). This was not found in induced MN4176 worms, where the transcription was actually downregulated (Fig. 9.2).

In conclusion, these data suggest that activation of the IIS pathway and transcription of HSP chaperons could play an important role Aβ toxicity, as demonstrated by comparing the results in CL4176 worms (showing Aβ-induced paralysis) with those in MN4176 worms (protected from paralysis).

DISCUSSION

The aim of this project was to identify genetic regulators involved in the toxicity or in the formation of Aβ oligomers, by using an unbiased genome-wide screening in a transgenic *C. elegans* model of AD.

Numerous genome-wide screenings have been employed in *C. elegans* models of protein misfolding and aggregation diseases. These screens have identified a multifaceted network of mediators of protein aggregation and toxicity. These mediators include proteins with a known role in maintaining homeostasis, but also proteins involved in unrelated pathways.

To the best of my knowledge, this is the first genome-wide screening ever performed in transgenic *C. elegans* expressing Aβ. In this model, the inducible expression of the human Aβ1-42 peptide in the body wall muscles leads to a rapid paralysis and death[257]. It was previously shown that the paralysis of these transgenic worms is strictly associated with the accumulation of Aβ oligomeric species[255].

After chemical mutagenesis by EMS, a viable mutant clone resistant to paralysis was obtained. Notably, this clone showed no paralysis even at longer induction times, suggesting that the effects of mutagenesis did not result just a delay in paralysis onset.

An extensive work was carried out to evaluate the Aβ expression in this clone. Genetic and biochemical studies confirmed that the chemical mutagenesis did not alter the Aβ coding sequence DNA, nor impaired Aβ mRNA transcription. More importantly, induced mutated worms were able to produce Aβ protein to similar levels compared to the control CL4176 strain. Finally, Aβ expression resulted in

the formation of Aβ oligomers in both strains. Thus, in MN4176 worms, resistance to paralysis was not due to defects in Aβ oligomers formation, and this simple model represent a unique *in vivo* system where the expression of Aβ oligomers do not cause toxicity.

Other clones other than MN4176 were identified after EMS mutagenesis. When induced to express Aβ oligomers, these worms showed different paralysis kinetics, compared to the control strain CL4176. The most striking differences were observed after 24 hours of temperature shift, where in most of the mutated worms no paralysis was observed. However, after 48 hours of temperature increase, these worms almost completely get paralyzed. It could possible that mutations in specific genes could completely abolish the toxic effect of Aβ oligomers (as observed in MN4176 worms), while mutations in other genes modulate and/or delayed the Aβ oligomers-induced paralysis.

Then, next generation sequencing was performed to identify the genes specifically mutated in the paralysis-resistant strain, in comparison with the control strain. Unexpectedly, in the first experiment we found a huge bacterial contamination in all the worm strains analyzed, which severely affected the quality of the sequencing. Thus, the recent establishment of high throughput DNA sequencing analysis necessitates to pay attention in developing strategies to avoid any contamination. We successfully eliminated any bacterial contamination from CL4176 and MN4176 worms, allowing us to obtain high quality worm DNA needed to perform whole genomic sequencing.

After the sequencing, we refined the analysis in order to select only homozygous mutations affecting protein function specific for MN4176 worms. Most of these mutations were G to A single substitutions, as expected with EMS mutagenesis[227]. Following this analysis, only two genes were found with mutations associated with a stop codon, suggesting the expression of truncated and, likely, inactive proteins. However, no functional data about these genes is reported, thus limiting possible considerations about their possible interaction with Aβ oligomers. RNAi- mediated silencing of the expression of these genes in CL4176 worms will provide important clues about their role in Aβ oligomers-mediated toxicity.

The rest of the mutations found in MN4176 worms were missense mutations, in which a single base substitution led to a change in the coded amino acid. However, it is difficult to predict if these types of mutations actually affect the protein function. The mutated genes found in MN4176 worms encodes for proteins involved in different biological functions, for example DNA/RNA metabolism, protein trafficking, determination of adult lifespan or lipid storage and metabolism. It has been previously demonstrated with polyglutammine proteins that aggregation can be regulated by a complex integration of biosynthetic events, from RNA synthesis to protein degradation[284]. Thus, it could also be possible that the genes mutated in MN4176 play in an orchestrated manner to mediate the formation or the toxicity of Aβ oligomers.

Among the candidate genes, one was mutated, named *pnk-1*, which in previous reports was correlated with nematode ageing.

pnk-1 is the ortholog of human PNK4 gene and encodes one of the two pantothenate kinase in *C. elegans*, the rate-limiting enzymes involved in the biosynthesis of coenzyme A[314]. Deletion of *pnk-1* leads to a decreased motility and

lifespan[314,315]. It has been also suggested that *pnk-1* could be a direct target of *daf-16*[311,316], the main downstream effector of the Insulin/Insulin-like growth factor signalling (IIS) cascade[238].

In *C. elegans* the IIS cascade is known to regulate energy and lipid metabolism, lifespan and protein homeostasis in response to different stress agents such as heat shock, oxidative stress and aggregated misfolded proteins[235,238]. *daf-16* is negatively regulated by *daf-2,* which encodes the worm insulin receptor; decreased *daf-2* activity extends worm lifespan. Interestingly, in mutant worms with reduced expression of *daf-2, pnk-1* mRNA levels were found increased up to 5 times[316]. However, the role of this gene in relation to Aβ oligomers-mediated toxicity has never been investigated; to address this point, a possible future strategy will be the use of RNA interference to downregulate the expression of *pnk-1* in CL4176 worms and then evaluate the effects on worm paralysis. A reduction or abrogation of paralysis, as observed in MN4176 worms, could help to elucidate the molecular mechanisms underlying the toxicity induced by Aβ.

Another gene found mutated in MN4176 worms was *sec-8,* which encode for a component of the exocyst complex, a multiple protein complex essential for targeting exocytic vesicles to specific docking sites on the plasma membrane, allowing the delivery of specific receptors to their location, for example NMDAR receptors targeted at post-synaptic densities[317]. Interestingly, like *pnk*-1, the promoter region of *sec-8* contain the DAF-16 binding DNA sequence TTGTTTAC[316]. It is possible that, as for many genes target of DAF-16, also the expression of *pnk-1* and *sec-8* could be regulated in response to Aβ oligomers.

Finally, another possible DAF-16 downstream gene found mutated in MN4176 worms was Y39F10C.1, encoding for a vitellogenin membrane outer layer protein,

likely involved in reproduction. In previous studies[312], inactivation of this gene led to an increase in lifespan, suggesting that the vast amount of energy a worm spend on reproduction could limit the resources needed for life maintenance.
How suppression of the expression of Y39F10C.1 may affect Aβ oligomer-mediated toxicity remains to be clarified and will be the subject of future studies.

Different lines of evidence suggest that a reduction of IIS protects from toxic protein aggregation. It has been shown that in worms expressing toxic aggregated polyQ stretches, a downregulation of components of the IIS cascade mediated by RNA interference led to a reduction of the toxicity[236]. These findings were also confirmed in transgenic worms expressing Aβ[235]. These studies have also demonstrated the role of molecular chaperones as important players in protection from proteotoxicity. Among them, the family of small heat shock proteins (*hsp*)-16, which expression is dependent of *daf-16*, has been found to be upregulated in response to Aβ aggregation and to interact directly with Aβ fibrils in transgenic *C. elegans*[251,257,258]. This chaperon family is homologous to human alphaB-crystallin, an intracellular ATP-independent heat shock protein which role is to prevent protein aggregation by binding to improperly folded proteins[318,319]. Notably, different studies have shown that alphaB-crystallin is increased in the brains of AD patients and is associated with senile plaques[320,321]. These observations also point to a significant role of the intracellular Aβ pool in Alzheimer's disease, thus confirming the validity of transgenic *C. elegans* expressing intracellular Aβ as a simple model to study the mechanisms of Aβ oligomers-induced toxicity. In this thesis, it has been demonstrated that, following Aβ oligomers expression in

CL4176 worms, the induction of *daf-18*, the sole regulator of the IIS cascade, led to an upregulation of *hsp-16 genes*, as previously shown[257,258]. Surprisingly, in mutagenized MN4176 worms, where Aβ oligomers did not cause paralysis, the expression of *hsp-16* genes was downregulated, although the induction levels of *daf-18* were comparable to those of CL4176. This observation may indicate that in *C. elegans*, different molecular pathways, other than the IIS cascade, regulate the expression of specific genes important for the response to toxic aggregated proteins. This is, for example, the case of HSF-1, which has been demonstrated to have a joint activity with DAF-16 in regulating proteotoxicity in *C. elegans*[235,238]. Another protein, MOAG-4, not related to the IIS cascade or other aging-related pathways, has been recently linked to the toxicity of misfolded proteins[277]. Future studies will evaluate the upregulation of HSF-1 and MOAG-4 in MN4176 worms, with or without induction of the expression of Aβ oligomers.

The finding that in MN4176 the downregulation of *hsp-16* genes is correlated with the absence of paralysis in the presence of Aβ, may suggest that alphaB-crystallin promotes the formation of toxic Aβ oligomers, by binding directly to the misfolded peptide. This hypothesis is in contrast with the general idea that the induction of DAF-16 target genes (including *hsp-16*) is a protective mechanism, either by mediating Aβ disaggregation or by fostering the aggregation of Aβ in higher molecular assemblies, with lower toxicity[238]. To find out the role of alphaB-crystallin it could be relevant to silence the expression of *hsp-16* in CL4176 worms and evaluate the effects of this downregulation on Aβ oligomers-induced paralysis.

In conclusion, the data obtained in this thesis work and the evidences found in literature suggest that, among the mutated genes found in MN4176 worms, there could be novel mediators of Aβ oligomers toxicity in *C. elegans*. How these genes and their related proteins act, for example by interacting directly with misfolded Aβ or by regulating specific molecular pathways such as the IIS cascade, has still to be elucidated. As demonstrated by various genome-wide screenings in *C. elegans* models of protein misfolded diseases, several proteins are involved in protein homeostasis. Thus, it cannot be excluded that, in CL4176 strain, different proteins participate in the Aβ oligomers-induced paralysis.

Although more studies are needed to confirm and substantiate the data obtained from the genome-wide screening, the mutated CL4176 strain obtained during the course of this thesis represent a novel tool to investigate in *C. elegans* the mechanisms of Aβ oligomer toxicity.

BIBLIOGRAPHY

1. Radford, S. E. & Dobson, C. M. From computer simulations to human disease: emerging themes in protein folding. *Cell* **97,** 291–298 (1999).
2. Dobson, C. M. Protein folding and misfolding. *Nature* **426,** 884–890 (2003).
3. Ingram, V. M. Gene mutations in human haemoglobin: the chemical difference between normal and sickle cell haemoglobin. *Nature* **180,** 326–328 (1957).
4. Hunt, J. A. & Ingram, V. M. Human haemoglobin E: the chemical effect of gene mutation. *Nature* **184,** 870–872 (1959).
5. Gibson, J. S. & Ellory, J. C. Membrane transport in sickle cell disease. *Blood Cells Mol. Dis.* **28,** 303–314 (2002).
6. Dobson, C. M. & Ellis, R. J. Protein folding and misfolding inside and outside the cell. in **17,** 5251–5254 (EMBO Press, 1998).
7. Dobson, C. M. & Karplus, M. The fundamentals of protein folding: bringing together theory and experiment. *Current Opinion in Structural Biology* **9,** 92–101 (1999).
8. Brockwell, D. J. & Radford, S. E. Intermediates: ubiquitous species on folding energy landscapes? *Current Opinion in Structural Biology* **17,** 30–37 (2007).
9. Dinner, A. R., Sali, A., Smith, L. J., Dobson, C. M. & Karplus, M. Understanding protein folding via free-energy surfaces from theory and experiment. *Trends in Biochemical Sciences* **25,** 331–339 (2000).
10. Ellis, R. J. Molecular chaperones: inside and outside the Anfinsen cage. *Curr. Biol.* **11,** R1038–40 (2001).
11. Bukau, B. & Horwich, A. L. The Hsp70 and Hsp60 chaperone machines. *Cell* **92,** 351–366 (1998).
12. Hartl, F. U. & Hayer-Hartl, M. Molecular chaperones in the cytosol: from nascent chain to folded protein. *Science* **295,** 1852–1858 (2002).
13. Balchin, D., Hayer-Hartl, M. & Hartl, F. U. In vivo aspects of protein folding and quality control. *Science* **353,** aac4354–aac4354 (2016).
14. Hayer-Hartl, M. K., Weber, F. & Hartl, F. U. Mechanism of chaperonin action: GroES binding and release can drive GroEL-mediated protein folding in the absence of ATP hydrolysis. *The EMBO Journal* **15,** 6111–6121 (1996).

15. Kim, Y. E., Hipp, M. S., Bracher, A., Hayer-Hartl, M. & Hartl, F. U. Molecular chaperone functions in protein folding and proteostasis. *Annu. Rev. Biochem.* **82,** 323–355 (2013).

16. Hartl, F. U., Bracher, A. & Hayer-Hartl, M. Molecular chaperones in protein folding and proteostasis. *Nature* **475,** 324–332 (2011).

17. Hardesty, B. & Kramer, G. Folding of a nascent peptide on the ribosome. *Prog. Nucleic Acid Res. Mol. Biol.* **66,** 41–66 (2001).

18. Schiene, C. & Fischer, G. Enzymes that catalyse the restructuring of proteins. *Current Opinion in Structural Biology* **10,** 40–45 (2000).

19. Brehme, M. *et al.* A chaperome subnetwork safeguards proteostasis in aging and neurodegenerative disease. *CellReports* **9,** 1135–1150 (2014).

20. Hipp, M. S., Park, S.-H. & Hartl, F. U. Proteostasis impairment in protein-misfolding and -aggregation diseases. *Trends Cell Biol.* **24,** 506–514 (2014).

21. Taipale, M. *et al.* A quantitative chaperone interaction network reveals the architecture of cellular protein homeostasis pathways. *Cell* **158,** 434–448 (2014).

22. Anckar, J. & Sistonen, L. Regulation of HSF1 function in the heat stress response: implications in aging and disease. *Annu. Rev. Biochem.* **80,** 1089–1115 (2011).

23. Walter, P. & Ron, D. The unfolded protein response: from stress pathway to homeostatic regulation. *Science* **334,** 1081–1086 (2011).

24. Hammond, C. & Helenius, A. Quality control in the secretory pathway. *Curr. Opin. Cell Biol.* **7,** 523–529 (1995).

25. Shemorry, A., Hwang, C.-S. & Varshavsky, A. Control of protein quality and stoichiometries by N-terminal acetylation and the N-end rule pathway. *Mol. Cell* **50,** 540–551 (2013).

26. Ciechanover, A. & Kwon, Y. T. Degradation of misfolded proteins in neurodegenerative diseases: therapeutic targets and strategies. *Exp. Mol. Med.* **47,** e147 (2015).

27. Qu, B. H., Strickland, E. & Thomas, P. J. Cystic fibrosis: a disease of altered protein folding. *J. Bioenerg. Biomembr.* **29,** 483–490 (1997).

28. Perlmutter, D. H. & Silverman, G. A. Hepatic fibrosis and carcinogenesis in α1-antitrypsin deficiency: a prototype for chronic tissue damage in gain-of-function disorders. *Cold Spring Harb Perspect Biol* **3,** a005801–a005801 (2011).

29. Lomas, D. A., Evans, D. L., Finch, J. T. & Carrell, R. W. The mechanism of Z alpha 1-antitrypsin accumulation in the liver. *Nature* **357,** 605–607 (1992).

30. Hidvegi, T., Schmidt, B. Z., Hale, P. & Perlmutter, D. H. Accumulation of mutant alpha1-antitrypsin Z in the endoplasmic reticulum activates caspases-4 and caspase-12, NFkappaB, and BAP31 but not the unfolded protein response. *Journal of Biological Chemistry* **280,** 39002–39015 (2005).

31. Soto, C. Unfolding the role of protein misfolding in neurodegenerative diseases. *Nat Rev Neurosci* **4,** 49–60 (2003).

32. Sunde, M. & Blake, C. The structure of amyloid fibrils by electron microscopy and X-ray diffraction. *Adv. Protein Chem.* **50,** 123–159 (1997).

33. Fändrich, M. & Dobson, C. M. The behaviour of polyamino acids reveals an inverse side chain effect in amyloid structure formation. *The EMBO Journal* **21,** 5682–5690 (2002).

34. Westermark, P. Aspects on human amyloid forms and their fibril polypeptides. *FEBS J.* **272,** 5942–5949 (2005).

35. Pedersen, J. S. *et al.* The changing face of glucagon fibrillation: structural polymorphism and conformational imprinting. *J. Mol. Biol.* **355,** 501–523 (2006).

36. Soto, C. Protein misfolding and disease; protein refolding and therapy. *FEBS Lett.* **498,** 204–207 (2001).

37. Teplow, D. B. Structural and kinetic features of amyloid beta-protein fibrillogenesis. *Amyloid* **5,** 121–142 (1998).

38. Mrak, R. E., Griffin, S. T. & Graham, D. I. Aging-associated changes in human brain. *J. Neuropathol. Exp. Neurol.* **56,** 1269–1275 (1997).

39. Chiti, F. & Dobson, C. M. Protein misfolding, functional amyloid, and human disease. *Annu. Rev. Biochem.* **75,** 333–366 (2006).

40. Caughey, B. & Lansbury, P. T. Protofibrils, pores, fibrils, and neurodegeneration: separating the responsible protein aggregates from the innocent bystanders. *Annu. Rev. Neurosci.* **26,** 267–298 (2003).

41. Bitan, G., Vollers, S. S. & Teplow, D. B. Elucidation of primary structure elements controlling early amyloid beta protein oligomerization. *Journal of Biological Chemistry* **278,** 34882–34889 (2003).

42. Harper, J. D. & Lansbury, P. T. Models of amyloid seeding in Alzheimer's disease and scrapie: mechanistic truths and physiological consequences of the time-dependent solubility of amyloid proteins. *Annu. Rev. Biochem.* **66,** 385–407 (1997).

43. Kane, M. D. *et al.* Evidence for seeding of beta -amyloid by intracerebral infusion of Alzheimer brain extracts in beta -amyloid precursor protein-transgenic mice. *J. Neurosci.* **20,** 3606–3611 (2000).

44. Griffith, J. S. Self-replication and scrapie. *Nature* **215,** 1043–1044 (1967).

45. Gajdusek, D. C. Transmissible and non-transmissible amyloidoses: autocatalytic post-translational conversion of host precursor proteins to beta-pleated sheet configurations. *J. Neuroimmunol.* **20,** 95–110 (1988).

46. Prusiner, S. B. Molecular biology of prion diseases. *Science* **252,** 1515–1522 (1991).

47. Walsh, D. M., Lomakin, A., Benedek, G. B., Condron, M. M. & Teplow, D. B. Amyloid beta-protein fibrillogenesis. Detection of a protofibrillar intermediate. *Journal of Biological Chemistry* **272,** 22364–22372 (1997).

48. Walsh, D. M. *et al.* Amyloid beta-protein fibrillogenesis. Structure and biological activity of protofibrillar intermediates. *Journal of Biological Chemistry* **274,** 25945–25952 (1999).

49. Martin, J. B. Molecular basis of the neurodegenerative disorders. *N Engl J Med* **340,** 1970–1980 (1999).

50. Mastrianni, J. A. The prion diseases: Creutzfeldt-Jakob, Gerstmann-Sträussler-Scheinker, and related disorders. *J Geriatr Psychiatry Neurol* **11,** 78–97 (1998).

51. Mastrianni, J. A. The genetics of prion diseases. *Genet. Med.* **12,** 187–195 (2010).

52. Shiga, Y. *et al.* Diffusion-weighted MRI abnormalities as an early diagnostic marker for Creutzfeldt-Jakob disease. *Neurology* **63,** 443–449 (2004).

53. Mastrianni, J. A. *et al.* Prion protein conformation in a patient with sporadic fatal insomnia. *N Engl J Med* **340,** 1630–1638 (1999).

54. Gambetti, P., Parchi, P., Petersen, R. B., Chen, S. G. & Lugaresi, E. Fatal familial insomnia and familial Creutzfeldt-Jakob disease: clinical, pathological and molecular features. *Brain Pathol.* **5,** 43–51 (1995).

55. Hsiao, K. K. *et al.* A prion protein variant in a family with the telencephalic form of Gerstmann-Sträussler-Scheinker syndrome. *Neurology* **41,** 681–684 (1991).

56. Reaume, A. G. *et al.* Motor neurons in Cu/Zn superoxide dismutase-deficient mice develop normally but exhibit enhanced cell death after axonal injury. *Nat. Genet.* **13,** 43–47 (1996).

57. Lundmark, K. *et al.* Transmissibility of systemic amyloidosis by a prion-like mechanism. *Proceedings of the National Academy of Sciences* **99,** 6979–6984 (2002).

58. Games, D. *et al.* Alzheimer-type neuropathology in transgenic mice overexpressing V717F beta-amyloid precursor protein. *Nature* **373,** 523–527 (1995).

59. Masliah, E. *et al.* Dopaminergic loss and inclusion body formation in alpha-synuclein mice: implications for neurodegenerative disorders. *Science* **287,** 1265–1269 (2000).

60. Mangiarini, L. *et al.* Exon 1 of the HD gene with an expanded CAG repeat is sufficient to cause a progressive neurological phenotype in transgenic mice. *Cell* **87,** 493–506 (1996).

61. Gurney, M. E. Transgenic-mouse model of amyotrophic lateral sclerosis. *N Engl J Med* **331,** 1721–1722 (1994).

62. Hsiao, K. K. *et al.* Spontaneous neurodegeneration in transgenic mice with mutant prion protein. *Science* **250,** 1587–1590 (1990).

63. Tsukada, M. & Ohsumi, Y. Isolation and characterization of autophagy-defective mutants of Saccharomyces cerevisiae. *FEBS Lett.* **333,** 169–174 (1993).

64. Mizushima, N., Levine, B., Cuervo, A. M. & Klionsky, D. J. Autophagy fights disease through cellular self-digestion. *Nature* **451,** 1069–1075 (2008).

65. Ravikumar, B., Duden, R. & Rubinsztein, D. C. Aggregate-prone proteins with polyglutamine and polyalanine expansions are degraded by autophagy. *Hum. Mol. Genet.* **11,** 1107–1117 (2002).

66. Webb, J. L., Ravikumar, B., Atkins, J., Skepper, J. N. & Rubinsztein, D. C. Alpha-Synuclein is degraded by both autophagy and the proteasome. *Journal of Biological Chemistry* **278,** 25009–25013 (2003).

67. Barmada, S. J. *et al.* Autophagy induction enhances TDP43 turnover and survival in neuronal ALS models. *Nat Chem Biol* **10,** 677–685 (2014).

68. Berger, Z. *et al.* Rapamycin alleviates toxicity of different aggregate-prone proteins. *Hum. Mol. Genet.* **15,** 433–442 (2006).

69. Williams, A. *et al.* Aggregate-prone proteins are cleared from the cytosol by autophagy:

therapeutic implications. *Curr. Top. Dev. Biol.* **76,** 89–101 (2006).

70. Nixon, R. A. *et al.* Extensive involvement of autophagy in Alzheimer disease: an immuno-electron microscopy study. *J. Neuropathol. Exp. Neurol.* **64,** 113–122 (2005).

71. Boland, B. *et al.* Autophagy induction and autophagosome clearance in neurons: relationship to autophagic pathology in Alzheimer's disease. *J. Neurosci.* **28,** 6926–6937 (2008).

72. Xing, Y. *et al.* Transmission of mouse senile amyloidosis. *Lab. Invest.* **81,** 493–499 (2001).

73. Schmidt, A. M., Yan, S. D., Yan, S. F. & Stern, D. M. The biology of the receptor for advanced glycation end products and its ligands. *Biochim. Biophys. Acta* **1498,** 99–111 (2000).

74. Yan, S. D. *et al.* Receptor-dependent cell stress and amyloid accumulation in systemic amyloidosis. *Nat Med* **6,** 643–651 (2000).

75. Sousa, M. M., Yan, S. D., Stern, D. & Saraiva, M. J. Interaction of the receptor for advanced glycation end products (RAGE) with transthyretin triggers nuclear transcription factor kB (NF-kB) activation. *Lab. Invest.* **80,** 1101–1110 (2000).

76. Schmidt, A. M., Hofmann, M., Taguchi, A., Yan, S. D. & Stern, D. M. RAGE: a multiligand receptor contributing to the cellular response in diabetic vasculopathy and inflammation. *Semin. Thromb. Hemost.* **26,** 485–493 (2000).

77. Pike, L. J. Rafts defined: a report on the Keystone Symposium on Lipid Rafts and Cell Function. in **47,** 1597–1598 (American Society for Biochemistry and Molecular Biology, 2006).

78. Simons, K. & Gerl, M. J. Revitalizing membrane rafts: new tools and insights. *Nat. Rev. Mol. Cell Biol.* **11,** 688–699 (2010).

79. Michel, V. & Bakovic, M. Lipid rafts in health and disease. *Biol. Cell* **99,** 129–140 (2007).

80. Bate, C. & Williams, A. Amyloid-β-induced synapse damage is mediated via cross-linkage of cellular prion proteins. *J. Biol. Chem.* **286,** 37955–37963 (2011).

81. Bate, C. & Williams, A. Neurodegeneration induced by clustering of sialylated glycosylphosphatidylinositols of prion proteins. *J. Biol. Chem.* **287,** 7935–7944 (2012).

82. Bate, C., Tayebi, M. & Williams, A. Phospholipase A2 inhibitors protect against prion and

Abeta mediated synapse degeneration. *Mol Neurodegeneration* **5,** 13 (2010).

83. Bate, C. & Williams, A. Amyloid-β(1-40) inhibits amyloid-β(1-42) induced activation of cytoplasmic phospholipase A2 and synapse degeneration. *J. Alzheimers Dis.* **21,** 985–993 (2010).

84. Wickner, R. B. [URE3] as an altered URE2 protein: evidence for a prion analog in Saccharomyces cerevisiae. *Science* **264,** 566–569 (1994).

85. Cummings, C. J. *et al.* Chaperone suppression of aggregation and altered subcellular proteasome localization imply protein misfolding in SCA1. *Nat. Genet.* **19,** 148–154 (1998).

86. Ii, K., Ito, H., Tanaka, K. & Hirano, A. Immunocytochemical co-localization of the proteasome in ubiquitinated structures in neurodegenerative diseases and the elderly. *J. Neuropathol. Exp. Neurol.* **56,** 125–131 (1997).

87. Uptain, S. M. & Lindquist, S. Prions as protein-based genetic elements. *Annu. Rev. Microbiol.* **56,** 703–741 (2002).

88. Behl, C., Davis, J. B., Lesley, R. & Schubert, D. Hydrogen peroxide mediates amyloid beta protein toxicity. *Cell* **77,** 817–827 (1994).

89. Hsu, L. J. *et al.* alpha-synuclein promotes mitochondrial deficit and oxidative stress. *Am. J. Pathol.* **157,** 401–410 (2000).

90. Brodaty, H. *et al.* The world of dementia beyond 2020. *J Am Geriatr Soc* **59,** 923–927 (2011).

91. Alzheimer's Association. 2015 Alzheimer's disease facts and figures. *Alzheimers Dement* **11,** 332–384 (2015).

92. McKhann, G. M. *et al.* The diagnosis of dementia due to Alzheimer's disease: recommendations from the National Institute on Aging-Alzheimer"s Association workgroups on diagnostic guidelines for Alzheimer"s disease. in **7,** 263–269 (Elsevier, 2011).

93. Alzheimer, A., Stelzmann, R. A., Schnitzlein, H. N. & Murtagh, F. R. *An English translation of Alzheimer's 1907 paper, "Uber eine eigenartige Erkankung der Hirnrinde". Clinical anatomy (New York, N.Y.)* **8,** 429–431 (Wiley Subscription Services, Inc., A Wiley Company, 1995).

94. Glenner, G. G. & Wong, C. W. Alzheimer's disease: initial report of the purification and characterization of a novel cerebrovascular amyloid protein. *Biochem. Biophys. Res. Commun.* **120,** 885–890 (1984).

95. Masters, C. L. *et al.* Amyloid plaque core protein in Alzheimer disease and Down syndrome. *Proceedings of the National Academy of Sciences* **82,** 4245–4249 (1985).

96. Glenner, G. G. & Wong, C. W. Alzheimer‘s disease and Down’s syndrome: sharing of a unique cerebrovascular amyloid fibril protein. *Biochem. Biophys. Res. Commun.* **122,** 1131–1135 (1984).

97. Olson, M. I. & Shaw, C. M. Presenile dementia and Alzheimer's disease in mongolism. *Brain* **92,** 147–156 (1969).

98. Kurt, M. A., Davies, D. C. & Kidd, M. Paired helical filament morphology varies with intracellular location in Alzheimer's disease brain. *Neurosci. Lett.* **239,** 41–44 (1997).

99. Grundke-Iqbal, I. *et al.* Microtubule-associated protein tau. A component of Alzheimer paired helical filaments. *Journal of Biological Chemistry* **261,** 6084–6089 (1986).

100. Su, J. H., Cummings, B. J. & Cotman, C. W. Plaque biogenesis in brain aging and Alzheimer's disease. I. Progressive changes in phosphorylation states of paired helical filaments and neurofilaments. *Brain Res.* **739,** 79–87 (1996).

101. Blennow, K. *et al.* Longitudinal stability of CSF biomarkers in Alzheimer's disease. *Neurosci. Lett.* **419,** 18–22 (2007).

102. Bird, T. D. Genetic aspects of Alzheimer disease. *Genet. Med.* **10,** 231–239 (2008).

103. Campion, D. *et al.* Early-onset autosomal dominant Alzheimer disease: prevalence, genetic heterogeneity, and mutation spectrum. *Am. J. Hum. Genet.* **65,** 664–670 (1999).

104. Sherrington, R. *et al.* Alzheimer's disease associated with mutations in presenilin 2 is rare and variably penetrant. *Hum. Mol. Genet.* **5,** 985–988 (1996).

105. Janssen, J. C. *et al.* Early onset familial Alzheimer's disease: Mutation frequency in 31 families. *Neurology* **60,** 235–239 (2003).

106. Raux, G. *et al.* Molecular diagnosis of autosomal dominant early onset Alzheimer's disease: an update. *J. Med. Genet.* **42,** 793–795 (2005).

107. Mawuenyega, K. G. *et al.* Decreased clearance of CNS beta-amyloid in Alzheimer's disease. *Science* **330,** 1774–1774 (2010).

108. Corder, E. H. *et al.* Gene dose of apolipoprotein E type 4 allele and the risk of Alzheimer's disease in late onset families. *Science* **261,** 921–923 (1993).

109. Bu, G. Apolipoprotein E and its receptors in Alzheimer's disease: pathways, pathogenesis and therapy. *Nat Rev Neurosci* **10,** 333–344 (2009).

110. Huang, Y. & Mucke, L. Alzheimer mechanisms and therapeutic strategies. *Cell* **148,** 1204–1222 (2012).

111. Farrer, L. A. *et al.* Effects of age, sex, and ethnicity on the association between apolipoprotein E genotype and Alzheimer disease. A meta-analysis. APOE and Alzheimer Disease Meta Analysis Consortium. *JAMA* **278,** 1349–1356 (1997).

112. Hardy, J. & Selkoe, D. J. The amyloid hypothesis of Alzheimer's disease: progress and problems on the road to therapeutics. *Science* **297,** 353–356 (2002).

113. Selkoe, D. J. & Hardy, J. The amyloid hypothesis of Alzheimer's disease at 25 years. *EMBO Mol Med* **8,** 595–608 (2016).

114. LaFerla, F. M., Green, K. N. & Oddo, S. Intracellular amyloid-beta in Alzheimer's disease. *Nat Rev Neurosci* **8,** 499–509 (2007).

115. Gandy, S. The role of cerebral amyloid beta accumulation in common forms of Alzheimer disease. *J. Clin. Invest.* **115,** 1121–1129 (2005).

116. De Strooper, B. Proteases and proteolysis in Alzheimer disease: a multifactorial view on the disease process. *Physiol. Rev.* **90,** 465–494 (2010).

117. Zhou, Z.-D. *et al.* The roles of amyloid precursor protein (APP) in neurogenesis: Implications to pathogenesis and therapy of Alzheimer disease. *Cell Adh Migr* **5,** 280–292 (2011).

118. Ghosal, K., Stathopoulos, A. & Pimplikar, S. W. APP intracellular domain impairs adult neurogenesis in transgenic mice by inducing neuroinflammation. *PLoS ONE* **5,** e11866 (2010).

119. Raychaudhuri, M. & Mukhopadhyay, D. AICD Overexpression in Neuro 2A Cells Regulates Expression of PTCH1 and TRPC5. *International Journal of Alzheimer's Disease* **2011,** 1–5 (2011).

120. Gowing, E. *et al.* Chemical characterization of A beta 17-42 peptide, a component of diffuse amyloid deposits of Alzheimer disease. *Journal of Biological Chemistry* **269,**

10987–10990 (1994).

121. De Strooper, B. Aph-1, Pen-2, and Nicastrin with Presenilin generate an active gamma-Secretase complex. *Neuron* **38,** 9–12 (2003).

122. Selkoe, D. J. & Wolfe, M. S. Presenilin: running with scissors in the membrane. *Cell* **131,** 215–221 (2007).

123. Iwatsubo, T. *et al.* Visualization of A beta 42(43) and A beta 40 in senile plaques with end-specific A beta monoclonals: evidence that an initially deposited species is A beta 42(43). *Neuron* **13,** 45–53 (1994).

124. Suzuki, N. *et al.* High tissue content of soluble beta 1-40 is linked to cerebral amyloid angiopathy. *Am. J. Pathol.* **145,** 452–460 (1994).

125. Wiltfang, J. *et al.* Highly conserved and disease-specific patterns of carboxyterminally truncated Abeta peptides 1-37/38/39 in addition to 1-40/42 in Alzheimer's disease and in patients with chronic neuroinflammation. *Journal of Neurochemistry* **81,** 481–496 (2002).

126. Portelius, E. *et al.* Amyloid-β(1-15/16) as a marker for γ-secretase inhibition in Alzheimer's disease. *J. Alzheimers Dis.* **31,** 335–341 (2012).

127. Esh, C. *et al.* Altered APP processing in PDAPP (Val717 --> Phe) transgenic mice yields extended-length Abeta peptides. *Biochemistry* **44,** 13807–13819 (2005).

128. Van Vickle, G. D. *et al.* Presenilin-1 280Glu-->Ala mutation alters C-terminal APP processing yielding longer abeta peptides: implications for Alzheimer's disease. *Mol. Med.* **14,** 184–194 (2008).

129. Welander, H. *et al.* Abeta43 is more frequent than Abeta40 in amyloid plaque cores from Alzheimer disease brains. *Journal of Neurochemistry* **110,** 697–706 (2009).

130. Selkoe, D. J., Abraham, C. R., Podlisny, M. B. & Duffy, L. K. Isolation of low-molecular-weight proteins from amyloid plaque fibers in Alzheimer's disease. *Journal of Neurochemistry* **46,** 1820–1834 (1986).

131. Mori, H., Takio, K., Ogawara, M. & Selkoe, D. J. Mass spectrometry of purified amyloid beta protein in Alzheimer's disease. *Journal of Biological Chemistry* **267,** 17082–17086 (1992).

132. Sergeant, N. *et al.* Truncated beta-amyloid peptide species in pre-clinical Alzheimer's disease as new targets for the vaccination approach. *Journal of Neurochemistry* **85,**

1581–1591 (2003).

133. Pike, C. J., Overman, M. J. & Cotman, C. W. Amino-terminal deletions enhance aggregation of beta-amyloid peptides in vitro. *Journal of Biological Chemistry* **270,** 23895–23898 (1995).

134. Kummer, M. P. & Heneka, M. T. Truncated and modified amyloid-beta species. *Alzheimers Res Ther* **6,** 28 (2014).

135. Schilling, S., Hoffmann, T., Manhart, S., Hoffmann, M. & Demuth, H.-U. Glutaminyl cyclases unfold glutamyl cyclase activity under mild acid conditions. *FEBS Lett.* **563,** 191–196 (2004).

136. Schilling, S. *et al.* Glutaminyl cyclase inhibition attenuates pyroglutamate Abeta and Alzheimer's disease-like pathology. *Nat Med* **14,** 1106–1111 (2008).

137. Naslund, J. *et al.* Relative abundance of Alzheimer A beta amyloid peptide variants in Alzheimer disease and normal aging. *Proceedings of the National Academy of Sciences* **91,** 8378–8382 (1994).

138. Heneka, M. T., O'Banion, M. K., Terwel, D. & Kummer, M. P. Neuroinflammatory processes in Alzheimer's disease. *J Neural Transm (Vienna)* **117,** 919–947 (2010).

139. Szendrei, G. I. *et al.* Aspartate-bond isomerization affects the major conformations of synthetic peptides. *Eur. J. Biochem.* **226,** 917–924 (1994).

140. Shapira, R., Austin, G. E. & Mirra, S. S. Neuritic plaque amyloid in Alzheimer's disease is highly racemized. *Journal of Neurochemistry* **50,** 69–74 (1988).

141. Tomiyama, T. *et al.* Racemization of Asp23 residue affects the aggregation properties of Alzheimer amyloid beta protein analogues. *Journal of Biological Chemistry* **269,** 10205–10208 (1994).

142. Tambo, K. *et al.* Racemization of the aspartic acid residue of amyloid-β peptide by a radical reaction. *Biosci. Biotechnol. Biochem.* **77,** 416–418 (2013).

143. Russo, C. *et al.* Pyroglutamate-modified amyloid beta-peptides--AbetaN3(pE)--strongly affect cultured neuron and astrocyte survival. *Journal of Neurochemistry* **82,** 1480–1489 (2002).

144. Weggen, S. & Beher, D. Molecular consequences of amyloid precursor protein and presenilin mutations causing autosomal-dominant Alzheimer's disease. *Alzheimers Res*

Ther **4,** 9 (2012).

145. Cai, X. D., Golde, T. E. & Younkin, S. G. Release of excess amyloid beta protein from a mutant amyloid beta protein precursor. *Science* **259,** 514–516 (1993).

146. Citron, M. *et al.* Mutation of the beta-amyloid precursor protein in familial Alzheimer's disease increases beta-protein production. *Nature* **360,** 672–674 (1992).

147. Citron, M. *et al.* Excessive production of amyloid beta-protein by peripheral cells of symptomatic and presymptomatic patients carrying the Swedish familial Alzheimer disease mutation. *Proceedings of the National Academy of Sciences* **91,** 11993–11997 (1994).

148. Mullan, M. *et al.* A pathogenic mutation for probable Alzheimer's disease in the APP gene at the N-terminus of beta-amyloid. *Nat. Genet.* **1,** 345–347 (1992).

149. Bergman, A. *et al.* APP intracellular domain formation and unaltered signaling in the presence of familial Alzheimer's disease mutations. *Exp. Cell Res.* **287,** 1–9 (2003).

150. Hecimovic, S. *et al.* Mutations in APP have independent effects on Abeta and CTFgamma generation. *Neurobiol. Dis.* **17,** 205–218 (2004).

151. Suzuki, N. *et al.* An increased percentage of long amyloid beta protein secreted by familial amyloid beta protein precursor (beta APP717) mutants. *Science* **264,** 1336–1340 (1994).

152. McGowan, E. *et al.* Abeta42 is essential for parenchymal and vascular amyloid deposition in mice. *Neuron* **47,** 191–199 (2005).

153. Haass, C. Take five--BACE and the gamma-secretase quartet conduct Alzheimer's amyloid beta-peptide generation. *The EMBO Journal* **23,** 483–488 (2004).

154. Baumketner, A., Krone, M. G. & Shea, J.-E. Role of the familial Dutch mutation E22Q in the folding and aggregation of the 15-28 fragment of the Alzheimer amyloid-beta protein. *Proc. Natl. Acad. Sci. U.S.A.* **105,** 6027–6032 (2008).

155. Miravalle, L. *et al.* Substitutions at codon 22 of Alzheimer's abeta peptide induce diverse conformational changes and apoptotic effects in human cerebral endothelial cells. *Journal of Biological Chemistry* **275,** 27110–27116 (2000).

156. Grant, M. A. *et al.* Familial Alzheimer's disease mutations alter the stability of the amyloid beta-protein monomer folding nucleus. *Proceedings of the National Academy of Sciences* **104,** 16522–16527 (2007).

157. Lazo, N. D., Grant, M. A., Condron, M. C., Rigby, A. C. & Teplow, D. B. On the nucleation of amyloid beta-protein monomer folding. *Protein Sci.* **14,** 1581–1596 (2005).

158. Davis, J. & Van Nostrand, W. E. Enhanced pathologic properties of Dutch-type mutant amyloid beta-protein. *Proceedings of the National Academy of Sciences* **93,** 2996–3000 (1996).

159. Murakami, K. *et al.* Neurotoxicity and physicochemical properties of Abeta mutant peptides from cerebral amyloid angiopathy: implication for the pathogenesis of cerebral amyloid angiopathy and Alzheimer's disease. *Journal of Biological Chemistry* **278,** 46179–46187 (2003).

160. Herzig, M. C., Eisele, Y. S., Staufenbiel, M. & Jucker, M. E22Q-mutant Abeta peptide (AbetaDutch) increases vascular but reduces parenchymal Abeta deposition. *Am. J. Pathol.* **174,** 722–726 (2009).

161. Terry, R. D. *et al.* Physical basis of cognitive alterations in Alzheimer's disease: synapse loss is the major correlate of cognitive impairment. *Ann. Neurol.* **30,** 572–580 (1991).

162. Perrin, R. J., Fagan, A. M. & Holtzman, D. M. Multimodal techniques for diagnosis and prognosis of Alzheimer's disease. *Nature* **461,** 916–922 (2009).

163. Hsia, A. Y. *et al.* Plaque-independent disruption of neural circuits in Alzheimer's disease mouse models. *Proceedings of the National Academy of Sciences* **96,** 3228–3233 (1999).

164. Mucke, L. *et al.* High-level neuronal expression of abeta 1-42 in wild-type human amyloid protein precursor transgenic mice: synaptotoxicity without plaque formation. *J. Neurosci.* **20,** 4050–4058 (2000).

165. Westerman, M. A. *et al.* The relationship between Abeta and memory in the Tg2576 mouse model of Alzheimer's disease. *J. Neurosci.* **22,** 1858–1867 (2002).

166. Lambert, M. P. *et al.* Diffusible, nonfibrillar ligands derived from Abeta1-42 are potent central nervous system neurotoxins. *Proceedings of the National Academy of Sciences* **95,** 6448–6453 (1998).

167. Oddo, S. *et al.* Triple-transgenic model of Alzheimer's disease with plaques and tangles: intracellular Abeta and synaptic dysfunction. *Neuron* **39,** 409–421 (2003).

168. Shankar, G. M. *et al.* Natural oligomers of the Alzheimer amyloid-beta protein induce reversible synapse loss by modulating an NMDA-type glutamate receptor-dependent

signaling pathway. *J. Neurosci.* **27,** 2866–2875 (2007).

169. Reddy, P. H. *et al.* Differential loss of synaptic proteins in Alzheimer's disease: implications for synaptic dysfunction. *J. Alzheimers Dis.* **7,** 103–17– discussion 173–80 (2005).

170. Chauhan, N. B. & Siegel, G. J. Reversal of amyloid beta toxicity in Alzheimer's disease model Tg2576 by intraventricular antiamyloid beta antibody. *J. Neurosci. Res.* **69,** 10–23 (2002).

171. McLean, C. A. *et al.* Soluble pool of Abeta amyloid as a determinant of severity of neurodegeneration in Alzheimer's disease. *Ann. Neurol.* **46,** 860–866 (1999).

172. Mc Donald, J. M. *et al.* The presence of sodium dodecyl sulphate-stable Abeta dimers is strongly associated with Alzheimer-type dementia. *Brain* **133,** 1328–1341 (2010).

173. Walsh, D. M. *et al.* Naturally secreted oligomers of amyloid beta protein potently inhibit hippocampal long-term potentiation in vivo. *Nature* **416,** 535–539 (2002).

174. Gong, Y. *et al.* Alzheimer's disease-affected brain: presence of oligomeric A beta ligands (ADDLs) suggests a molecular basis for reversible memory loss. *Proceedings of the National Academy of Sciences* **100,** 10417–10422 (2003).

175. Kayed, R. *et al.* Common structure of soluble amyloid oligomers implies common mechanism of pathogenesis. *Science* **300,** 486–489 (2003).

176. Lacor, P. N. *et al.* Synaptic targeting by Alzheimer's-related amyloid beta oligomers. *J. Neurosci.* **24,** 10191–10200 (2004).

177. Townsend, M., Shankar, G. M., Mehta, T., Walsh, D. M. & Selkoe, D. J. Effects of secreted oligomers of amyloid beta-protein on hippocampal synaptic plasticity: a potent role for trimers. *J. Physiol. (Lond.)* **572,** 477–492 (2006).

178. Klyubin, I. *et al.* Amyloid beta protein dimer-containing human CSF disrupts synaptic plasticity: prevention by systemic passive immunization. *J. Neurosci.* **28,** 4231–4237 (2008).

179. Shankar, G. M. *et al.* Biochemical and immunohistochemical analysis of an Alzheimer's disease mouse model reveals the presence of multiple cerebral Abeta assembly forms throughout life. *Neurobiol. Dis.* **36,** 293–302 (2009).

180. Xia, W. *et al.* A specific enzyme-linked immunosorbent assay for measuring beta-amyloid

protein oligomers in human plasma and brain tissue of patients with Alzheimer disease. *Arch. Neurol.* **66,** 190–199 (2009).

181. Lambert, M. P. *et al.* Vaccination with soluble Abeta oligomers generates toxicity-neutralizing antibodies. *Journal of Neurochemistry* **79,** 595–605 (2001).

182. Lambert, M. P. *et al.* Monoclonal antibodies that target pathological assemblies of Abeta. *Journal of Neurochemistry* **100,** 23–35 (2007).

183. Rasool, S., Martinez-Coria, H., Wu, J. W., LaFerla, F. & Glabe, C. G. Systemic vaccination with anti-oligomeric monoclonal antibodies improves cognitive function by reducing Aβ deposition and tau pathology in 3xTg-AD mice. *Journal of Neurochemistry* **126,** 473–482 (2013).

184. Smith, I. *et al.* Amyloid-beta protein dimers isolated directly from Alzheimer's brains impair synaptic plasticity and memory. *Nat Med* **14,** 837–842 (2008).

185. Shankar, G. M. *et al.* Biochemical and immunohistochemical analysis of an Alzheimer's disease mouse model reveals the presence of multiple cerebral Abeta assembly forms throughout life. *Neurobiol. Dis.* **36,** 293–302 (2009).

186. Mc Donald, J. M. *et al.* The presence of sodium dodecyl sulphate-stable Abeta dimers is strongly associated with Alzheimer-type dementia. *Brain* **133,** 1328–1341 (2010).

187. Townsend, M., Shankar, G. M., Mehta, T., Walsh, D. M. & Selkoe, D. J. Effects of secreted oligomers of amyloid beta-protein on hippocampal synaptic plasticity: a potent role for trimers. *J. Physiol. (Lond.)* **572,** 477–492 (2006).

188. Zahs, K. R. & Ashe, K. H. β-Amyloid oligomers in aging and Alzheimer's disease. *Front Aging Neurosci* **5,** 28 (2013).

189. Bernstein, S. L. *et al.* Amyloid-β protein oligomerization and the importance of tetramers and dodecamers in the aetiology of Alzheimer's disease. *Nat Chem* **1,** 326–331 (2009).

190. Benilova, I., Karran, E. & De Strooper, B. The toxic Aβ oligomer and Alzheimer's disease: an emperor in need of clothes. *Nat Neurosci* **15,** 349–357 (2012).

191. Campioni, S. *et al.* A causative link between the structure of aberrant protein oligomers and their toxicity. *Nat Chem Biol* **6,** 140–147 (2010).

192. Matsumura, S. *et al.* Two distinct amyloid beta-protein (Abeta) assembly pathways leading to oligomers and fibrils identified by combined fluorescence correlation

spectroscopy, morphology, and toxicity analyses. *J. Biol. Chem.* **286,** 11555–11562 (2011).

193. Kayed, R. *et al.* Fibril specific, conformation dependent antibodies recognize a generic epitope common to amyloid fibrils and fibrillar oligomers that is absent in prefibrillar oligomers. *Mol Neurodegeneration* **2,** 18 (2007).

194. Yamin, G. NMDA receptor-dependent signaling pathways that underlie amyloid beta-protein disruption of LTP in the hippocampus. *J. Neurosci. Res.* **87,** 1729–1736 (2009).

195. Dineley, K. T. *et al.* Beta-amyloid activates the mitogen-activated protein kinase cascade via hippocampal alpha7 nicotinic acetylcholine receptors: In vitro and in vivo mechanisms related to Alzheimer's disease. *J. Neurosci.* **21,** 4125–4133 (2001).

196. Zhao, W.-Q. *et al.* Amyloid beta oligomers induce impairment of neuronal insulin receptors. *FASEB J.* **22,** 246–260 (2008).

197. Laurén, J., Gimbel, D. A., Nygaard, H. B., Gilbert, J. W. & Strittmatter, S. M. Cellular prion protein mediates impairment of synaptic plasticity by amyloid-beta oligomers. *Nature* **457,** 1128–1132 (2009).

198. Balducci, C. *et al.* Synthetic amyloid-beta oligomers impair long-term memory independently of cellular prion protein. *Proc. Natl. Acad. Sci. U.S.A.* **107,** 2295–2300 (2010).

199. Calella, A. M. *et al.* Prion protein and Abeta-related synaptic toxicity impairment. *EMBO Mol Med* **2,** 306–314 (2010).

200. Cisse, M. *et al.* Ablation of Cellular Prion Protein Does Not Ameliorate Abnormal Neural Network Activity or Cognitive Dysfunction in the J20 Line of Human Amyloid Precursor Protein Transgenic Mice. *Journal of Neuroscience* **31,** 10427–10431 (2011).

201. Um, J. W. *et al.* Alzheimer amyloid-β oligomer bound to postsynaptic prion protein activates Fyn to impair neurons. *Nat Neurosci* **15,** 1227–1235 (2012).

202. Fluharty, B. R. *et al.* An N-terminal fragment of the prion protein binds to amyloid-β oligomers and inhibits their neurotoxicity in vivo. *J. Biol. Chem.* **288,** 7857–7866 (2013).

203. Nicoll, A. J. *et al.* Amyloid-β nanotubes are associated with prion protein-dependent synaptotoxicity. *Nat Comms* **4,** 2416 (2013).

204. Kostylev, M. A. *et al.* Prion-Protein-interacting Amyloid-β Oligomers of High Molecular

Weight Are Tightly Correlated with Memory Impairment in Multiple Alzheimer Mouse Models. *J. Biol. Chem.* **290,** 17415–17438 (2015).

205. Campioni, S. *et al.* A causative link between the structure of aberrant protein oligomers and their toxicity. *Nat Chem Biol* **6,** 140–147 (2010).

206. Ladiwala, A. R. A. *et al.* Conformational differences between two amyloid β oligomers of similar size and dissimilar toxicity. *J. Biol. Chem.* **287,** 24765–24773 (2012).

207. Stravalaci, M. *et al.* Specific recognition of biologically active amyloid-β oligomers by a new surface plasmon resonance-based immunoassay and an in vivo assay in Caenorhabditis elegans. *J. Biol. Chem.* **287,** 27796–27805 (2012).

208. Sepulveda, F. J., Parodi, J., Peoples, R. W., Opazo, C. & Aguayo, L. G. Synaptotoxicity of Alzheimer beta amyloid can be explained by its membrane perforating property. *PLoS ONE* **5,** e11820 (2010).

209. Stravalaci, M. *et al.* The Anti-Prion Antibody 15B3 Detects Toxic Amyloid-β Oligomers. *J. Alzheimers Dis.* **Preprint,** 1–13 (2016).

210. Driscoll, M. & Chalfie, M. Developmental and abnormal cell death in C. elegans. *Trends Neurosci.* **15,** 15–19 (1992).

211. Shaham, S. Glial development and function in the nervous system of Caenorhabditis elegans. *Cold Spring Harb Perspect Biol* **7,** a020578 (2015).

212. Bargmann, C. I. Chemosensation in C. elegans. *WormBook* 1–29 (2006). doi:10.1895/wormbook.1.123.1

213. Stiernagle, T. Maintenance of C. elegans. *WormBook* 1–11 (2006). doi:10.1895/wormbook.1.101.1

214. C. elegans Sequencing Consortium. Genome sequence of the nematode C. elegans: a platform for investigating biology. *Science* **282,** 2012–2018 (1998).

215. Shaye, D. D. & Greenwald, I. OrthoList: a compendium of C. elegans genes with human orthologs. *PLoS ONE* **6,** e20085 (2011).

216. Kaletta, T. & Hengartner, M. O. Finding function in novel targets: C. elegans as a model organism. *Nat Rev Drug Discov* **5,** 387–398 (2006).

217. Culetto, E. & Sattelle, D. B. A role for Caenorhabditis elegans in understanding the function and interactions of human disease genes. *Hum. Mol. Genet.* **9,** 869–877 (2000).

218. Fire, A. *et al.* Potent and specific genetic interference by double-stranded RNA in Caenorhabditis elegans. *Nature* **391,** 806–811 (1998).

219. Sulston, J. E. Neuronal cell lineages in the nematode Caenorhabditis elegans. *Cold Spring Harb. Symp. Quant. Biol.* **48 Pt 2,** 443–452 (1983).

220. Sulston, J. E., Schierenberg, E., White, J. G. & Thomson, J. N. The embryonic cell lineage of the nematode Caenorhabditis elegans. *Dev. Biol.* **100,** 64–119 (1983).

221. Sulston, J. E. & Horvitz, H. R. Post-embryonic cell lineages of the nematode, Caenorhabditis elegans. *Dev. Biol.* **56,** 110–156 (1977).

222. Ward, S., Thomson, N., White, J. G. & Brenner, S. Electron microscopical reconstruction of the anterior sensory anatomy of the nematode Caenorhabditis elegans.?2UU. *J. Comp. Neurol.* **160,** 313–337 (1975).

223. Francis, R. & Waterston, R. H. Muscle cell attachment in Caenorhabditis elegans. *J. Cell Biol.* **114,** 465–479 (1991).

224. Byerly, L., Cassada, R. C. & Russell, R. L. The life cycle of the nematode Caenorhabditis elegans. I. Wild-type growth and reproduction. *Dev. Biol.* **51,** 23–33 (1976).

225. Hu, P. J. Dauer. *WormBook* 1–19 (2007). doi:10.1895/wormbook.1.144.1

226. Kenyon, C., Chang, J., Gensch, E., Rudner, A. & Tabtiang, R. A C. elegans mutant that lives twice as long as wild type. *Nature* **366,** 461–464 (1993).

227. Brenner, S. The Genetics of Caenorhabdtis elegans. 71–94 (1974).

228. Jorgensen, E. M. & Mango, S. E. The art and design of genetic screens: caenorhabditis elegans. *Nat. Rev. Genet.* **3,** 356–369 (2002).

229. Kutscher, L. M. & Shaham, S. Forward and reverse mutagenesis in C. elegans. *WormBook* 1–26 (2014). doi:10.1895/wormbook.1.167.1

230. Doitsidou, M., Poole, R. J., Sarin, S., Bigelow, H. & Hobert, O. C. elegans mutant identification with a one-step whole-genome-sequencing and SNP mapping strategy. *PLoS ONE* **5,** e15435 (2010).

231. Zuryn, S., Le Gras, S., Jamet, K. & Jarriault, S. A strategy for direct mapping and identification of mutations by whole-genome sequencing. *Genetics* **186,** 427–430 (2010).

232. Minevich, G., Park, D. S., Blankenberg, D., Poole, R. J. & Hobert, O. CloudMap: a cloud-based pipeline for analysis of mutant genome sequences. *Genetics* **192,** 1249–1269

(2012).

233. Frøkjaer-Jensen, C. Exciting prospects for precise engineering of Caenorhabditis elegans genomes with CRISPR/Cas9. *Genetics* **195,** 635–642 (2013).

234. Waaijers, S. & Boxem, M. Engineering the Caenorhabditis elegans genome with CRISPR/Cas9. *Methods* **68,** 381–388 (2014).

235. Cohen, E., Bieschke, J., Perciavalle, R. M., Kelly, J. W. & Dillin, A. Opposing activities protect against age-onset proteotoxicity. *Science* **313,** 1604–1610 (2006).

236. Morley, J. F., Brignull, H. R., Weyers, J. J. & Morimoto, R. I. The threshold for polyglutamine-expansion protein aggregation and cellular toxicity is dynamic and influenced by aging in Caenorhabditis elegans. *Proceedings of the National Academy of Sciences* **99,** 10417–10422 (2002).

237. Kimura, K. D., Tissenbaum, H. A., Liu, Y. & Ruvkun, G. daf-2, an insulin receptor-like gene that regulates longevity and diapause in Caenorhabditis elegans. *Science* **277,** 942–946 (1997).

238. Cohen, E. & Dillin, A. The insulin paradox: aging, proteotoxicity and neurodegeneration. *Nat Rev Neurosci* **9,** 759–767 (2008).

239. Taguchi, A. & White, M. F. Insulin-like signaling, nutrient homeostasis, and life span. *Annu. Rev. Physiol.* **70,** 191–212 (2008).

240. Ogg, S. & Ruvkun, G. The C. elegans PTEN homolog, DAF-18, acts in the insulin receptor-like metabolic signaling pathway. *Mol. Cell* **2,** 887–893 (1998).

241. Rabindran, S. K., Haroun, R. I., Clos, J., Wisniewski, J. & Wu, C. Regulation of heat shock factor trimer formation: role of a conserved leucine zipper. *Science* **259,** 230–234 (1993).

242. Tonkiss, J. & Calderwood, S. K. Regulation of heat shock gene transcription in neuronal cells. *Int J Hyperthermia* **21,** 433–444 (2005).

243. Dong, M.-Q. *et al.* Quantitative mass spectrometry identifies insulin signaling targets in C. elegans. *Science* **317,** 660–663 (2007).

244. Barral, J. M., Broadley, S. A., Schaffar, G. & Hartl, F. U. Roles of molecular chaperones in protein misfolding diseases. *Semin. Cell Dev. Biol.* **15,** 17–29 (2004).

245. Link, C. D. Invertebrate models of Alzheimer's disease. *Genes Brain Behav* **4,** 147–156 (2005).

246. Fay, D. S., Fluet, A., Johnson, C. J. & Link, C. D. In vivo aggregation of beta-amyloid peptide variants. *Journal of Neurochemistry* **71,** 1616–1625 (1998).

247. Link, C. D. Expression of human beta-amyloid peptide in transgenic Caenorhabditis elegans. *Proceedings of the National Academy of Sciences* **92,** 9368–9372 (1995).

248. Link, C. D. *et al.* Visualization of fibrillar amyloid deposits in living, transgenic Caenorhabditis elegans animals using the sensitive amyloid dye, X-34. *Neurobiology of Aging* **22,** 217–226 (2001).

249. Selkoe, D. J. Alzheimer's disease: genes, proteins, and therapy. *Physiol. Rev.* **81,** 741–766 (2001).

250. McColl, G. *et al.* The Caenorhabditis elegans A beta 1-42 model of Alzheimer disease predominantly expresses A beta 3-42. *J. Biol. Chem.* **284,** 22697–22702 (2009).

251. Florez-McClure, M. L., Hohsfield, L. A., Fonte, G., Bealor, M. T. & Link, C. D. Decreased insulin-receptor signaling promotes the autophagic degradation of beta-amyloid peptide in C. elegans. *Autophagy* **3,** 569–580 (2007).

252. Fonte, V. *et al.* Interaction of intracellular beta amyloid peptide with chaperone proteins. *Proceedings of the National Academy of Sciences* **99,** 9439–9444 (2002).

253. Gouras, G. K. *et al.* Intraneuronal Abeta42 accumulation in human brain. *Am. J. Pathol.* **156,** 15–20 (2000).

254. Wirths, O. *et al.* Intraneuronal Abeta accumulation precedes plaque formation in beta-amyloid precursor protein and presenilin-1 double-transgenic mice. *Neurosci. Lett.* **306,** 116–120 (2001).

255. Diomede, L. *et al.* Tetracycline and its analogues protect Caenorhabditis elegans from β amyloid-induced toxicity by targeting oligomers. *Neurobiol. Dis.* **40,** 424–431 (2010).

256. Wu, Y., Cao, Z., Klein, W. L. & Luo, Y. Heat shock treatment reduces beta amyloid toxicity in vivo by diminishing oligomers. *Neurobiology of Aging* **31,** 1055–1058 (2010).

257. Link, C. Gene expression analysis in a transgenic Caenorhabditis elegans Alzheimer's disease model. *Neurobiology of Aging* **24,** 397–413 (2003).

258. Hassan, W. M., Dostal, V., Huemann, B. N., Yerg, J. E. & Link, C. D. Identifying Aβ-specific pathogenic mechanisms using a nematode model of Alzheimer's disease. *Neurobiology of Aging* **36,** 857–866 (2015).

259. Diomede, L. *et al.* Expression of A2V-mutated Aβ in Caenorhabditis elegans results in oligomer formation and toxicity. *Neurobiol. Dis.* **62,** 521–532 (2014).

260. Dosanjh, L. E., Brown, M. K., Rao, G., Link, C. D. & Luo, Y. Behavioral phenotyping of a transgenic Caenorhabditis elegans expressing neuronal amyloid-beta. *J. Alzheimers Dis.* **19,** 681–690 (2010).

261. Di Fede, G. *et al.* A recessive mutation in the APP gene with dominant-negative effect on amyloidogenesis. *Science* **323,** 1473–1477 (2009).

262. Jorgensen, E. M. & Mango, S. E. The art and design of genetic screens: caenorhabditis elegans. *Nat. Rev. Genet.* **3,** 356–369 (2002).

263. Boutros, M. & Ahringer, J. The art and design of genetic screens: RNA interference. *Nat. Rev. Genet.* **9,** 554–566 (2008).

264. Anderson, P. Mutagenesis. *Methods Cell Biol.* **48,** 31–58 (1995).

265. Davis, M. W. *et al.* Rapid single nucleotide polymorphism mapping in C. elegans. *BMC Genomics* **6,** 118 (2005).

266. Bargmann, C. I. Neurobiology of the Caenorhabditis elegans genome. *Science* **282,** 2028–2033 (1998).

267. Ophoff, R. A. *et al.* Familial hemiplegic migraine and episodic ataxia type-2 are caused by mutations in the Ca2+ channel gene CACNL1A4. *Cell* **87,** 543–552 (1996).

268. Sulston, J. E. & Horvitz, H. R. Abnormal cell lineages in mutants of the nematode Caenorhabditis elegans. *Dev. Biol.* **82,** 41–55 (1981).

269. Beitel, G. J., Tuck, S., Greenwald, I. & Horvitz, H. R. The Caenorhabditis elegans gene lin-1 encodes an ETS-domain protein and defines a branch of the vulval induction pathway. *Genes Dev.* **9,** 3149–3162 (1995).

270. Egan, S. E. *et al.* Association of Sos Ras exchange protein with Grb2 is implicated in tyrosine kinase signal transduction and transformation. *Nature* **363,** 45–51 (1993).

271. Timmons, L., Tabara, H., Mello, C. C. & Fire, A. Z. Inducible systemic RNA silencing in Caenorhabditis elegans. *Mol. Biol. Cell* **14,** 2972–2983 (2003).

272. Timmons, L., Court, D. L. & Fire, A. Ingestion of bacterially expressed dsRNAs can produce specific and potent genetic interference in Caenorhabditis elegans. *Gene* **263,** 103–112 (2001).

273. Tabara, H., Grishok, A. & Mello, C. C. RNAi in C. elegans: soaking in the genome sequence. *Science* **282,** 430–431 (1998).

274. Tavernarakis, N., Wang, S. L., Dorovkov, M., Ryazanov, A. & Driscoll, M. Heritable and inducible genetic interference by double-stranded RNA encoded by transgenes. *Nat. Genet.* **24,** 180–183 (2000).

275. Kamath, R. S. *et al.* Systematic functional analysis of the Caenorhabditis elegans genome using RNAi. *Nature* **421,** 231–237 (2003).

276. Kamath, R. S. & Ahringer, J. Genome-wide RNAi screening in Caenorhabditis elegans. *Methods* **30,** 313–321 (2003).

277. van Ham, T. J. *et al.* Identification of MOAG-4/SERF as a regulator of age-related proteotoxicity. *Cell* **142,** 601–612 (2010).

278. Sin, O., Michels, H. & Nollen, E. A. A. Genetic screens in Caenorhabditis elegans models for neurodegenerative diseases. *Biochim. Biophys. Acta* **1842,** 1951–1959 (2014).

279. Blum, E. S., Schwendeman, A. R. & Shaham, S. PolyQ disease: misfiring of a developmental cell death program? *Trends Cell Biol.* **23,** 168–174 (2013).

280. Blum, E. S., Schwendeman, A. R. & Shaham, S. PolyQ disease: misfiring of a developmental cell death program? *Trends Cell Biol.* **23,** 168–174 (2013).

281. Faber, P. W., Alter, J. R., MacDonald, M. E. & Hart, A. C. Polyglutamine-mediated dysfunction and apoptotic death of a Caenorhabditis elegans sensory neuron. *Proceedings of the National Academy of Sciences* **96,** 179–184 (1999).

282. Parker, J. A. *et al.* Expanded polyglutamines in Caenorhabditis elegans cause axonal abnormalities and severe dysfunction of PLM mechanosensory neurons without cell death. *Proceedings of the National Academy of Sciences* **98,** 13318–13323 (2001).

283. Brignull, H. R., Moore, F. E., Tang, S. J. & Morimoto, R. I. Polyglutamine proteins at the pathogenic threshold display neuron-specific aggregation in a pan-neuronal Caenorhabditis elegans model. *J. Neurosci.* **26,** 7597–7606 (2006).

284. Nollen, E. A. A. *et al.* Genome-wide RNA interference screen identifies previously undescribed regulators of polyglutamine aggregation. *Proceedings of the National Academy of Sciences* **101,** 6403–6408 (2004).

285. Silva, M. C. *et al.* A genetic screening strategy identifies novel regulators of the

proteostasis network. *PLoS Genet.* **7,** e1002438 (2011).

286. Falsone, S. F. *et al.* SERF protein is a direct modifier of amyloid fiber assembly. *CellReports* **2,** 358–371 (2012).

287. Lejeune, F.-X. *et al.* Large-scale functional RNAi screen in C. elegans identifies genes that regulate the dysfunction of mutant polyglutamine neurons. *BMC Genomics* **13,** 91 (2012).

288. de Lau, L. M. L. & Breteler, M. M. B. Epidemiology of Parkinson's disease. *The Lancet Neurology* **5,** 525–535 (2006).

289. Inamdar, N. N., Arulmozhi, D. K., Tandon, A. & Bodhankar, S. L. Parkinson's disease: genetics and beyond. *Curr Neuropharmacol* **5,** 99–113 (2007).

290. Dauer, W. & Przedborski, S. Parkinson's disease: mechanisms and models. *Neuron* **39,** 889–909 (2003).

291. Chung, K. K. *et al.* Parkin ubiquitinates the alpha-synuclein-interacting protein, synphilin-1: implications for Lewy-body formation in Parkinson disease. *Nat Med* **7,** 1144–1150 (2001).

292. Abeliovich, A. *et al.* Mice lacking alpha-synuclein display functional deficits in the nigrostriatal dopamine system. *Neuron* **25,** 239–252 (2000).

293. Clayton, D. F. & George, J. M. The synucleins: a family of proteins involved in synaptic function, plasticity, neurodegeneration and disease. *Trends Neurosci.* **21,** 249–254 (1998).

294. van Ham, T. J. *et al.* C. elegans model identifies genetic modifiers of alpha-synuclein inclusion formation during aging. *PLoS Genet.* **4,** e1000027 (2008).

295. van der Goot, A. T. *et al.* Delaying aging and the aging-associated decline in protein homeostasis by inhibition of tryptophan degradation. *Proc. Natl. Acad. Sci. U.S.A.* **109,** 14912–14917 (2012).

296. Fung, H.-C. *et al.* Genome-wide genotyping in Parkinson's disease and neurologically normal controls: first stage analysis and public release of data. *The Lancet Neurology* **5,** 911–916 (2006).

297. Kuwahara, T. *et al.* A systematic RNAi screen reveals involvement of endocytic pathway in neuronal dysfunction in alpha-synuclein transgenic C. elegans. *Hum. Mol. Genet.* **17,**

2997–3009 (2008).

298. Collins, B. M., McCoy, A. J., Kent, H. M., Evans, P. R. & Owen, D. J. Molecular architecture and functional model of the endocytic AP2 complex. *Cell* **109,** 523–535 (2002).

299. Kraemer, B. C., Burgess, J. K., Chen, J. H., Thomas, J. H. & Schellenberg, G. D. Molecular pathways that influence human tau-induced pathology in Caenorhabditis elegans. *Hum. Mol. Genet.* **15,** 1483–1496 (2006).

300. Wang, H.-Y., Li, W., Benedetti, N. J. & Lee, D. H. S. Alpha 7 nicotinic acetylcholine receptors mediate beta-amyloid peptide-induced tau protein phosphorylation. *Journal of Biological Chemistry* **278,** 31547–31553 (2003).

301. Livak, K. J. & Schmittgen, T. D. Analysis of relative gene expression data using real-time quantitative PCR and the 2(-Delta Delta C(T)) Method. *Methods* **25,** 402–408 (2001).

302. Langmead, B. & Salzberg, S. L. Fast gapped-read alignment with Bowtie 2. *Nat Meth* **9,** 357–359 (2012).

303. McKenna, A. *et al.* The Genome Analysis Toolkit: a MapReduce framework for analyzing next-generation DNA sequencing data. *Genome Research* **20,** 1297–1303 (2010).

304. Kent, W. J. *et al.* The human genome browser at UCSC. *Genome Research* **12,** 996–1006 (2002).

305. Jonsson, T. *et al.* A mutation in APP protects against Alzheimer's disease and age-related cognitive decline. *Nature* **488,** 96–99 (2012).

306. Benilova, I. *et al.* The Alzheimer disease protective mutation A2T modulates kinetic and thermodynamic properties of amyloid-β (Aβ) aggregation. *J. Biol. Chem.* **289,** 30977–30989 (2014).

307. White, C. V., Darby, B. J., Breeden, R. J. & Herman, M. A. A Stenotrophomonas maltophilia Strain Evades a Major Caenorhabditis elegans Defense Pathway. *Infect. Immun.* **84,** 524–536 (2015).

308. Marroquin, L. D., Elyassnia, D., Griffitts, J. S., Feitelson, J. S. & Aroian, R. V. Bacillus thuringiensis (Bt) toxin susceptibility and isolation of resistance mutants in the nematode Caenorhabditis elegans. *Genetics* **155,** 1693–1699 (2000).

309. Bravo, A., Gill, S. S. & Soberón, M. Mode of action of Bacillus thuringiensis Cry and Cyt

toxins and their potential for insect control. *Toxicon* **49,** 423–435 (2007).

310. Garigan, D. *et al.* Genetic analysis of tissue aging in Caenorhabditis elegans: a role for heat-shock factor and bacterial proliferation. *Genetics* **161,** 1101–1112 (2002).

311. Samuelson, A. V., Carr, C. E. & Ruvkun, G. Gene activities that mediate increased life span of C. elegans insulin-like signaling mutants. *Genes Dev.* **21,** 2976–2994 (2007).

312. Hamilton, B. *et al.* A systematic RNAi screen for longevity genes in C. elegans. *Genes Dev.* **19,** 1544–1555 (2005).

313. Libina, N., Berman, J. R. & Kenyon, C. Tissue-specific activities of C. elegans DAF-16 in the regulation of lifespan. *Cell* **115,** 489–502 (2003).

314. Srinivasan, B. *et al.* Extracellular 4'-phosphopantetheine is a source for intracellular coenzyme A synthesis. *Nat Chem Biol* **11,** 784–792 (2015).

315. Siudeja, K. *et al.* Impaired Coenzyme A metabolism affects histone and tubulin acetylation in Drosophila and human cell models of pantothenate kinase associated neurodegeneration. *EMBO Mol Med* **3,** 755–766 (2011).

316. Lee, S. S., Kennedy, S., Tolonen, A. C. & Ruvkun, G. DAF-16 target genes that control C. elegans life-span and metabolism. *Science* **300,** 644–647 (2003).

317. Sans, N. *et al.* NMDA receptor trafficking through an interaction between PDZ proteins and the exocyst complex. *Nat. Cell Biol.* **5,** 520–530 (2003).

318. Basha, E., O'Neill, H. & Vierling, E. Small heat shock proteins and α-crystallins: dynamic proteins with flexible functions. *Trends in Biochemical Sciences* **37,** 106–117 (2012).

319. Garrido, C., Paul, C., Seigneuric, R. & Kampinga, H. H. The small heat shock proteins family: the long forgotten chaperones. *Int. J. Biochem. Cell Biol.* **44,** 1588–1592 (2012).

320. Shinohara, H., Inaguma, Y., Goto, S., Inagaki, T. & Kato, K. Alpha B crystallin and HSP28 are enhanced in the cerebral cortex of patients with Alzheimer's disease. *J. Neurol. Sci.* **119,** 203–208 (1993).

321. Renkawek, K., Voorter, C. E., Bosman, G. J., van Workum, F. P. & de Jong, W. W. Expression of alpha B-crystallin in Alzheimer's disease. *Acta Neuropathol.* **87,** 155–160 (1994).